

Westinghouse Non-Proprietary Class 3



WCAP - 15834

**WCOBRA/TRAC AP1000
ADS-4/IRWST Phase
Modeling**

Westinghouse Electric Company LLC



WCAP-15834

**WCOBRA/TRAC AP1000
ADS-4/IRWST Phase Modeling**

W. L. Brown
Systems Analysis Engineering

R. M. Kemper
Systems Analysis Engineering

May 2002

Westinghouse Electric Company LLC
P.O. Box 355
Pittsburgh, PA 15230-0355

© 2002 Westinghouse Electric Company LLC
All Rights Reserved

TABLE OF CONTENTS

LIST OF TABLES.....v

LIST OF FIGURES..... vii

LIST OF ACRONYMS AND ABBREVIATIONSxi

EQUATION NOMENCLATURE xii

SUMMARY xiii

1 INTRODUCTION..... 1-1

 1.1 NOTRUMP APPLICATION TO PASSIVE PLANT SMALL BREAK
 LOSS-OF-COOLANT ACCIDENT ANALYSIS 1-2

 1.1.1 Background 1-2

 1.1.2 PIRT Issues..... 1-4

 1.2 USE OF WCOBRA/TRAC TO SUPPLEMENT NOTRUMP..... 1-5

 1.3 REFERENCES..... 1-6

2 WCOBRA/TRAC APPLICATION TO THE ADS-4 IRWST INITIATION PHASE 2-1

 2.1 INTRODUCTION..... 2-1

 2.2 FLOW MODELS AND VALIDATION 2-1

 2.2.1 Models and Correlations 2-2

 2.2.2 Separate Effects Test Validation..... 2-16

 2.2.3 References 2-21

 2.3 OSU APEX FACILITY VALIDATION OF WCOBRA/TRAC-AP 2-46

 2.3.1 WCOBRA/TRAC OSU Test Facility Model 2-47

 2.3.2 Assessment of WCOBRA/TRAC-AP Predictions 2-51

 2.3.3 References 2-52

3 AP1000 PLANT SIMULATIONS 3-1

 3.1 PLANT MODELING..... 3-1

 3.1.1 Vessel Component..... 3-1

 3.1.2 Primary Loop 3-2

 3.1.3 Pressurizer..... 3-2

 3.1.4 Steam Generators 3-2

 3.1.5 Reactor Coolant Pumps..... 3-2

 3.1.6 Loop Lines 3-2

 3.1.7 Accumulators 3-2

 3.1.8 Core Makeup Tanks 3-3

 3.1.9 Passive Residual Heat Removal Heat Exchanger/In-Containment
 Refueling Water Storage Tank..... 3-3

 3.1.10 In-Containment Refueling Water Storage Tank (IRWST)..... 3-3

 3.1.11 Automatic Depressurization System Stage 1 to 3 Valves..... 3-3

 3.1.12 Automatic Depressurization System Stage 4 Valves..... 3-3

 3.1.13 Safety Injection During the ADS-4 IRWST Initiation Phase 3-3

TABLE OF CONTENTS (cont.)

3.1.14 Break Component..... 3-4

3.1.15 Initial and Boundary Conditions 3-4

3.2 LIMITING CASE RESULTS 3-4

3.2.1 Double-Ended DVI Line Break..... 3-4

3.2.2 Inadvertent ADS Actuation Scenario 3-5

3.3 REFERENCES..... 3-6

4 CONCLUSIONS..... 4-1

LIST OF TABLES

Table 2-1 Test Matrix Parameters..... 2-24

LIST OF FIGURES

Figure 1-1	AP1000 Passive Safety Injection Flow Schematic	1-7
Figure 2-1	Generalized Flow Regime Map for Horizontal Two-Phase Flow	2-27
Figure 2-2	Equilibrium Liquid Level vs. Martinelli Parameter, X	2-28
Figure 2-3	Basic Mesh Cell	2-29
Figure 2-4	<u>W</u> COBRA/TRAC-AP Representation of Interfacial Heat Transfer	2-30
Figure 2-5	Schematic Diagram of the Experimental System (Lim, et al., 1981)	2-31
Figure 2-6	<u>W</u> COBRA/TRAC Noding	2-32
Figure 2-7	Measured Water Thickness Versus Axial Position for Various Liquid (WI) Flowrates and Inlet Water Layer Thickness of 1.583 cm.....	2-33
Figure 2-8	Measured Water Thickness at 0.157 m From the Channel Inlet Versus Liquid and Steam Flowrates	2-34
Figure 2-9	Calculated Liquid Level (Run 275)	2-35
Figure 2-10	Calculated and Measured Liquid Levels Versus Axial Position (Run 275)	2-36
Figure 2-11	Calculated Steam Pressure (Run 275).....	2-37
Figure 2-12	Calculated and Measured Steam Pressure Versus Axial Position (Run 275)	2-38
Figure 2-13	Calculated Steam Flowrate (Run 275).....	2-39
Figure 2-14	Calculated and Measured Steam Flowrate Versus Axial Position (Run 275)	2-40
Figure 2-15	Comparison of Condensation Heat Transfer Correlations	2-41
Figure 2-16	Predicted Versus Measured Liquid Level at Various Axial Locations	2-42
Figure 2-17	Predicted Versus Measured Steam Flowrate at Various Axial Locations.....	2-43
Figure 2-18	Predicted Versus Measured Liquid Temperature at the Channel Exit.....	2-44
Figure 2-19	Predicted Versus Measured Steam Pressure Drop at Various Axial Locations	2-45
Figure 2-20	OSU <u>W</u> COBRA/TRAC Schematic Diagram.....	2-53
Figure 2-21	OSU <u>W</u> COBRA/TRAC Vessel Model (Front View)	2-54

LIST OF FIGURES (cont.)

Figure 2-22 OSU Vessel Model – Section 1 2-55

Figure 2-23 OSU Vessel Model – Section 2 2-56

Figure 2-24 OSU Vessel Model – Section 3 2-57

Figure 2-25 OSU Vessel Model – Section 4 2-58

Figure 2-26 OSU Vessel Model – Section 5 2-59

Figure 2-27 OSU Vessel Model – Section 6 2-60

Figure 2-28 OSU Vessel Model – Section 7 2-61

Figure 2-29 WCOBRA/TRAC Prediction vs. Test SB18 Data: Pressurizer Collapsed
Liquid Level..... 2-62

Figure 2-30 WCOBRA/TRAC Prediction vs. Test SB18 Data: Total ADS-4 Integrated
Liquid Flow Rate 2-63

Figure 2-31 WCOBRA/TRAC Prediction of Test SB18 Downcomer Collapsed Liquid Level.... 2-64

Figure 2-32 WCOBRA/TRAC Prediction of Test SB18 Core Collapsed Liquid Level..... 2-65

Figure 2-33 WCOBRA/TRAC Prediction of Test SB18 Core/Upper Plenum Collapsed
Liquid Level..... 2-66

Figure 2-34 WCOBRA/TRAC Prediction vs. Test SB18 Data: Downcomer Pressure 2-67

Figure 3-1 AP1000 WCOBRA/TRAC Vessel Model (Front View) 3-7

Figure 3-2 AP1000 Vessel Model – Section 1 3-8

Figure 3-3 AP1000 Vessel Model – Section 2 3-9

Figure 3-4 AP1000 Vessel Model – Section 3 3-10

Figure 3-5 AP1000 Vessel Model – Section 4 3-11

Figure 3-6 AP1000 Vessel Model – Section 5 3-12

Figure 3-7 AP1000 Vessel Model – Section 6 3-13

Figure 3-8 AP1000 WCOBRA/TRAC Schematic Diagram..... 3-14

Figure 3-9 AP1000 DEDVI Break Downcomer Pressure 3-15

LIST OF FIGURES (cont.)

Figure 3-10 AP1000 DEDVI Break IRWST Flow Rate..... 3-16

Figure 3-11 AP1000 DEDVI Break CMT and Accumulator Flow Rate 3-17

Figure 3-12 AP1000 DEDVI Break Intact Loop ADS-4 – Integrated Liquid Flow 3-18

Figure 3-13 AP1000 DEDVI Break Intact Loop ADS-4 – Integrated Vapor Flow 3-19

Figure 3-14 AP1000 DEDVI Break Single Failure Loop ADS-4 – Integrated Liquid Flow..... 3-20

Figure 3-15 AP1000 DEDVI Break Single Failure Loop ADS-4 – Integrated Vapor Flow..... 3-21

Figure 3-16 AP1000 DEDVI Break Vessel Mass Inventory 3-22

Figure 3-17 AP1000 DEDVI Break Integrated Core Inlet Flow 3-23

Figure 3-18 AP1000 Inadvertent ADS Actuation Scenario – Downcomer Pressure..... 3-24

Figure 3-19 AP1000 Inadvertent ADS Actuation Scenario – Total IRWST Injection
Flow Rate..... 3-25

Figure 3-20 AP1000 Inadvertent ADS Actuation Scenario – Total CMT Injection Flow Rate..... 3-26

Figure 3-21 AP1000 Inadvertent ADS Actuation Scenario Intact Loop ADS-4 –
Integrated Liquid Flow 3-27

Figure 3-22 AP1000 Inadvertent ADS Actuation Scenario Intact Loop ADS-4 –
Integrated Vapor Flow 3-28

Figure 3-23 AP1000 Inadvertent ADS Actuation Scenario Single Failure Loop ADS-4 –
Integrated Liquid Flow 3-29

Figure 3-24 AP1000 Inadvertent ADS Actuation Scenario Single Failure Loop ADS-4 –
Integrated Vapor Flow 3-30

Figure 3-25 AP1000 Inadvertent ADS Actuation Scenario Break Vessel Mass Inventory..... 3-31

Figure 3-26 AP1000 Inadvertent ADS Actuation Scenario Break Integrated Core Inlet Flow 3-32

LIST OF ACRONYMS AND ABBREVIATIONS

ACC	accumulators
ADS	automatic depressurization system
CCFL	counter current flow limitation
CMT	core makeup tank
CVS	chemical and volume control system
DCD	design control document
ECCS	emergency core cooling system
H2TS	hierarchical, two-tiered scaling
HX	heat exchanger
IRWST	in-containment refueling water storage tank
LOCA	loss-of-coolant accident
LTC	long-term cooling
NRC	Nuclear Regulatory Commission
OSU	Oregon State University
PCS	passive containment cooling system
PIRT	phenomena identification and ranking tables
PRHR	passive residual heat removal
PXS	passive core cooling system
RCP	reactor coolant pump
RCS	reactor coolant system
RNS	normal residual heat removal system
SAR	Safety Analysis Report
SBLOCA	small-break loss-of-coolant accident
SG	steam generator
SIMARC	simulator advanced real-time code

EQUATION NOMENCLATURE

A	Area	<u>Greek</u>
d	Offtake diameter	ρ Density
D	Pipe diameter	δ Angle
D_H	Hydraulic diameter	ν Kinematic viscosity
F_r	Froude Number	α Void fraction
g	Gravitational acceleration	σ Surface tension
h_L	Mixture level	μ Viscosity
H	Heat Transfer coefficient	τ Interfacial shear stress
i	Interfacial	
k	Thermal conductivity	<u>Subscripts</u>
K	Interfacial friction factor	b Bubble
N_μ	Viscosity number	g Saturated vapor
P	Pressure	l Liquid field
P_r	Prandtl number	v Vapor field
R_e	Reynolds number	f Saturated liquid
T	Temperature	
V_s	Settling velocity	<u>Superscripts</u>
x	Vertical direction, Cartesian coordinates	e Entrained field
X	Phasic pressure drop ratio in two-phase flow	k Continuous phase
U	Vertical velocity component, Subchannel coordinates	x Vertical direction, Cartesian Coordinate
z	Transverse direction, Cartesian coordinates	S Superficial
Z	Transverse direction, Subchannel Coordinates	

SUMMARY

In NUREG-1512, "Final Safety Evaluation Report Related to the Certification of the AP600 Standard Design," dated September 1998, the NRC approved the use of the Westinghouse NOTRUMP safety analysis code for the purpose of performing small break loss of coolant accidents (SBLOCA) for the AP600, in accordance with Appendix K of 10 CFR Part 50. In this evaluation, the staff identified that the NOTRUMP code did not include an explicit modeling of some phenomena that may affect the performance of the passive safety systems during the SBLOCA events. To compensate for the lack of an explicit momentum flux model in NOTRUMP, Westinghouse imposed penalties to the NOTRUMP code calculations to effectively inhibit the depressurization capability of the automatic depressurization system, and thus reduce the predicted safety injection flow, for the purpose of conservatively bounding the effect of momentum flux on the NOTRUMP predictions. This conservative approach was found to be acceptable for the AP600, due to several factors, including the following:

- Validation of the NOTRUMP code against AP600 separate effects and integral systems test programs.
- Large conservatisms inherent in the approved methodology (including Appendix K decay heat of 120 percent of nominal).
- Large safety margins of the passive safety systems, demonstrated in the confirmatory tests that were conducted by the NRC at the APEX test facility, at Oregon State University, and the ROSA-AP600 test facility, at the Japan Atomic Energy Research Institute.
- Large safety margins of the AP600 SBLOCA analysis results, which show that SBLOCA is a non-limiting LOCA event with no core uncover for break sizes up to, and including the double-ended rupture of a direct vessel injection line break (DEDVI), which disables 50 percent of the installed safety injection flow paths.

In the AP1000 Pre-Certification review, Westinghouse demonstrated, through the evaluation of important phenomena and through scaling of the AP600 tests, that the AP600 test program used to support Design Certification was applicable to the AP1000. This leads to the conclusion that the safety analysis codes that were validated and approved for the AP600 are then appropriate for use in performing AP1000 safety analysis in support of AP1000 Design Certification. In the AP1000 Design Control Document, submitted as part of the Westinghouse Application for Design Certification, it can be seen that the AP1000 plant behavior is similar to the AP600, and the performance of the AP1000 safety systems demonstrate margin to the regulatory limits.

One of the considerations in the approval of the NOTRUMP code for AP1000 was the Westinghouse commitment to perform a supplemental analysis of the AP1000 SBLOCA event, for the period of time in the transient when phenomena, such as momentum flux and hot leg / upper plenum entrainment, could affect the predicted analytical results from the NOTRUMP code. This supplemental analysis is performed with a version of the WCOBRA-TRAC computer code with models and correlations to predict important phenomena during the ADS-4 IRWST initiation Phase of an AP1000 SBLOCA are included. The reason for using the WCOBRA-TRAC code is that this code is a modern, state-of-the-art analysis code that models the phenomena that were not explicitly modeled in NOTRUMP. The purpose of this supplemental

analysis is to demonstrate that NOTRUMP provides a conservative simulation of ADS-4 venting and the onset of IRWST injection for AP1000.

This report provides a description of the supplemental analysis model, and includes validation of this model against suitable test data. It is shown that this model performs a reasonable simulation of a suitable test performed at the APEX test facility. This model is then used to perform plant calculations. The results of these plant calculations are then compared to the NOTRUMP calculations presented in Chapter 15 of the AP1000 Design Control Document. Based on a comparison of these calculations to the DCD analyses, it is demonstrated that the NOTRUMP DCD analyses provide a conservative prediction of the ECCS performance of the AP1000. It is concluded that the NOTRUMP DCD calculational approach compensates for the lack of explicit phenomenological modeling in NOTRUMP (such as momentum flux and upper plenum / hot leg entrainment) that could affect the predictions of the SBLOCA accident. Large margin to regulatory limits are demonstrated in the analytical results of the SBLOCA events for AP1000.

1 INTRODUCTION

Westinghouse Electric Company has designed an advanced 600 MWe nuclear power plant called the AP600. The AP600 uses passive safety systems to enhance plant safety and to satisfy U.S. licensing requirements. The use of passive safety systems provides significant and measurable improvements in plant simplification, safety, reliability, investment protection, and plant costs. These systems use only natural forces such as gravity, natural circulation, and compressed gas to provide the driving forces for the systems to adequately cool the reactor core following an accident. The AP600 received Design Certification by the Nuclear Regulatory Commission (NRC) in December 1999.

To further improve AP600 economics, Westinghouse initiated development of the AP1000 standard nuclear reactor design, with an output of approximately 1000 MWe, based upon the AP600 design. The design features of the plant, including the passive safety systems, have been selected to preserve key features and performance characteristics embodied in the AP600. By preserving the design basis of the AP600 in the AP1000, Westinghouse seeks to preserve the licensing basis of the plant as well. The AP1000 passive safety injection systems are shown in Figure 1-1.

The AP1000 is a Westinghouse advanced reactor designed to enhance plant safety with accident mitigation features that, once actuated, depend only on natural forces, such as gravity and natural circulation, to perform all required safety functions.

The AP1000 primary system is a two-loop design. Each loop contains one hot leg, two cold legs, and one steam generator (SG) with two canned motor reactor coolant pumps (RCPs) attached directly to the SG outlet channel head. The passive safety systems comprise the following:

- Two full-pressure core makeup tanks (CMTs) that provide borated makeup water to the primary system at full system pressure.
- Two accumulators (ACCs) that provide borated water to the reactor vessel if the primary pressure ≤ 700 psia.
- A passive residual heat removal (PRHR) heat exchanger (HX), comprised of a C-shaped tube bundle submerged in the in-containment refueling water storage tank (IRWST), that can remove heat from the primary system at full system pressure.
- The automatic depressurization system (ADS), which is comprised of a set of valves connected to the reactor coolant system (RCS) at the pressurizer steam space and the two hot legs. The valves connected to the pressurizer vent to the IRWST through a sparger. The valves connected to the hot leg vent to the containment. These valves are opened sequentially to provide controlled depressurization of the primary system.
- An IRWST that provides a large source of core cooling water, which drains by gravity after the ADS has actuated.
- A passive containment cooling system (PCS) that utilizes the AP1000 steel containment shell to transfer heat to the environment (ultimate heat sink).

Westinghouse submitted the “AP1000 PIRT and Scaling Assessment” (Reference 2) report to the NRC. The report provides Phenomena Identification and Ranking Tables (PIRT) for the AP1000 and demonstrates through scaling that the AP600 test program is applicable to the AP1000 and sufficiently covers the range of conditions expected for the AP1000. The report concludes that the AP600 test program provides a test database sufficient for code validation for AP1000 in accordance with 10CFR Part 52. The Reference 2 PIRT increases the importance of some post-ADS phenomena.

This report documents the approach to supplement the NOTRUMP code approved for AP600 in its application to AP1000 Design Certification by using WCOBRA/TRAC to predict the ADS-4 IRWST initiation phase.

Section 2 provides the validation of the WCOBRA/TRAC code for predicting phenomena during ADS-4 operation and addresses the acceptability of the WCOBRA/TRAC code for the analysis of AP1000 loss-of-coolant accident (LOCA) events during this phase. Section 3 provides an analysis of AP1000 during this phase. Section 4 provides conclusions regarding the capability of NOTRUMP to conservatively predict AP1000 small break LOCA transients.

1.1 NOTRUMP APPLICATION TO PASSIVE PLANT SMALL BREAK LOSS-OF-COOLANT ACCIDENT ANALYSIS

1.1.1 Background

The NOTRUMP code used for the AP600/AP1000 calculations consists of the modeling features that meet the requirements of Appendix K to 10CFR Part 50. The NOTRUMP code was previously approved by the NRC for small break LOCA (SBLOCA) analyses on conventional Westinghouse Pressurized Water Reactors (PWRs). The acceptance criteria for Emergency Core Cooling Systems (ECCS) for light-water nuclear power reactors, given in 10CFR50.46 (Reference 1), require that ECCS performance be calculated in accordance with an acceptable evaluation model. Two approaches may be taken to demonstrate that an acceptable model has been applied to an ECCS design. In one approach (commonly referred to as a “best estimate”), the evaluation model must contain sufficient supporting justification to show that the analytical technique realistically describes the behavior of the reactor system during a LOCA. This necessitates comparisons to applicable experimental data along with identification and assessment of uncertainty in the analysis methods and inputs so that the uncertainty in the calculated results can be estimated. This uncertainty must then be accounted for in subsequent calculations. Alternatively, an ECCS evaluation model may be developed in conformance with the required and acceptable features of 10CFR Part 50, Appendix K, and ECCS evaluation models. Westinghouse chose to demonstrate the acceptability of the SBLOCA response of the AP600 passive reactor design using an Appendix K ECCS evaluation model.

To support this effort, a version of the NOTRUMP code, modified for the AP600 application, was developed and is documented in WCAP-14807, "NOTRUMP Final Verification and Validation Report for AP600" (Reference 3). Modifications performed to the basic NOTRUMP model enabled proper analysis of the AP600 and the supporting test matrix. A summary of the features added to NOTRUMP, which comprises the AP600 version (notrump-ap600), is as follows:

- SIMARC (SIMulator Advanced Real-time Code) drift flux methodology implementation
- General drift flux model modifications
 - Modified Yeh drift flux correlation for use with the SIMARC drift flux method
 - Inclusion of general droplet flow correlation when void fractions are between 0.95 and 1.0 when using the improved TRAC-PF1 flow regime map
 - Modification of the bubbly and slug flow distribution parameter (C_0)
- Use of a net volumetric flow-based momentum equation
- Implementation of the EPRI/Flooding vertical drift flux model
- Modifications to allow over-riding of the default NOTRUMP contact coefficient terms for formation of regions
- Implementation of internally calculated liquid reflux flow links
- Implementation of the Mixture Level Overshoot model
- Modified Bubble Rise/Droplet Fall model logic
- Activation of the simplified pump model
- Implicit Fluid Node Gravitational Head model implementation
- Horizontal Levelizing model implementation
- Revised Unchoking model implementation
- Implementation of a revised Condensation heat link model
- Implementation of Zuber Critical Heat Flux model
- Revised Two-Phase Friction Multiplier logic
- Addition of the Henry-Fauske/HEM Critical Flow Correlation
 - The Henry-Fauske subcooled correlation used for a subcooled donor node

- Homogeneous equilibrium model correlation used for superheated donor node and saturated donor node at quality greater than []^{a,c}
- For a saturated donor node below this transition quality, the minimum of the Henry-Fauske saturated correlation and a quality-adjusted HEM value is used
- Improved Flux Node Stacking model logic
- Revised iteration method for Transition Boiling Correlation in metal node heat links

NOTRUMP was validated against the AP600 test data that includes all the unique features of the AP600 passive safety system design. This validation includes the Automatic Depressurization System (ADS), Core Makeup Tank, and integrated system response from SPES-2 and OSU APEX. The AP1000 Code Applicability Report (Reference 4) discusses NOTRUMP and its application to the AP1000 SBLOCA analysis, providing the basis for NRC review of NOTRUMP for the AP1000 design. The purpose for the integral systems tests was to provide the database to cover the range of applicability for NOTRUMP, as well as other codes; the NOTRUMP code was compared to the separate effects AP600 test results and both integral systems tests.

In the AP1000 Pre-Certification review, the NRC concurred with Westinghouse that the AP600 test facilities used to support AP600 Design Certification are sufficiently sealed to AP1000 such that the test data from these facilities are applicable to AP1000 (Reference 5). Therefore, analysis codes validated against these tests can be used to perform analysis of the AP1000.

For application to the AP1000 plant design, the same NOTRUMP computer code, as approved for AP600 analyses, is utilized with the code error corrections, as reported and assessed in the annual 10CFR50.46 reporting letters. In addition, to counteract the lack of momentum flux, the ADS-4 resistance is increased in accordance with the result of a stand-alone momentum flux model of the ADS-4 flow path.

1.1.2 PIRT Issues

A review of the PIRT was performed in Section 2.0 of the AP1000 PIRT and Scaling Assessment report (Reference 2) and concluded the following related to important SBLOCA phenomena:

- ADS-4 subsonic, two-phase pressure drop should be raised to a high importance.
- Upper plenum/hot leg entrainment during the post-ADS period should be raised to a high importance level.
- Pressurizer surge line countercurrent flow/flooding during the ADS-IRWST period should be raised to a medium importance level.

The above items are not really new phenomena but rather the change in rankings is a result of the lessons learned from the AP600 test and analysis program. The issues identified above apply to both the AP600 and AP1000 designs and do not constitute new issues.

1.2 USE OF WCOBRA/TRAC TO SUPPLEMENT NOTRUMP

Items raised in importance level in the AP1000 PIRT highlight previously identified issues regarding NOTRUMP predictions of the ADS-4 IRWST injection phase phenomena. In addition to the steps taken within NOTRUMP to address deficiencies, a supplementary analysis using WCOBRA/TRAC is performed to demonstrate the conservative nature of NOTRUMP results. This supplemental calculation is intended to demonstrate that:

- The thermal-hydraulic models in NOTRUMP, with the adjustment to increase ADS Stage 4 flowpath resistance, provide an appropriate, conservative prediction of the AP1000 small break LOCA ECCS performance.
- The injection of water from the IRWST does not occur prematurely in NOTRUMP.

In this way, the issues in ADS Stage 4 IRWST initiation predictions associated with the NOTRUMP predictive capabilities are addressed through an analysis that uses more suitable models for highly ranked PIRT phenomena.

This supplemental calculation to support the adjusted NOTRUMP result is performed using the “AP” version of the WCOBRA/TRAC computer code, which contains the detailed models necessary to calculate the pertinent phenomena during this phase of the transient. The phenomena which led to the imposition of an IRWST level penalty in the AP600 licensing analysis, and the adjustment to increase ADS Stage 4 line resistance in the AP1000 NOTRUMP small break LOCA analysis cases are momentum flux two-phase pressure drop in the ADS-4 flowpaths and entrainment in the hot legs and ADS-4 flowpaths. With its more detailed models, WCOBRA/TRAC-AP provides a physically-based calculation of these phenomena.

The use of the WCOBRA/TRAC analysis tool as a supplemental calculation is a desirable approach as it leverages the use of state of the art technology to address the identified deficiencies in the NOTRUMP code. The methodology involves starting the WCOBRA/TRAC calculation at the time of the ADS-4 actuation setpoint. Following the opening of the ADS-4 valves, the flow through the ADS-4 valves for AP1000 is initially choked. The WCOBRA/TRAC simulations, which include a complete treatment of momentum flux, are utilized to confirm and demonstrate the overall conservative nature of the NOTRUMP results.

The phase separation at Tee junctions in the hot legs connected to the ADS-4 paths was identified as an issue for NOTRUMP due to the use of an ad-hoc model. Entrainment/phase separation can impact the flow quality encountered at the ADS-4 discharge valves and affect the IRWST injection flow. The ad-hoc model to account for the effects of entrainment/phase separation was utilized in the NOTRUMP analysis of the AP600 and integral test facilities and was determined to have a negligible impact on calculated results. For application to the AP1000 design, WCOBRA/TRAC-AP contains specific models to determine the onset of entrainment into a branch line and the quality present in the branch line, as well as entrainment within the reactor vessel upper plenum.

Due to the issues with NOTRUMP ADS-4 flowpath modeling, increases in ADS-4 resistance were implemented on AP1000 to account for the lack of a momentum flux model in the NOTRUMP code. The

resistance increases utilized were based on the results of a detailed stand-alone momentum flux model of the ADS-4 flowpaths as discussed in the response to AP600 RAI 440.796, Part a. As such, with the implementation of the ADS-4 resistance increases, it is expected that the pertinent phenomena were captured.

The WCOBRA/TRAC “AP” code version used in the AP1000 small break LOCA supplemental calculations is validated for this application against the ADS Stage 4 IRWST initiation phase of OSU integral effects facility Test SB18. The WCOBRA/TRAC “AP” code version includes models for important processes such as entrainment to predict the OSU integral effects test during the ADS-IRWST transition phase. As the OSU integral effects tests have been shown to be acceptably scaled to AP1000, the test-validated models serve as the basis on which the code will be used to predict the behavior of the AP1000 during the ADS-IRWST transition phase. Initial and boundary conditions are supplied from the test data and the NOTRUMP simulation of the tests to accomplish the validation. The use of WCOBRA/TRAC with its more detailed models for momentum flux and entrainment provides more in-depth understanding of these phenomena to support the treatment of ADS-4 resistance in NOTRUMP analysis of the AP1000.

Among the phenomena which are important to AP1000 performance during the ADS-4 IRWST initiation phase are those that deal with flow patterns in the hot legs and the removal of liquid and vapor from the hot legs into the ADS-4 flowpaths. The models and correlations that have been added to the large break LOCA version of WCOBRA/TRAC to calculate these phenomena for horizontal pipe flow are presented in Section 2, together with results of the separate effects test validation calculation performed.

1.3 REFERENCES

1. 10CFR50.46, “Acceptance Criteria for Emergency Core Cooling Systems for Light Water Cooled Nuclear Power Reactors.”
2. WCAP-15613, “AP1000 PIRT and Scaling Assessment,” Westinghouse Electric Company LLC, February 2001.
3. WCAP-14807, Revision 5, “NOTRUMP Final Verification and Validation Report for AP600,” Fittante, R. L., et al., 1998.
4. WCAP-15644, “AP1000 Code Applicability Report,” May 2001.
5. NRC Letter Lyons to Cummins, “Applicability of AP600 Standard Plant Design Analysis Codes, Test Program and Exemptions to the AP1000 Standard Plant Design,” dated 3/25/2002.

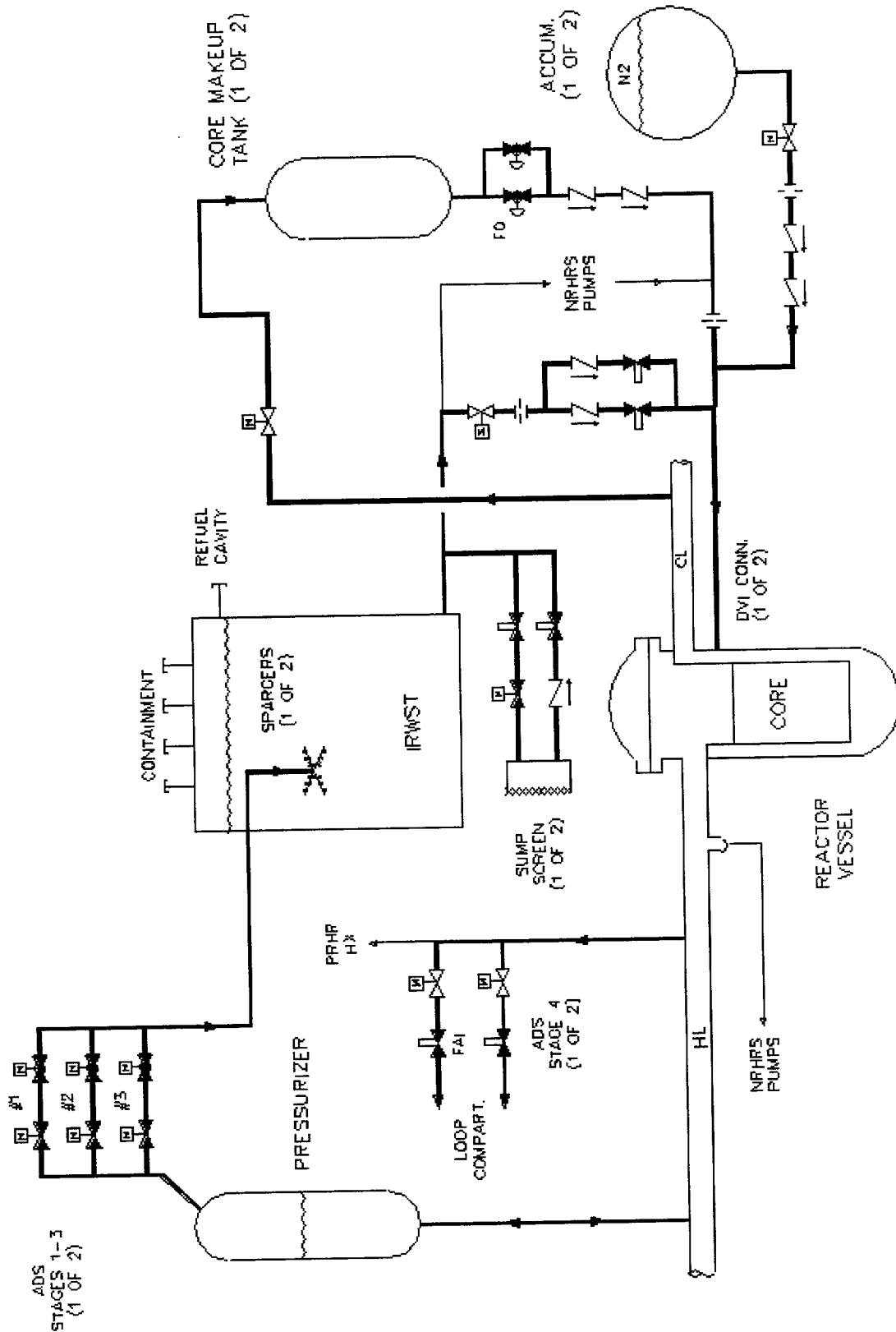


Figure 1-1 AP1000 Passive Safety Injection Flow Schematic

2 WCOBRA/TRAC APPLICATION TO THE ADS-4 IRWST INITIATION PHASE

2.1 INTRODUCTION

The Automatic Depressurization System (ADS) Stage 4 in-containment refueling water storage tank (IRWST) initiation phase of the small break LOCA event for AP1000 is characterized by the following phenomena: significant momentum flux pressure drop in the ADS-4 flowpaths, entrainment in the reactor vessel and hot legs, and draining of the pressurizer and surge line mass. To account for these phenomena, a modified version of WCOBRA/TRAC-MOD7A designated as "WCOBRA/TRAC-AP" is used to supplement NOTRUMP. In comparison to the NOTRUMP code, WCOBRA/TRAC provides a more detailed model of the physical processes encountered during these conditions as follows:

The momentum equation as solved in the TRAC components used for ADS Stage 4 (ADS-4) piping contains all significant terms, including the momentum flux terms, as discussed in Section 2-5 of WCAP-12945-P-A (Reference 3).

COBRA channels are used to model the hot legs in the AP1000 supplemental calculation. Within the hot legs, horizontal flow regimes are identified using the Taitel-Dukler flow map (Reference 1). The Ishii-Grolmes (Reference 2) criteria are used to predict the onset of entrainment off the horizontal surface. Entrainment into the ADS Stage 4 offtake piping atop the hot legs is determined using a Froude-number relationship. In the event that entrainment is predicted to occur, the quality in the ADS-4 pipe is calculated using a correlation for a vertical upward branch connection.

Prediction of the mixture swell in a WCOBRA/TRAC channel depends on interfacial drag between the vapor and liquid phases. Models and correlations are available that calculate interfacial shear in both vertical and horizontal flows. Models for flow regime transition and bubble rise in the code allow for phase separation and entrainment.

Subsection 2.2 is intended to describe the models and correlations that have been included in the WCOBRA/TRAC-AP code to enable it to compute the important phenomena during the ADS-4 IRWST initiation phase of a small break LOCA in AP1000. The subsection presents the code features for modeling horizontal flow behaviors and for calculating the entrainment into the branch line at a "TEE" vertical connection, such as the ADS-4 offtake piping atop the hot legs in the AP1000 design. The performance of the code in predicting the horizontal flow behaviors observed in a separate effect test conducted at atmospheric pressure is also presented. Subsection 2.3 presents the OSU APEX facility integral systems validation using Test SB18.

2.2 FLOW MODELS AND VALIDATION

Horizontal stratification, counter-current flow and counter-current flow limitations (CCFL), and transition between flow regimes in WCOBRA/TRAC depend on interfacial drag between phases in lateral flow. WCOBRA/TRAC-AP allows for horizontal flow regime modeling using correlations for drag to allow stratification. Section 15 of Volume 3 of WCAP-12945-P-A (Reference 3) reported an assessment and calculations of flow in horizontal pipes represented by COBRA channels. The evaluation showed that

WCOBRA/TRAC has the capability to predict counterflow and CCFL at horizontal locations within the reactor coolant system. A further assessment of WCOBRA/TRAC-AP presented in subsection 2.2.2 shows it capable of predicting horizontal stratified flow behaviors with the accuracy necessary for the ADS-4 IRWST initiation phase of small break LOCA analyses for AP1000.

Horizontal flow regimes and the transition criteria from one regime to another have been the subjects of several studies. The most notable result is the Taitel-Dukler flow regime map for horizontal flows (Reference 1), which takes into account both pipe diameters and fluid properties on each of the flow pattern transitions. The Taitel-Dukler flow regime map and transition criteria include a dependence on pipe diameter. This provides a means of examining the scale diameter dependence of the WCOBRA/TRAC models for horizontal flow.

Subsection 2.2.2 presents the results of WCOBRA/TRAC simulations of tests reported in Lim (Reference 4) investigating the horizontal two-phase flow in a channel. The wavy or stratified flow regime condensation and pressure drop data were obtained, together with steam flowrate and water layer thickness data at various locations in a four-foot long experimental channel.

The carry over of droplets from the upper plenum into the hot legs by the flow of steam above the mixture level is assigned a medium (M) ranking for the ADS-4 operation time period in the AP1000 small break LOCA PIRT in WCAP-15613 (Reference 5). Entrainment in the flow from the hot legs into the ADS-4 piping is assigned a high (H) ranking for AP1000, increased from the medium (M) ranking of AP600. This carryover by drops entrained in the steam is modeled in detail in WCOBRA/TRAC-AP.

2.2.1 Models and Correlations

2.2.1.1 Liquid Entrainment Onset Correlations

General Form of Entrainment Onset Correlations into Branch Pipes

The general form of most entrainment onset correlations for offtake pipes found in the literature is as follows:

$$Fr_g \left(\frac{\rho_g}{\rho_l - \rho_g} \right)^{0.5} = C_1 \left[\frac{z_b}{d} \right]^{C_2} \quad (2-1)$$

The key elements of this correlation form consist of the Froude number (Fr), density ratio ($\rho/\Delta\rho$), and a geometric ratio (z/d) of entrainment onset height (z) to offtake diameter (d). The coefficient C_1 and exponent C_2 are functions of the orientation and geometry of the offtake.

Side Offtake Orientation

Craya (Reference 6) developed a theoretical onset of liquid entrainment for discharge from a side offtake neglecting viscosity and surface tension effects. Craya's theoretical result was obtained by treating the offtake as a potential flow point sink. From this he arrived at onset correlations for orifice-type offtakes and slot-type offtakes as follows:

$$Fr_g \left(\frac{\rho_g}{\rho_\ell - \rho_g} \right)^{0.5} = C_1 \left[\frac{z_b}{d} \right]^{2.5} \quad \text{for orifice} \quad (2-2)$$

$$Fr_g \left(\frac{\rho_g}{\rho_\ell - \rho_g} \right)^{0.5} = C_1 \left[\frac{z_b}{d} \right]^{1.5} \quad \text{for slot} \quad (2-3)$$

Note that the form is similar for orifice and slot, however, the exponents for the geometric ratio (z/d) are 2.5 and 1.5, respectively.

Top Offtake Orientation

Rouse (Reference 7) developed a correlation for onset of liquid entrainment for top offtake configurations as follows:

$$Fr_g \left(\frac{\rho_g}{\rho_\ell - \rho_g} \right)^{0.5} = C_1 \left[\frac{z_b}{d} \right]^2 \quad (2-4)$$

It is important to note here that the exponent for the geometric ratio is 2.0, which is different from those obtained by Craya for side offtake orientations. Ardron and Bryce (Reference 8) provide a summary of exponents and coefficients recommended for use in Froude number type correlations in the open literature. For the top offtake orientation, Ardron and Bryce propose the vertical upward branch correlation of Schrock et al. (Reference 9) to compute the discharge flow quality in the offtake branch when entrainment occurs as presented in subsection 2.2.1.5.

Issues with General Correlation Form for Entrainment

While it appears from several data sets that the general correlation form for entrainment onset provides reasonable agreement or representation, there is room for improvement in several areas:

1. Viscous effects are neglected. Interfacial shear stress between the gas and liquid phases would be expected to play some role in liquid entrainment such as found in the work of Ishii and Grolmes (Reference 2). However, there is no viscosity term or viscosity-related non-dimensional parameter in the general correlation.
2. Liquid surface tension and intermolecular force effects are neglected. It is expected that surface tension is important in resisting the onset of entrainment. Intermolecular liquid forces are

probably involved in a liquid siphoning-type effect that is seen in experiments once entrainment onset is reached.

3. The offtake branch, orifice, or slot is treated in most cases (with the exception of the work by Soliman and Sims [Reference 10]) as a point sink. This treatment may be appropriate for very large tanks or reservoirs with relatively small diameter offtakes, but may not be so good for reactor coolant piping connected to a branch pipe.
4. The potential flow solution treatment such as that of Craya and others neglects liquid velocity in liquid phase streamlines and even neglects the very presence of the liquid phase itself in obtaining a potential flow solution for the flowing gas field. Again, neglecting liquid velocity in large reservoirs or tanks may be reasonable, but it would be a more difficult case to make for reactor coolant piping connected to a breakflow path.

A liquid entrainment correlation for flow into branch pipes using a more realistic potential flow, Bernoulli type solution which addresses the concerns outlined earlier (i.e., viscosity, surface tension, etc.) has not been developed and correlated against data sets. Therefore, [

] ^{a,c}

2.2.1.2 Horizontal Flow Regime Map

Model Basis

Predicting the flow regime for two-phase flow in horizontal pipes is important in representing the ADS-4 IRWST initiation phase of a small break LOCA transient for AP1000; the realistic, mechanistic model of Taitel and Dukler (Reference 1) for predicting flow regime transitions provides this capability in WCOBRA/TRAC-AP. This physically based, semi-theoretical model provides an unambiguous analytical prediction of the transition between horizontal flow regimes. It is a preferred approach because it takes into account the different influences of pipe diameter and fluid properties on each flow pattern transition.

Five flow regimes (Reference 1) are considered in this model: intermittent (slug and plug), stratified smooth, stratified wavy, dispersed bubble, and annular/annular dispersed liquid flow. Transitions between horizontal pipe flow regimes are determined using the following dimensionless groups:

$$X = \left[\frac{(dP/dx)_l^S}{(dP/dx)_v^S} \right]^{1/2} \tag{2-5}$$

$$T = \left[\frac{|(dP/dx)_l^S|}{(\rho_l - \rho_v)g \cos \delta} \right]^{1/2} \tag{2-6}$$

$$F = \sqrt{\frac{\rho_v}{(\rho_\ell - \rho_v)}} \frac{U_v^s}{\sqrt{Dg \cos \delta}} \quad (2-7)$$

$$K = \left[\frac{\rho_v U_v^{s2} U_\ell^s}{(\rho_\ell - \rho_v) g_\ell v_\ell \cos \delta} \right]^{1/2} \quad (2-8)$$

Each quantity in the above groups is available from the prevailing flow conditions.

The horizontal tube flow regime flow transition boundaries are shown in Figure 2-1. Specific transitions are controlled by the dimensionless groups as follows:

Stratified to annular	X, F
Stratified to intermittent	X, F
Intermittent to dispersed bubble	X, T
Stratified smooth to stratified wavy	X, K
Annular dispersed liquid to intermittent and to dispersed bubble	X

where:

- X is the phasic pressure drop ratio (Lockhart and Martinelli, 1949) where $(dP/dx)^s$ designates the pressure drop of one phase flowing alone
- T considers the ratio of turbulent to gravity forces acting on the gas
- F is the Froude number times the square root of the density ratio
- K is the product of F and the square root of the superficial Reynolds number of the liquid
- δ is the angle at which the pipe is inclined to the horizontal

In Reference 1, Taitel-Dukler show that predictions from this model agree very well with data for cocurrent flow through pipes.

Model as Coded

Flowrates, fluid conditions and properties, pressures, and diameter are available from WCOBRA/TRAC input and output for a given timestep. The VESSEL channel formulation calculates the flow between two cells for three separate fields: continuous liquid, continuous vapor, and entrained liquid droplets.

The fluid properties [

] ^{a,c}

[

] ^{a,c}

Next, the equilibrium liquid level $\left(\frac{h_L}{D}\right)$ is calculated for the $\delta = 0$ case from the Taitel-Dukler function that is graphically represented in Figure 2-2.

Referring to Figure 2-1, $X = 1.6$ is the limit line B.

For Curve A, Froude number (F) is calculated [

] ^{a,c}

[

] ^{a,c}

Lastly, curve D is defined.

On curve D, parameter T, which is the ratio of turbulent force to the gravity force acting on gas, is calculated from:

$$T = \left[\frac{8\bar{A}_G}{\bar{S}_i \bar{U}_L^2 (\bar{U}_L \bar{D}_L)^{-0.2}} \right]^{1/2} \quad (2-12)$$

[

] ^{a,c}

By equating

$$T = \left[\frac{4 C_{FF} (Re_f^{-0.2}) (\rho_l U_L^S)^2}{D \cdot 2 \rho_l} \right]^{1/2} \frac{1}{(\rho_l - \rho_v) g} \quad (2-13)$$

and solving for, U_L^S as,

$$U_L^S = \frac{1}{\rho_l} \left[\frac{T^2 \cdot (\rho_l - \rho_v) g}{\frac{2 C_{FF}}{D \rho_l} Re_f^{-0.2}} \right]^{1/2} \quad (2-14)$$

The gap superficial velocities are compared against $X = 1.6$, Equations 2-13 and 2-14, to determine the flow regime. Currently, four flow regimes, namely, stratified, annular dispersed liquid, dispersed bubble, and intermittent are recognized.

Scaling Considerations

Pipe diameter is one of the parameters that affects the flow regime transitions in the Taitel-Dukler horizontal flow regime map, through its presence in the "F" term. Therefore, the method is general, and may be used with confidence to predict flow regimes at various scales of operation; at larger diameters the regime boundaries are displaced relative to their location with a small pipe diameter.

Likewise, the use of prevailing fluid properties in this model considers variations in pressure, temperature, and quality such as those that occur during the ADS-4 IRWST initiation phase of a small break LOCA transient.

Conclusions

The Taitel-Dukler method for determining flow regime transitions in horizontal two-phase flow has been incorporated into WCOBRA/TRAC-AP. This method provides a mechanistic prediction of flow regime based on realistic theoretical considerations. The agreement with concurrent flow data is judged to be very good in Reference 1.

2.2.1.3 Horizontal Stratified Interfacial Drag

Model Basis

This model is based on stratified flow steam-water data in a rectangular channel (Jensen, Reference 11). The model is mechanistically based on the turbulent motion of the liquid near the interface. In addition, the interfacial shear and interfacial heat transfer are consistent with each other.

The interfacial friction factor K is computed according to Equations 5.5 and 5.6 of Jensen (Reference 11):

$$K_{ix,vl,HS} = 0.5 \cdot f_i \cdot |W_{vl}| \cdot A_{HS} / \Delta Z \quad (2-15)$$

where:

A_{HS} is the vapor/liquid stratified interface area

$$f_i = 0.01 \quad \text{if } U' < 17.6 \quad (2-16)$$

$$= 14.6 \times 10^{-6} (U')^{1.8} \quad \text{if } U' \geq 17.6 \quad (2-17)$$

where:

$$U' = \frac{U_v - U_\ell}{1.414 \left(\frac{\sigma(\rho_\ell - \rho_v)g}{\rho_\ell^2} \right)^{1/4}} \quad (2-18)$$

U_v and U_ℓ are the vapor and liquid velocities, respectively.

Model as Coded

Note that the friction factors are discontinuous at $U' = 17.6$ and also between developed and undeveloped flows.

The horizontal stratification is checked []^{a,c} to identify the flow regime according to the Taitel-Dukler (Reference 1) flow regime map. The parameters used in the determination of the horizontal flow regime are the total liquid superficial velocity, total vapor superficial velocity, gap average vapor density, gap average liquid density, the vapor viscosity, liquid viscosity, total gap void fraction, hydraulic diameter of flow channel, and mixture level.

The drag term for the horizontally stratified flow is modified in []^{a,c}

[]^{a,c}

Conclusions

The ability to identify horizontal stratified flow regimes has been implemented in WCOBRA/TRAC-AP, together with a method for calculating the interfacial drag for two-phase flow in these regimes.

2.2.1.4 Entrainment in Horizontal Stratified Flow

Model Basis

When horizontal stratification is identified, the Ishii-Grolmes (Reference 2) criteria are checked; if the criteria are satisfied, the calculation of entrainment off of the horizontal surface is enabled.

Ishii and Grolmes describe entrainment in horizontal cocurrent flow as the stripping of drops from the top of waves. They describe four mechanisms, but the shearing off of the top of roll waves by turbulent gas flow is expected to be significant for the ADS-4 IRWST initiation. Ishii and Grolmes state that this mechanism is valid for liquid $Re > 160$ in horizontal concurrent flow. For roll wave entrainment, Ishii and Grolmes provide two correlations based upon Re :

For $Re > 1635$:

$$\frac{\mu_{\ell} U_g}{\sigma} \sqrt{\frac{\rho_g}{\rho_{\ell}}} \geq N_{\mu}^{0.8} \text{ for } N_{\mu} < \frac{1}{15}$$

$$\frac{\mu_{\ell} U_g}{\sigma} \sqrt{\frac{\rho_g}{\rho_{\ell}}} \geq 0.1146 \text{ for } N_{\mu} < \frac{1}{15}$$

For $Re < 1635$:

$$\frac{\mu_{\ell} U_g}{\sigma} \sqrt{\frac{\rho_g}{\rho_{\ell}}} \geq 11.78 N_{\mu}^{0.8} Re_{\ell}^{-1/3} \text{ for } N_{\mu} < \frac{1}{15}$$

$$\frac{\mu_{\ell} U_g}{\sigma} \sqrt{\frac{\rho_g}{\rho_{\ell}}} \geq 1.35 Re_{\ell}^{-1/3} \text{ for } N_{\mu} < \frac{1}{15}$$

Re is based upon liquid film thickness, U_g is the minimum gas velocity for entrainment to occur, and N_{μ} represents viscosity number.

The entrainment source term in the continuity cell is evaluated when the Ishii-Grolmes criteria are satisfied for gap flow connections according to the model used by Hanratty (Reference 12):

$$Re = K_a U_v \sqrt{\rho_v \rho_{\ell}} \text{ (lb/s - ft}^2\text{)} \quad (2-19)$$

where:

$K_a = 0.2$ is currently used.

The size of the entrained droplets is determined by Tatterson's (Reference 13) model:

$$D_e = 0.0112 \left(\frac{D_g \sigma}{0.5 f_i \rho_v U_v^2} \right)^{1/2} \quad (2-20)$$

This correlation is for vertical annular flow, and the characteristic length is the pipe diameter. It will be implemented here by assuming that the characteristic length is the hydraulic diameter (D_g) of the gap above the mixture elevation.

De-entrainment onto the interface is assumed to be dominated by the terminal velocity of the droplets. The settling velocity (V_s) is the minimum of the Stokes flow solution Equation 9.13 (Wallis, Reference 14):

$$V_{s,1} = \frac{1}{18} \frac{D_e^2 g (\rho_\ell - \rho_v)}{\mu_\ell} \quad (2-21)$$

and the turbulent flow solution Equation 12.29 (Wallis):

$$V_{s,2} = \sqrt{\frac{D_e (\rho_\ell - \rho_v) g}{\rho_v}} \quad (2-22)$$

where:

D_e is the average diameter of the entrained drops in the vapor above the mixture. The net flux of droplets into the mixture is:

$$R_{de} = \rho_\ell \alpha_e (V_s - U_{v,ver}) \quad (2-23)$$

where:

$U_{v,ver}$ is the average vertical vapor velocity above the mixture and $V_s = \min(V_{s,1}, V_{s,2})$.

Model as Coded

As previously described, the horizontal stratified flow model is activated []^{a,c} to identify the flow regime according to the Taitel-Dukler flow regime map. The parameters used in the determination of the horizontal flow regime are the total liquid superficial velocity, total vapor superficial velocity, gap average vapor density, gap average liquid density, the vapor viscosity, liquid viscosity, total gap void fraction, hydraulic diameter of flow channel, and mixture level.

Within the structure of WCOBRA/TRAC, entrainment must be treated []^{a,c}

The

entrainment and de-entrainment source calculations are then performed using the techniques described earlier in this section.

Scaling Considerations

In WCOBRA/TRAC-AP, entrainment is modeled [

] ^{a,c}

Conclusions

The ability to identify horizontal stratified flow regimes has been implemented in WCOBRA/TRAC-AP, together with the calculation of entrainment at the vapor-liquid stratified interface for two-phase flow in these regimes.

2.2.1.5 Flow Regime Conditions Upstream of the ADS-4 Delivery Piping (Entrainment/Vapor Pull-through Model)

Model Basis

During the ADS-4 IRWST initiation phase of a small break LOCA event, flow in the hot leg pipes will eventually become two-phase and stratify. A stratified flow regime near or upstream of the ADS-4 valves may lead to liquid entrainment in the hot legs and in the ADS-4 delivery piping depending upon local characteristics such as the velocity of the gas phase and the height of liquid in the pipe relative to the ADS-4 branch elevation.

Nearly all entrainment onset correlations found in the literature were developed from stratified, potential flow, Bernoulli-type solutions. In these correlations, the Froude number (ratio of inertia to gravity forces) is usually a predominant term.

The general form of most entrainment onset correlations found in the literature is as follows:

$$Fr_k = \frac{U_k}{\sqrt{d \cdot g \frac{\Delta\rho}{\rho_k}}} = C_1 \left[\frac{Z_b}{d} \right]^{C_2} \quad (2-24)$$

where:

k indicates the continuous phase.

The key elements of this correlation form consist of the Froude number (Fr), density ratio $\Delta\rho/\rho_k$, and a geometric ratio (Z_b/d) of entrainment onset height (Z_b) to offtake diameter (d). The coefficient C_1 and exponent C_2 are functions of the orientation and geometry of the offtake.

Different offtake orientations lead to different values of C_1 and C_2 in the equation 2-24 for the flow.

The following exponent and multiplier values in the correlation form for entrainment are provided by Anderson (Reference 15):

$$C_1 = 0.35, C_2 = 2.50 \text{ for liquid entrainment into a top branch} \quad (2-25)$$

The above values are used in WCOBRA/TRAC-AP to predict the AP600 integral effects tests during the ADS-4 IRWST initiation phase.

When entrainment is predicted to occur, the quality in the offtake will differ from that in the donor cell. In WCOBRA/TRAC-AP, the discharge flow quality in the offtake branch is calculated by the following correlation as proposed by Ardron and Bryce (Reference 8):

Vertical upward branch, from Schrock et al., (Reference 9):

$$x = R^{3.25(1-R)^2} \quad (2-26)$$

where:

$$R = |h / Z_b|$$

and h is the distance between the branch pipe and the liquid surface,

Z_b is the critical distance at which the entrainment begins.

Model as Coded

The model as coded proceeds through a sequence of calculational steps to determine the entrainment from a channel in the hot leg pipes. [

] ^{a,c}

[

] ^{a,c}

Scaling Considerations

Ardron and Bryce (Reference 8) based their selections of correlations from a review of several series of tests carried out to study two-phase flow in offtake branches at top, bottom and central position connections to a larger diameter horizontal pipe containing stratified flow. In these experiments, pressures ranged from 0.2-6.2MPa. Ardron and Bryce concluded that this data base was adequate to assess the modeling of horizontal stratification entrainment to a PWR RCS loop pipe break.

Conclusions

Appropriate correlations are included in WCOBRA/TRAC-AP to provide the capability to calculate: (1) the onset of entrainment from the hot legs into the ADS-4 pipes and (2) the flow quality in the ADS-4 pipes during the ADS-4 IRWST initiation phase for a postulated AP1000 small break LOCA event.

2.2.1.6 Interfacial Heat Transfer in the Horizontal Stratified Regime

The horizontal stratified heat transfer model is utilized in a continuity cell where the horizontal stratified flow is identified in the connecting gap according to the Taitel-Dukler (Reference 1) flow regime map.

If the flow regime is determined to be annular-dispersed or dispersed bubble according to the Taitel-Dukler flow regime map, the appropriate interfacial heat/mass transfer is used.

Model Basis

The interfacial heat transfer model developed by Jensen (Reference 11) is mechanistically based on the turbulent motion of the liquid near the interface, and is consistent with the interfacial drag model. Equation 5.11 (Jensen) states:

$$\frac{Nu_x}{Pr_l^{0.5}} = 0.0405 \cdot \left(\frac{u^* \cdot x}{\nu} \right)^{1.1} \quad (2-27)$$

where:

$$Nu_x = \frac{h_{i\ell} \cdot x}{k_l}$$

$$u^* = \sqrt{\frac{\tau}{\rho_l}} = \sqrt{\frac{f_i \cdot \rho_v \cdot U_r^2}{2 \cdot \rho_l}} \quad (2-28)$$

where x is the lateral distance, τ is the interfacial shear stress, U_r is the relative velocity, and ν is the kinematic viscosity. Note that while this is not the final recommended correlation, it is not very different from the final version (Figure 5.24 of Jensen). The interfacial friction is obtained from the value without condensation (subsection 2.2.1.3), but needs to be adjusted to account for condensation. This is done by applying Equation 2.31 (Jensen, Reference 11) as follows:

$$\tau_c = \tau + \frac{\Gamma_c \cdot U_v}{144 \cdot g_c} \quad (2-29)$$

where the τ is in psia and the condensation rate (Γ_c) is in lb/ft²/s.

Rearranging Equation 2-27 yields,

$$h_{il} = 0.0405 \cdot k_l \cdot Pr_l^{0.5} \cdot \left(\frac{u^*}{\nu} \right)^{1.1} \cdot x^{0.1} \quad (2-30)$$

Model as Coded

Since h_{il} is a very weak function of the lateral distance x , the [

]^{a,c} (2-31)

The heat transfer coefficient h_{il} is then multiplied by the appropriate interfacial area to yield the condensation heat transfer coefficient (HASCL) as:

$$HASCL = h_{il} \cdot \text{Area}$$

where Area = continuity cell area as seen in Figure 2-3.

Conclusions

The ability to identify horizontal stratified flow regimes has been implemented in WCOBRA/TRAC-AP, together with a method for calculating the interfacial heat transfer for two-phase flow in these regimes. The capability of WCOBRA/TRAC-AP to predict the thermal conditions in the stratified horizontal two-phase flow regime is demonstrated by the test simulations shown in the following subsection.

2.2.2 Separate Effects Test Validation

The predicted performance of AP1000 during the ADS-4 IRWST initiation phase of a small break LOCA transient is influenced by the two-phase flow regime present in the horizontal hot leg pipes. In the WCOBRA/TRAC-AP computer code, the Taitel and Dukler flow regime map (Reference 1) is used to define the horizontal pipe flow regime. At the relatively low flowrates associated with ADS-4 operation during a small break LOCA, the horizontal two-phase flow is often in the stratified wavy and/or stratified smooth flow regimes.

Within WCOBRA/TRAC-AP logic, the horizontal flow regime is []^{a,c} the Taitel and Dukler regime map. If the path is determined to be stratified, the Jensen and Yuen model (Reference 11) is applied to calculate the interfacial drag and condensation that occurs; entrainment at the interface between gas and liquid is calculated when the Ishii-Grolmes criteria are satisfied (Reference 2). Because the interfacial drag and entrainment modeling for horizontal stratified flow are basic processes that are directly related to high-ranked items in the AP1000 small break LOCA PIRT given in WCAP-15613 (Reference 5), individual validation of each of these models is needed to confirm their accuracy. This is accomplished using the experimental WCOBRA/TRAC-AP simulations presented in the following sections.

Physical Processes

In the condition of a smooth, equilibrium-stratified flow, the wall resistance of the liquid is similar to that for open-channel flow and that of the gas is similar to closed-duct flow. Because the gas phase velocity is much larger than the velocity at the gas-liquid interface, the gas side interfacial shear stress is evaluated using the equation for gas wall shear. The interfacial drag is thus easily defined theoretically.

Entrainment from the liquid film at the stratified flow two-phase interface is accounted for in determining the mass inventory of the RCS during the ADS-4 IRWST initiation phase of a small break LOCA in AP1000.

WCOBRA/TRAC-AP Models

Phenomena associated with the ADS-4 IRWST initiation phase of a small break LOCA—the interfacial drag, entrainment, and condensation—are discussed in this section.

Interfacial Drag

The models and correlations used to calculate interfacial drag in horizontal stratified flow are described in subsection 2.2.1.3. In particular, the work reported by Jensen and Yuen (Reference 11) is used.

Entrainment

Subsection 2.2.1.4 describes the models and correlations in WCOBRA/TRAC-AP that are used to calculate the horizontal flow processes.

In general, entrainment is the result of interfacial shear between vapor and a liquid film. In WCOBRA/TRAC-AP, liquid is moved from the continuous liquid field to the entrained field when the interfacial shear forces acting on the liquid are sufficient. In de-entrainment, liquid is moved from the entrained field to the continuous liquid field. A summary of the applicable models in WCOBRA/TRAC-AP is as follows:

- Entrainment in Film Flow

WCOBRA/TRAC determines film entrainment rates by comparing the entrainment rate based on a stable film flow to an empirical entrainment rate based on the work of Walley (Reference 17). Refer to subsection 4-6-2 of Reference 3 for details.

- Entrainment in Bottom Reflood

The model for entrainment in the core near the quench front is based on a model by Kataoka and Ishii (Reference 16) assuming vapor bubbling through a liquid pool.

- Entrainment at a Horizontally Stratified Surface

In the ADS-4 IRWST initiation phase of small break LOCA events, if the vapor velocity is sufficient, entrainment can occur from a horizontal interface of vapor and liquid. Refer to subsection 2.2.1.4.

- De-entrainment in Film Flow and Crossflow De-entrainment

The model to estimate the de-entrainment of entrained drops into the continuous liquid field uses an empirical model by Cousins (Reference 18). Entrained liquid in the upper plenum can de-entrain on structures there as the two-phase mixture flows from the vessel into the hot legs. WCOBRA/TRAC uses a model based on experiments by Dallman and Kirchner (Reference 19) to determine the amount of de-entrainment in the upper plenum and other regions of the reactor vessel. These models, which are used in large break LOCA analyses, are not applied in the WCOBRA/TRAC analyses presented in this report.

- De-entrainment at Area Changes

De-entrainment occurs as a two-phase mixture encounters a flow restriction such as a tie plate. WCOBRA/TRAC uses a simple area ratio to de-entrain a fraction of the droplet field where an area reduction occurs in the reactor vessel.

- De-entrainment at Solid Surfaces and Liquid Pools

Drops are assumed to de-entrain when the drops flow into a cell with a solid surface at the opposite face or when the drops flow into a cell which is in a bubbly flow regime.

Condensation

WCOBRA/TRAC-AP uses a model for interfacial heat and mass transfer similar to other best estimate codes. As described in Section 5 of WCAP-12945 (Reference 3), four components are evaluated to calculate interfacial heat and mass transfer; they may be described as:

$$\begin{aligned}
 \Gamma_{SCL} &= \frac{HA_{SCL}(T_f - T_i)}{H_v - H_f} \\
 \Gamma_{SHL} &= \frac{HA_{SHL}(T_f - T_i)}{H_g - H_f} \\
 \Gamma_{SCV} &= \frac{HA_{SCV}(T_v - T_i)}{H_v - H_f} \\
 \Gamma_{SHV} &= \frac{HA_{SHV}(T_v - T_i)}{H_g - H_f}
 \end{aligned}
 \tag{2-32}$$

where:

Γ_{SCL} = condensation to subcooled liquid

Γ_{SHL} = evaporation from superheated liquid

Γ_{SCV} = condensation from subcooled vapor

Γ_{SHV} = evaporation to superheated vapor

Figure 2-4 provides a pictorial representation of the WCOBRA/TRAC-AP approach. []^{a,c}

Assessment of WCOBRA/TRAC-AP Horizontal Stratified Flow Models

The performance of the horizontal stratified flow models in WCOBRA/TRAC-AP are established in predicting a pertinent separate effect test to demonstrate that the models are adequate for the ADS-4 IRWST initiation phase of AP1000 small break LOCA applications. The interfacial drag predictive capability is validated against relevant experimental data (Reference 4); these data are also used to validate the interfacial condensation heat transfer.

Test Facility Description and Modeling

The test facility of Lim (Reference 4) used a rectangular channel to measure condensation of steam in cocurrent, horizontal flow. The channel was constructed of stainless steel with Pyrex glass windows; its dimensions were 160.1 cm long, 6.35 cm high, and 30.48 cm wide. Data were taken in the course of 35 runs. Controlled parameters in the experiments included water and steam inlet temperatures, mass flowrates, and water layer thickness at the inlet. The range of steam (maximum velocity 18 m/s) and water (maximum velocity 41 cm/s) flowrates were restricted by either the initiation of bridging

phenomena or the occurrence of a hydraulic jump. Inlet steam pressure was approximately 1 atmosphere. Steam velocity, static pressure (for some experiments), and water layer thicknesses were measured at five locations along the channel. The water inlet temperature was also measured. Figure 2-5 is a schematic diagram of the experimental system.

Figure 2-6 presents the WCOBRA/TRAC noding of the test facility. [

] ^{a,c}

As shown in Figure 2-6, the experimental channel is modeled axially [^{a,c} This was considered sufficient to provide enough resolution to compare with experimental measurements, which are available at only five axial locations.

The experimental channel is divided [

] ^{a,c}

The experimental report (Lim, et al., 1981) offers no data on liquid level in the discharge tank during the experiments and on the tank dimensions. Because it is impractical to simulate a constant liquid level in the tank due to condensation in the channel, the liquid level in the tank was allowed to rise during the simulation, but it was always kept below the liquid level in the channel. Condensation was turned off in [

] ^{a,c}

[

] ^{a,c}

The liquid level at the channel inlet [

] ^{a,c} As shown in

Figures 2-7 and 2-8, the liquid profile away from the channel inlet is determined only by the steam and water flowrates. The “line” in Figure 2-8 is a linear correlation plane oriented in parallel to the reader’s line of sight. Because essentially all of the variation in the liquid water thickness in the experimental channel can be attributed to the variations in steam and water flowrates, the effect of the initial water layer thickness on the flow pattern away from the inlet can be ignored.

The experimental results used in this analysis are reported to be at steady-state. That is, the water level, pressure, temperature, and steam flow in the channel were stable and not varying significantly.

The WCOBRA/TRAC simulations were run [

] ^{a,c}

Calculational Results

A total of 35 tests are reported in Lim (Reference 4) as shown in Table 2-1. Those tests in which the horizontal two-phase flow is fully within the wavy or stratified flow regimes (32 in number) were simulated. The experimental results and test conditions for the tests simulated with WCOBRA/TRAC-AP are shown in Table 2-1. Steam density and steam and water velocities were input as boundary conditions in the model's steam and liquid fill components, respectively.

In Table 2-1, steam flowrate and water layer thickness data at locations 1, 2, 3, 4, and 5 correspond to 6.18, 12.05, 23.08, 34.18, and 48.14 inches from the experimental channel inlet. Static pressure difference measurements at 4.88, 10.75, 21.77, 32.87, and 47.24 inches are listed as being at locations 1 through 5. Nomenclature is provided on the table.

Steam density input is calculated using NIST/ASME steam properties for given values of the steam inlet temperature and constant pressure of 16 psi. Due to small variations in the liquid temperature and density among the tests and along the experimental channel, a constant liquid density corresponding to the average liquid temperature of 148.6°F is assumed. Steam and water inlet velocities in the model fill components (Figure 2-6) are calculated using a constant flow area of 0.2083 ft².

The WCOBRA/TRAC-AP predictions for a typical case (Run 275) are presented in Figures 2-9, 2-11, and 2-13. Predicted values of liquid level, steam pressure, and steam flowrate are shown for the duration of the test at a number of axial locations. In Figures 2-10, 2-12, and 2-14, the average calculated values of these parameters are compared with the experimental data. There is a reasonably good agreement between the measured and predicted average values of liquid level and pressure drop¹ in the channel as seen in Figures 2-10 and 2-12. While the liquid level at 47.27 inches is significantly underpredicted, the observed trend of the liquid level to recover toward the channel outlet is well reproduced by WCOBRA/TRAC-AP (Figure 2-10). WCOBRA/TRAC-AP overpredicted the steam flowrate axially as seen in Figure 2-14; underpredicting the steam condensation rate is the cause. This matter was investigated further; the condensation heat transfer correlation used in WCOBRA/TRAC-AP (Reference 11), and one derived from the experimental data, were compared to each other for typical flow conditions in the channel. This comparison is presented in Figure 2-15: the solid line is the WCOBRA/TRAC correlation result, and the dashed line(s) the correlation from the experiment.

The alternative correlation for a smooth interface based on this test data (Lim, et al., 1981) is given by:

$$\text{Nu}_{x_{As}} := 0.631 \cdot (\text{Re}_g)^{0.58} \cdot (\text{Re}_l)^{0.09} \cdot (\text{Pr}_l)^{0.3} \quad (2-33)$$

where:

$\text{Nu}_{x_{As}}$ = is the Nusselt number (Nu)

¹ Note that the pressure actually increases as the steam flow proceeds through the channel.

The principal difference between the correlations is that the Nu value in WCOBRA/TRAC-AP is [

]^{a,c}

The cumulative results of all tests simulated are shown in Figures 2-16 through 2-19, which show scatter plots of predicted versus measured quantities of the liquid level, steam mass flowrate, liquid temperature at the channel exit, and the pressure drop in the channel, respectively. For most of the cases, liquid level predictions are within ± 0.2 inches of the measurements. The steam flowrate is overestimated almost everywhere in the test section, particularly near the channel exit. As a result, the liquid temperature at the channel exit is underpredicted by 20° to 40°F. The large majority (approximately 80 percent) of the pressure drop predictions is within ± 33 percent of the experimental data, as shown in Figure 2-19.

Conclusions

WCOBRA/TRAC-AP predictions of two-phase flow in a horizontal channel were verified against data for a rectangular channel with cocurrent water flow at atmospheric pressure. A model of the experimental channel, consisting of []^{a,c} The pertinent cases among the 35 test cases reported in Lim (Reference 4) were simulated. For most of the cases, liquid level predictions are within ± 0.2 inches of the measurements. Depending on the axial position, steam flowrate can be overestimated by a factor of 2 or more (near the channel exit). As a result, the liquid temperature at the channel exit is underpredicted by 20° to 40°F. To address this, values of the condensation heat transfer coefficient calculated by the code were compared with those given by the correlation used in WCOBRA/TRAC-AP and one derived from the experimental data. The difference in the condensation heat transfer coefficient is determined to be due to the correlation used in the code. Condensation heat transfer in AP1000 hot leg horizontal stratified flow is a minor effect during the ADS-4 IRWST initiation phase as saturated or near-saturated conditions exist during this phase of the transient.

Most of the pressure drop predictions are within ± 33 percent of the experimental data, and the number of points for which the pressure drop is underpredicted is approximately the same as the number for which it is overpredicted. Inasmuch as hot leg steam velocities are low when horizontal stratified flow conditions exist in the AP1000 hot legs during the ADS-4 IRWST initiation phase of a small break LOCA event, the hot leg pressure drop prediction is not of major importance in predicting ADS-4 performance.

2.2.3 References

1. Taitel, Y., and Dukler, A. E., 1976, "A Model for Predicting Flow Regime Transitions in Horizontal and Near Horizontal Gas-Flow," *AICHE Journal*, Vol. 22, No. 1, pp. 47-55.
2. Ishii, M. and Grolmes, M., 1975, "Inception Criteria for Droplet Entrainment in Two-Phase Concurrent Film Flow," *AICHE Journal*, Vol. 21, No. 2, pp. 308-318.

3. Bajorek, S. M., et al., 1998, "Code Qualification Document for Best Estimate LOCA Analysis," WCAP-12945-P-A, Volumes 1 and 3.
4. Lim, I. S., et al., 1981, "Cocurrent Steam-water Flow in a Horizontal Channel," NUREG/CR-2289.
5. WCAP-15613, "AP1000 PIRT and Scaling Assessment," Westinghouse Electric Company LLC, February 2001.
6. Craya, A., 1949, "Theoretical Research on the Flow of Non-homogeneous Fluids," La Houille Blanche, pp. 44-55.
7. Rouse, H., 1956, "Seven Exploratory Studies in Hydraulics," Proc. ASCE, Vol. 82.
8. Ardron, K. H., and Bryce, W. M., 1990, "Assessment of Horizontal Stratification Entrainment Model in RELAP5/MOD2 by comparison with Separate Effects Experiments," Nuclear Engineering and Design, Vol. 122, pp. 263-271.
9. Schrock, V. E., et al., "Small Break Critical Discharge – the Roles of Vapor and Liquid Entrainment in a Stratified Two-Phase Region Upstream of the Break," USNRC Report NUREG/CR-4761 (December 1986).
10. Soliman, H. M. and Sims, G. E., 1992, "Theoretical Analysis of the Onset of Liquid Entrainment for Orifices of Finite Diameter," Int. Journal of Multiphase Flow, Vol. 18, pp. 229-235.
11. Jensen, R. J. and Yuen, M. C., 1982, "Interphase Transport in Horizontal Stratified Cocurrent Flow," NUREG/CR-2334.
12. Hanratty, T. J., and Engen, J. M., 1957, "Interaction Between a Turbulent Air Stream and a Moving Water Surface," AIChE Journal, Vol. 3, No. 3, p. 299.
13. Tatterson, D. F., et al., 1977, "Drop Sizes in Annular Gas-Liquid Flows," AIChE Journal, Vol. 23, No. 1, pp. 68-76.
14. Wallis, G. B., 1969, One-Dimensional Two-Phase Flow, McGraw-Hill.
15. Anderson, J. L. and Benedetti, R. L., 1986, "Critical Flow Through Small Pipe Breaks," EPRI/NP-4532.
16. Kataoka, I. and Ishii, M., 1983, "Mechanistic Modeling and Correlations for Pool Entrainment Phenomena," NUREG/CR-3304.
17. Walley, P. B., et al., 1973, "Experimental Wave and Entrainment Measurements in Vertical Annular Two-Phase Flow," AERE-R7521, Atomic Energy Research Establishment, Harwell, England.

18. Cousins, L. B., et al., 1965, "Liquid Mass Transfer in Annular Two-Phase Flow," Paper C4, Symposium on Two-Phase Flow, Vol. 2, Exeter, England.
19. Dallman, J. C. and Kirchner, W. L., 1980, "De-Entrainment Phenomena on Vertical Tubes in Droplet Cross Flow," NUREG/CR-1421.

No.	Units ^(a)	Location						W_L^{in} (lb/s)	T_G^{in} (°F)	T_L^{in} (°F)	T_L^{ex} (°F)
		Inlet	1	2	3	4	5				
211	W_G (lb/s)	0.09	0.083	0.077	0.069	0.065	0.064	0.866	281	76.7	160
	δ_L (in)	0.623	0.534	0.393	0.223	0.222	0.241				
	ΔP (psi)	0	7E-05	1E-04	2E-04	3E-04	3E-04				
231	W_G (lb/s)	0.09	0.082	0.074	0.063	0.06	0.059	0.896	271	33.8	118
	δ_L (in)	0.623	0.626	0.487	0.317	0.293	0.317				
	ΔP (psi)	0	1E-04	2E-04	3E-04	4E-04	5E-04				
251	W_G (lb/s)	0.09	0.077	0.072	0.06	0.055	0.054	1.17	272	33.8	98.1
	δ_L (in)	0.623	0.624	0.55	0.349	0.403	0.436				
	ΔP (psi)	0	3E-04	5E-04	7E-04	7E-04	7E-04				
253	W_G (lb/s)	0.143	0.129	0.12	0.086	0.063	0.039	1.447	281	70.88	156
	δ_L (in)	0.623	0.569	0.444	0.3	0.417	0.484				
	ΔP (psi)	0	7E-04	1E-03	0.002	0.002	0.002				
255	W_G (lb/s)	0.204	0.188	0.167	0.113	0.081	0.061	1.57	278	72.68	175
	δ_L (in)	0.623	0.411	0.291	0.208	0.218	0.433				
	ΔP (psi)	0	0.001	0.002	0.004	0.004	0.004				
257	W_G (lb/s)	0.275	0.248	0.222	0.163	0.128	0.101	1.573	287	72.86	190
	δ_L (in)	0.623	0.298	0.208	0.173	0.178	0.23				
	ΔP (psi)	0	0.002	0.004	0.006	0.007	0.007				
273	W_G (lb/s)	0.144	0.119	0.096	0.061	0.042	0.025	2.253	280	77.54	144
	δ_L (in)	0.623	0.783	0.643	0.525	0.591	0.642				
	ΔP (psi)	0	7E-04	0.001	0.002	0.002	0.002				
275	W_G (lb/s)	0.202	0.169	0.14	0.097	0.069	0.047	2.244	285	79.7	163
	δ_L (in)	0.623	0.623	0.51	0.403	0.352	0.622				
	ΔP (psi)	0	0.001	0.002	0.004	0.004	0.005				

a. Definitions for all units are listed at the end of this table.

No.	Units	Location						W_L^{in} (lb/s)	T_G^{in} (°F)	T_L^{in} (°F)	T_L^{ex} (°F)
		Inlet	1	2	3	4	5				
277	W_G (lb/s)	0.277	0.24	0.212	0.156	0.117	0.08	2.289	287	76.1	175
	δ_L (in)	0.623	0.427	0.334	0.307	0.283	0.314				
	ΔP (psi)	0	0.002	0.004	0.006	0.007	0.008				
293	W_G (lb/s)	0.144	0.106	0.084	0.05	0.033	0.019	3.17	279	76.82	126
	δ_L (in)	0.623	0.956	0.819	0.658	0.702	0.754				
	ΔP (psi)	0	7E-04	0.002	0.002	0.002	0.003				
295	W_G (lb/s)	0.199	0.155	0.127	0.08	0.055	0.034	3.148	284	78.44	144
	δ_L (in)	0.623	0.869	0.693	0.551	0.652	0.726				
	ΔP (psi)	0	5E-04	0.002	0.004	0.004	0.005				
297	W_G (lb/s)	0.276	0.224	0.193	0.141	0.101	0.064	3.165	287	79.34	161
	δ_L (in)	0.623	0.605	0.444	0.446	0.389	0.419				
	ΔP (psi)	0	0.001	0.004	0.006	0.007	0.008				
353	W_G (lb/s)	0.144	0.132	0.127	0.09	0.067	0.043	1.5	281	76.73	160
	δ_L (in)	0.873	0.653	0.528	0.309	0.242	0.451				
357	W_G (lb/s)	0.274	0.255	0.231	0.173	0.138	0.109	1.489	288	77	192
	δ_L (in)	0.873	0.493	0.303	0.203	0.173	0.213				
373	W_G (lb/s)	0.141	0.125	0.114	0.077	0.049	0.03	2.233	281	75.92	139
	δ_L (in)	0.873	0.828	0.665	0.453	0.363	0.585				
377	W_G (lb/s)	0.272	0.246	0.218	0.155	0.112	0.074	2.236	288	76.1	175
	δ_L (in)	0.873	0.653	0.456	0.316	0.282	0.302				
393	W_G (lb/s)	0.141	0.118	0.102	0.06	0.042	0.024	3.143	280	78.62	127
	δ_L (in)	0.873	0.931	0.776	0.562	0.606	0.711				
397	W_G (lb/s)	0.277	0.233	0.201	0.144	0.104	0.067	3.095	288	77.36	161
	δ_L (in)	0.873	0.688	0.638	0.441	0.367	0.393				
153	W_G (lb/s)	0.146	0.13	0.117	0.071	0.05	0.031	1.5	221	73.04	165
	δ_L (in)	0.375	0.568	0.524	0.414	0.541	0.573				
157	W_G (lb/s)	0.285	0.254	0.227	0.169	0.135	0.124	1.463	241	75.74	194
	δ_L (in)	0.375	0.306	0.279	0.196	0.241	0.484				
173	W_G (lb/s)	0.147	0.128	0.105	0.063	0.043	0.041	2.311	220	73.4	144
	δ_L (in)	0.375	0.779	0.71	0.546	0.663	0.681				

Table 2-1 Test Matrix Parameters (cont.)

No.	Units	Location					W_L^{in} (lb/s)	T_G^{in} (°F)	T_L^{in} (°F)	T_L^{ex} (°F)	
		Inlet	1	2	3	4					5
177	W_G (lb/s)	0.285	0.262	0.217	0.159	0.115	0.086				
	δ_L (in)	0.375	0.503	0.438	0.335	0.36	0.381	2.315	241	80.06	177
453	W_G (lb/s)	0.142	0.131	0.123	0.099	0.08	0.063				
	δ_L (in)	0.623	0.6	0.544	0.43	0.535	0.567	1.504	280	122.2	182
455	W_G (lb/s)	0.207	0.193	0.176	0.138	0.119	0.108				
	δ_L (in)	0.623	0.445	0.361	0.299	0.305	0.507	1.5	284	119.5	190
457	W_G (lb/s)	0.282	0.261	0.238	0.199	0.179	0.165				
	δ_L (in)	0.623	0.407	0.293	0.257	0.252	0.263	1.496	287	118.4	197
459	W_G (lb/s)	0.344	0.315	0.294	0.254	0.236	0.223				
	δ_L (in)	0.623	0.329	0.257	0.227	0.214	0.249	1.562	288	125.8	201
473	W_G (lb/s)	0.141	0.125	0.112	0.084	0.064	0.045				
	δ_L (in)	0.623	0.766	0.663	0.526	0.61	0.675	2.344	280	123.8	172
475	W_G (lb/s)	0.199	0.176	0.156	0.119	0.094	0.079				
	δ_L (in)	0.623	0.635	0.53	0.444	0.367	0.632	2.286	284	119.5	180
477	W_G (lb/s)	0.285	0.256	0.233	0.187	0.158	0.132				
	δ_L (in)	0.623	0.491	0.367	0.336	0.298	0.333	2.337	287	117.9	189
493	W_G (lb/s)	0.143	0.118	0.102	0.072	0.056	0.037				
	δ_L (in)	0.623	0.906	0.825	0.665	0.728	0.77	3.002	278	119.7	164
495	W_G (lb/s)	0.2	0.17	0.149	0.109	0.083	0.064				
	δ_L (in)	0.623	0.812	0.735	0.546	0.451	0.721	3.007	285	119.8	172
497	W_G (lb/s)	0.282	0.252	0.225	0.178	0.142	0.11				
	δ_L (in)	0.623	0.622	0.458	0.426	0.392	0.426	3.156	287	119.3	181

- W_G = steam mass flowrate
- δ_L = water layer thickness
- ΔP = differential pressure
- W_L^{in} = inlet liquid mass flowrate
- T_G^{in} = inlet vapor temperature
- T_L^{in} = inlet liquid temperature
- T_L^{ex} = outlet liquid temperature

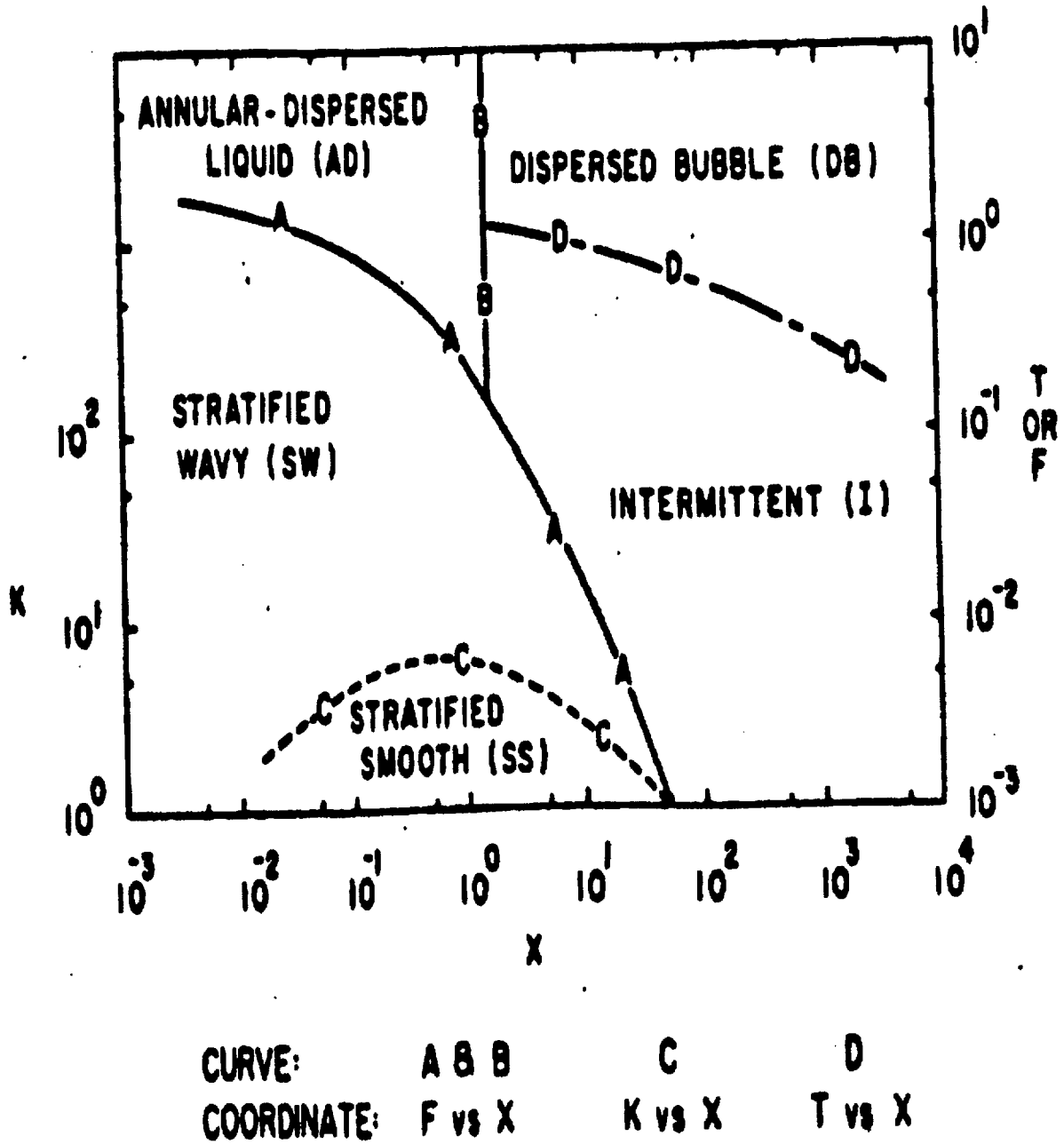


Figure 2-1 Generalized Flow Regime Map for Horizontal Two-Phase Flow

Equilibrium Liquid Level (HL/D)

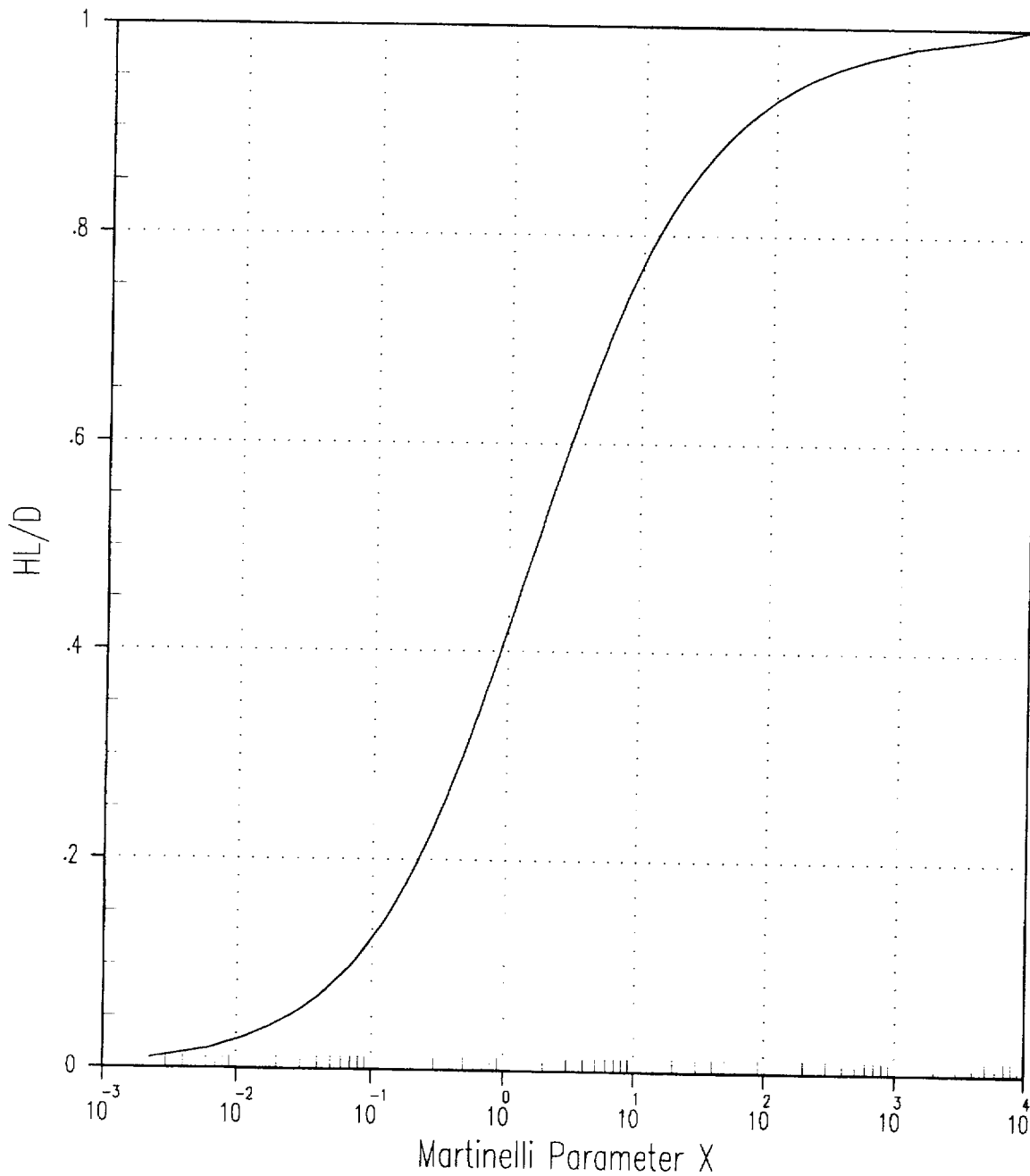


Figure 2-2 Equilibrium Liquid Level vs. Martinelli Parameter, X

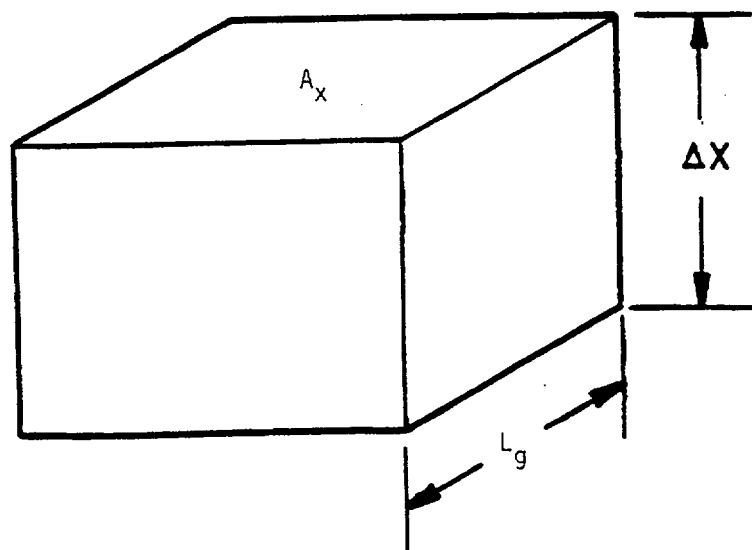


Figure 2-3 Basic Mesh Cell

a,c

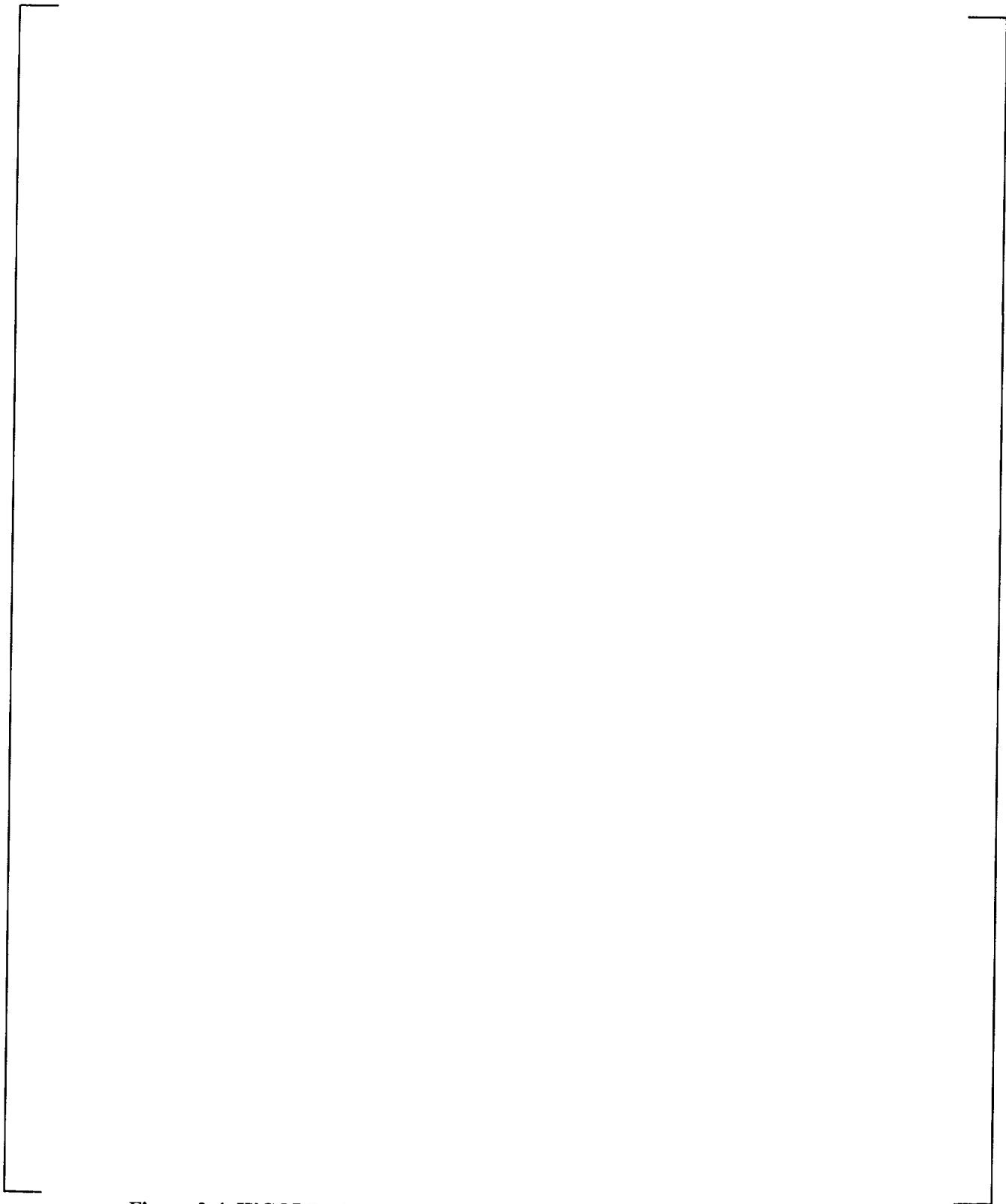


Figure 2-4 WCOBRA/TRAC-AP Representation of Interfacial Heat Transfer

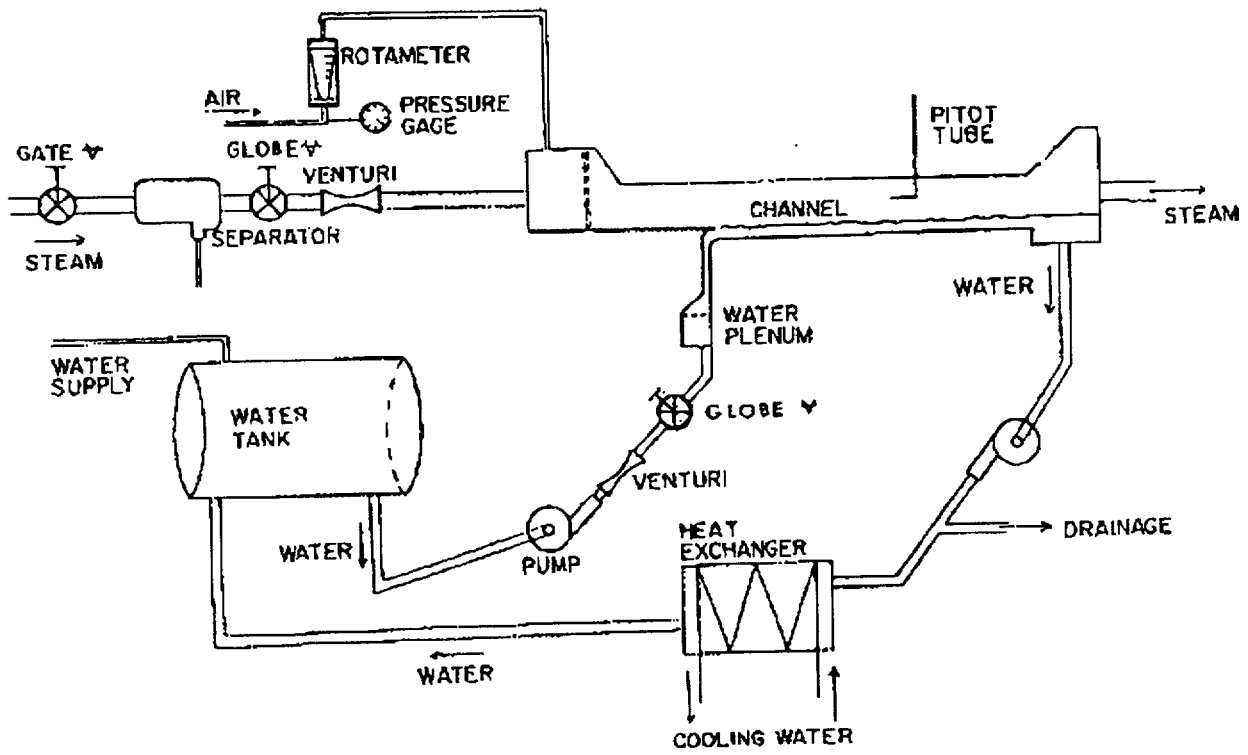


Figure 2-5 Schematic Diagram of the Experimental System (Lim, et al., 1981)

a,c

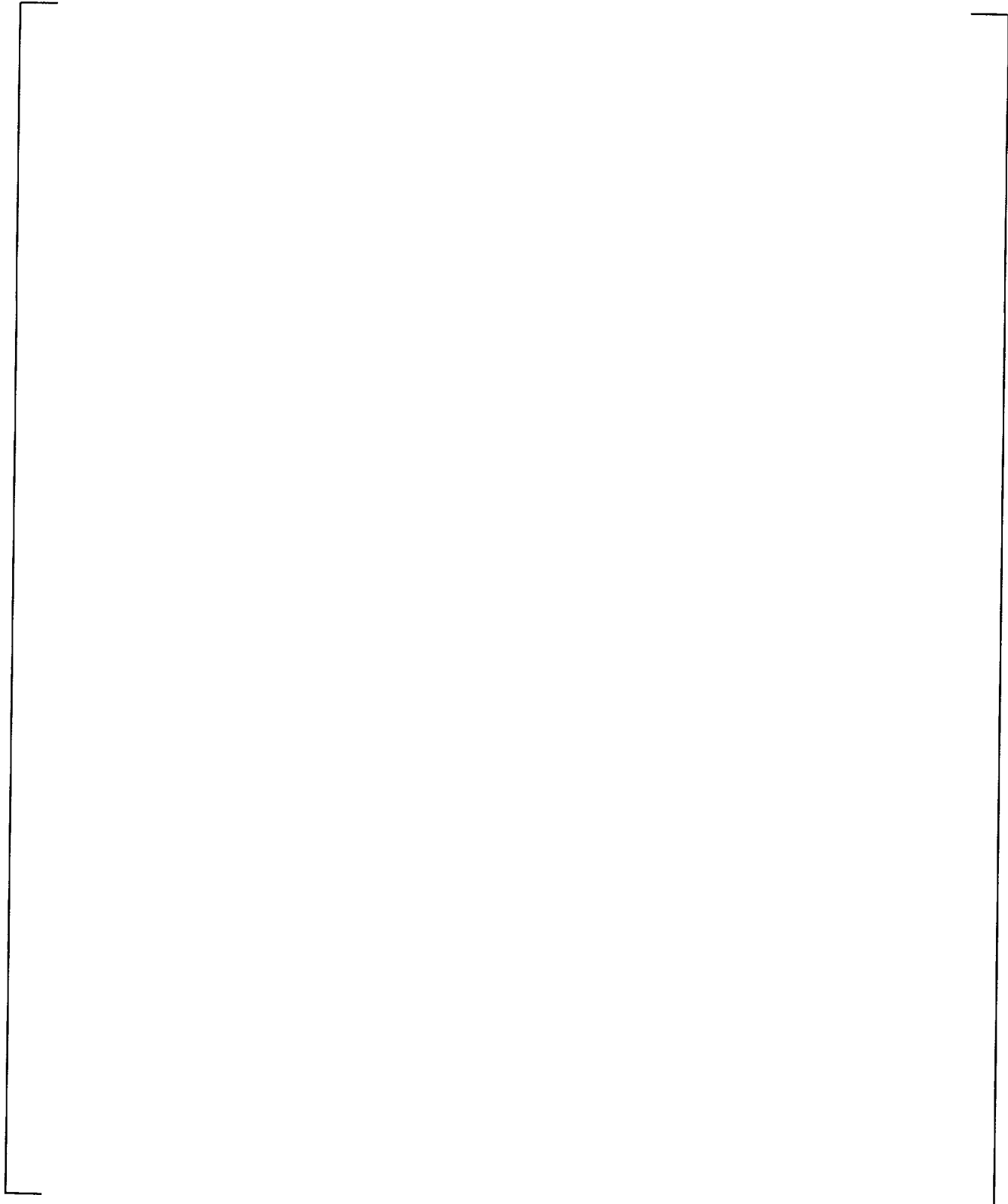


Figure 2-6 WCOBRA/TRAC Noding

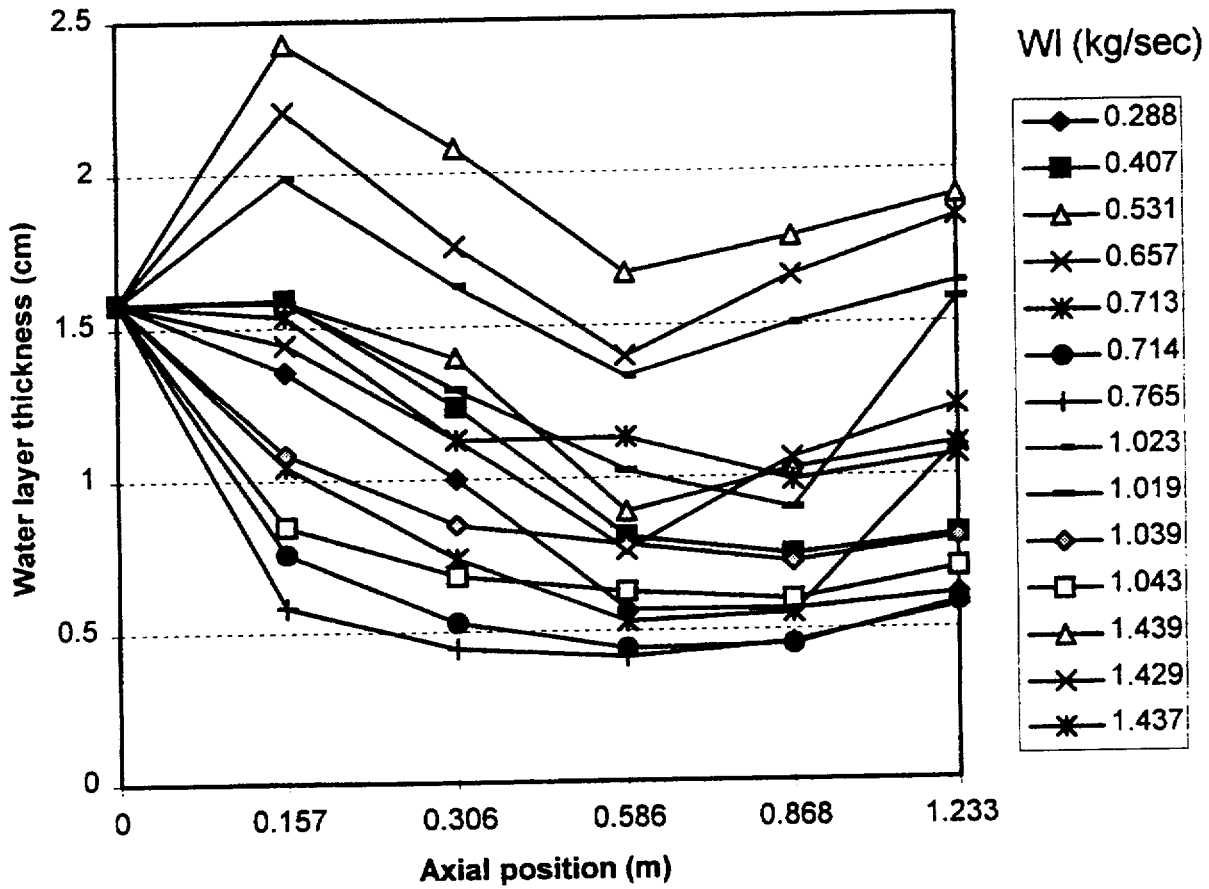


Figure 2-7 Measured Water Thickness Versus Axial Position for Various Liquid (WI) Flowrates and Inlet Water Layer Thickness of 1.583 cm

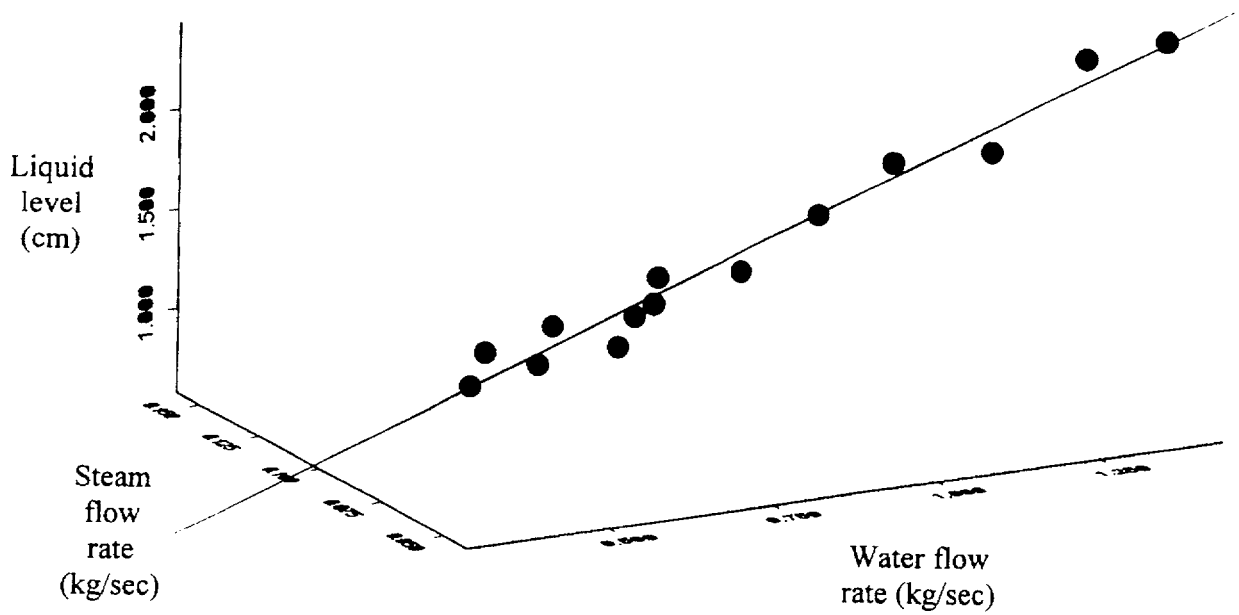


Figure 2-8 Measured Water Thickness at 0.157 m From the Channel Inlet Versus Liquid and Steam Flowrates

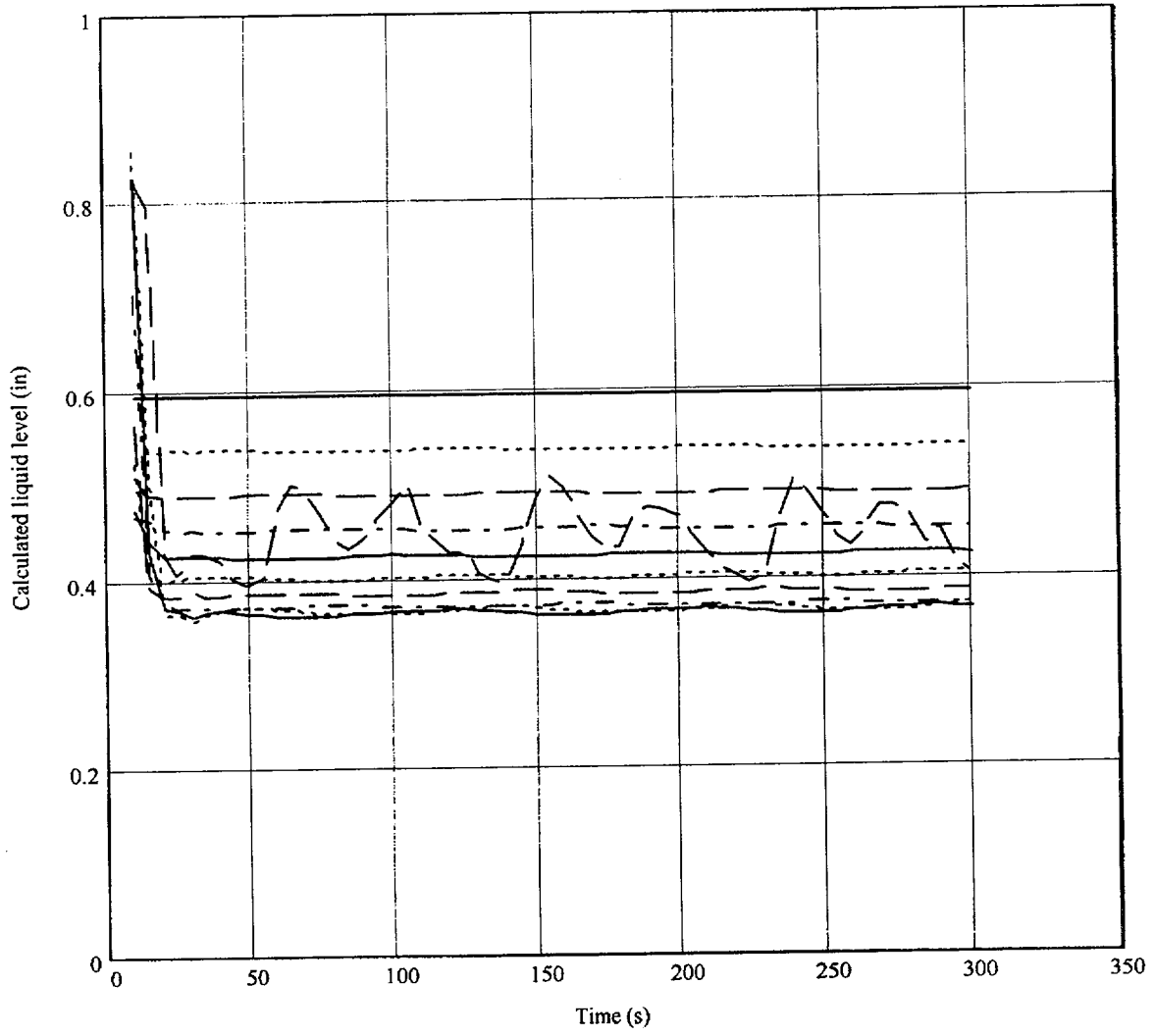


Figure 2-9 Calculated Liquid Level (Run 275)

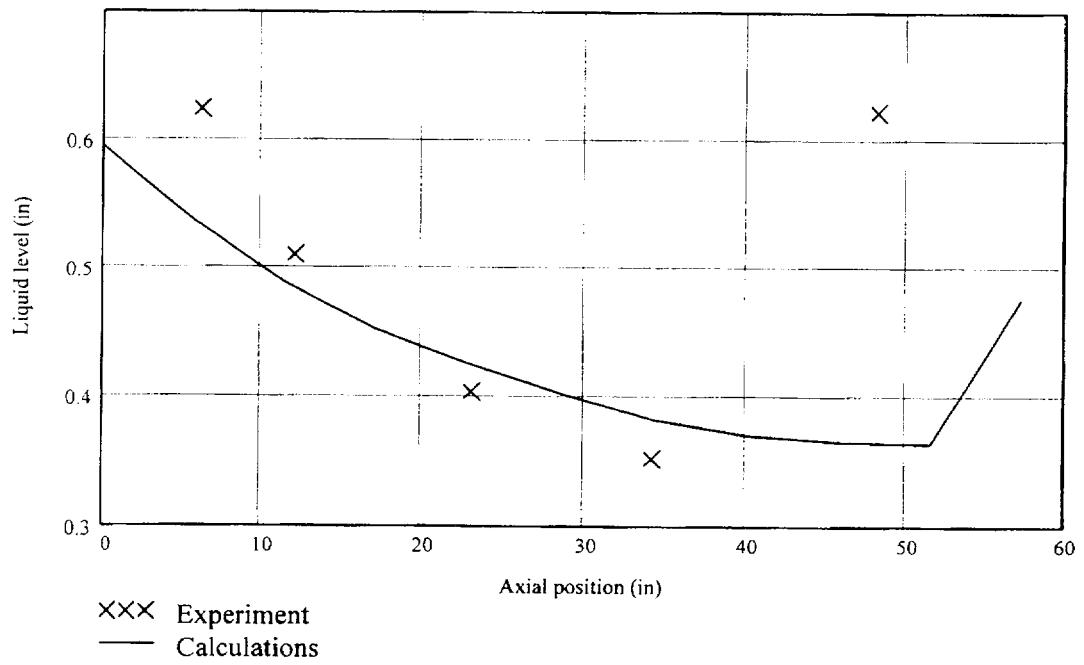


Figure 2-10 Calculated and Measured Liquid Levels Versus Axial Position (Run 275)

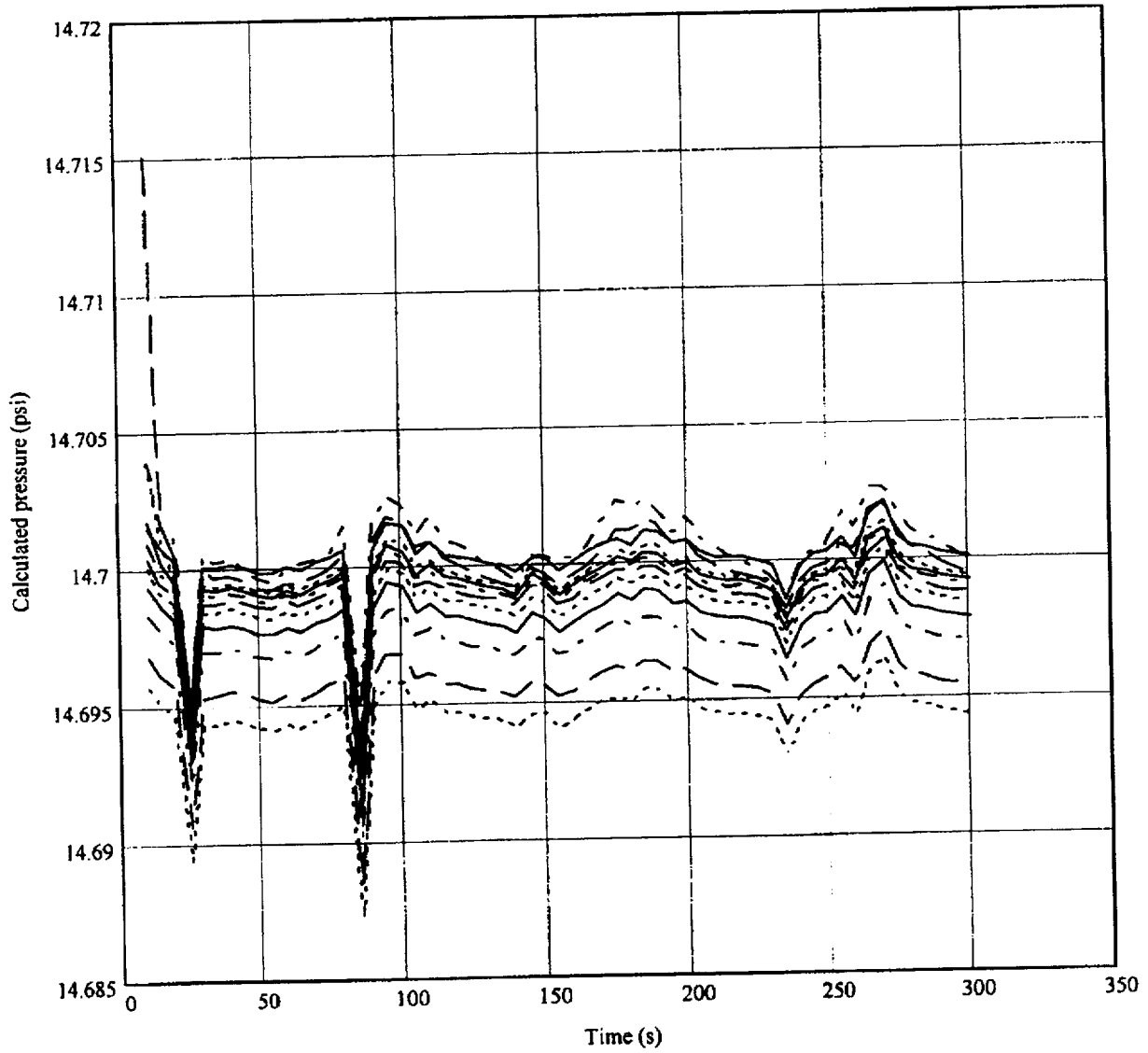


Figure 2-11 Calculated Steam Pressure (Run 275)

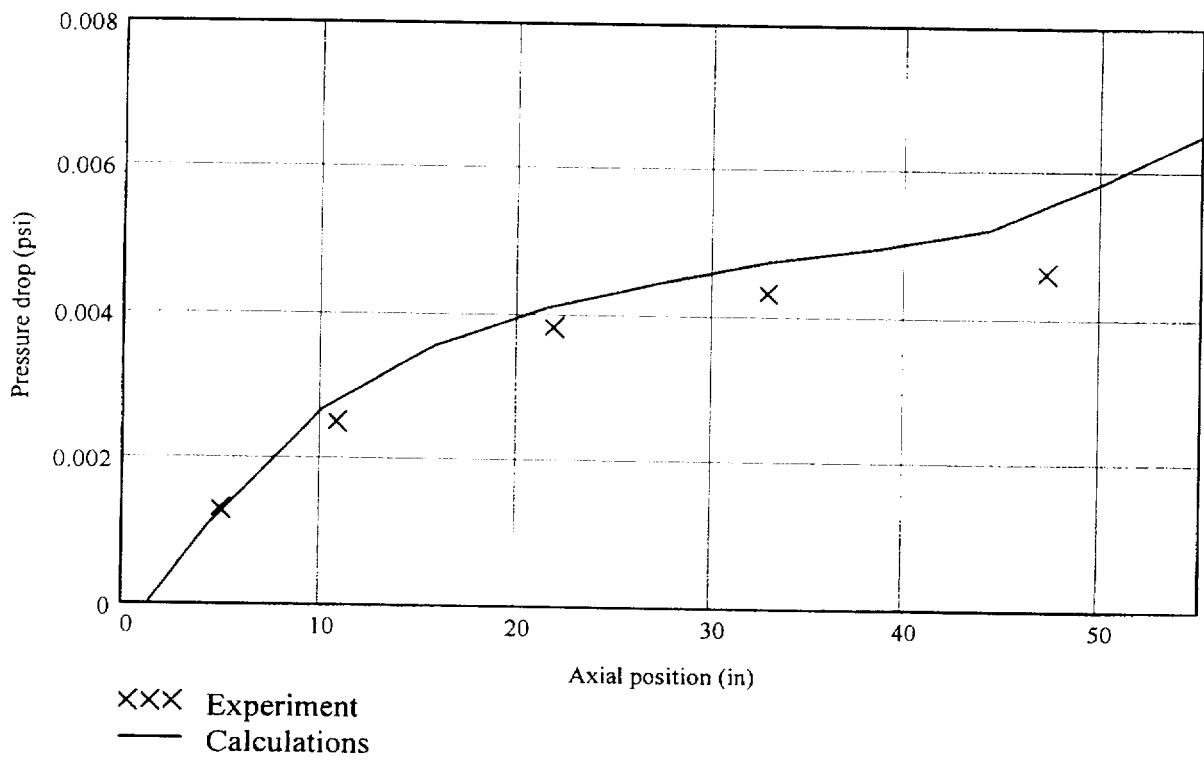


Figure 2-12 Calculated and Measured Steam Pressure Versus Axial Position (Run 275)

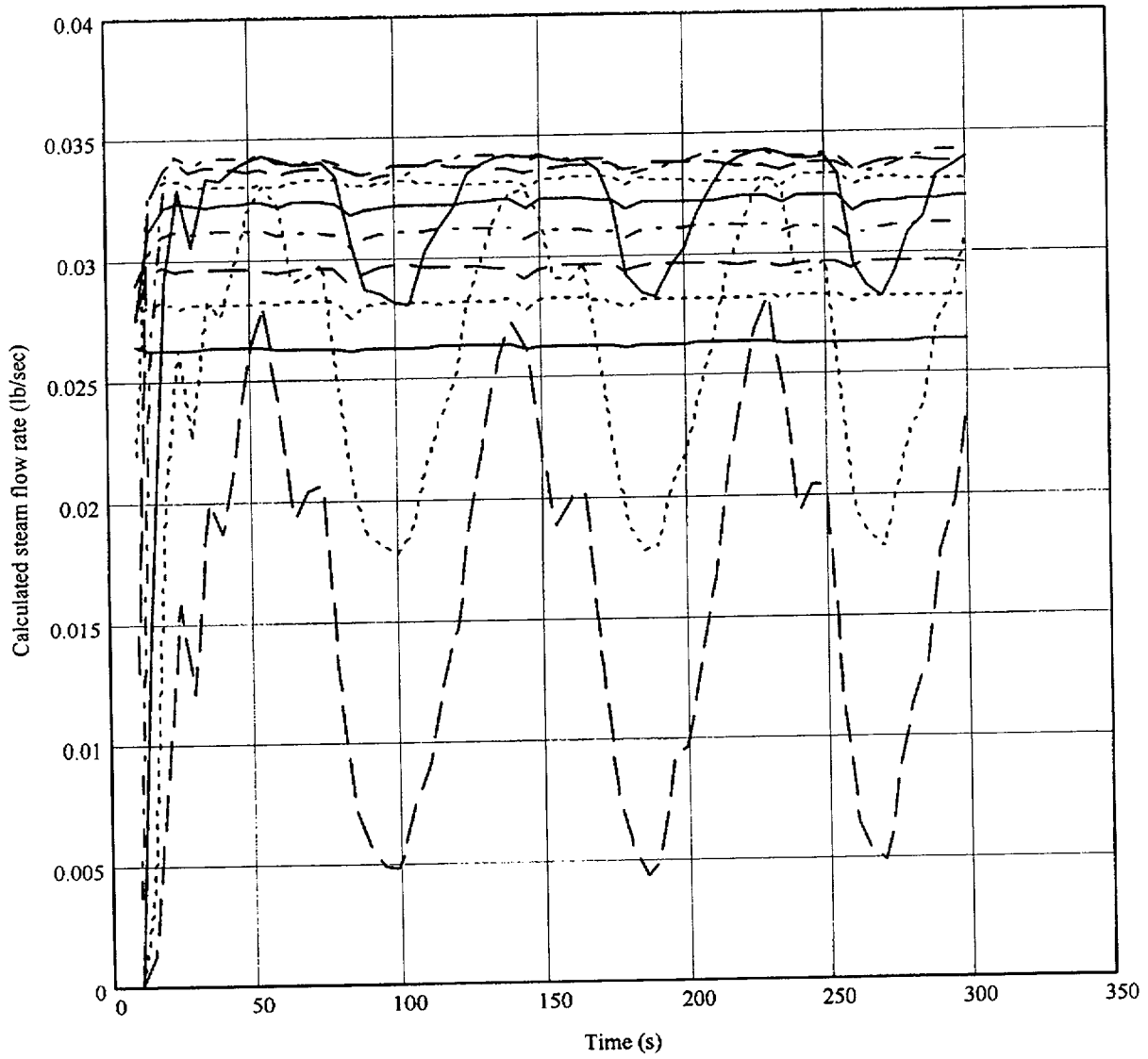


Figure 2-13 Calculated Steam Flowrate (Run 275)

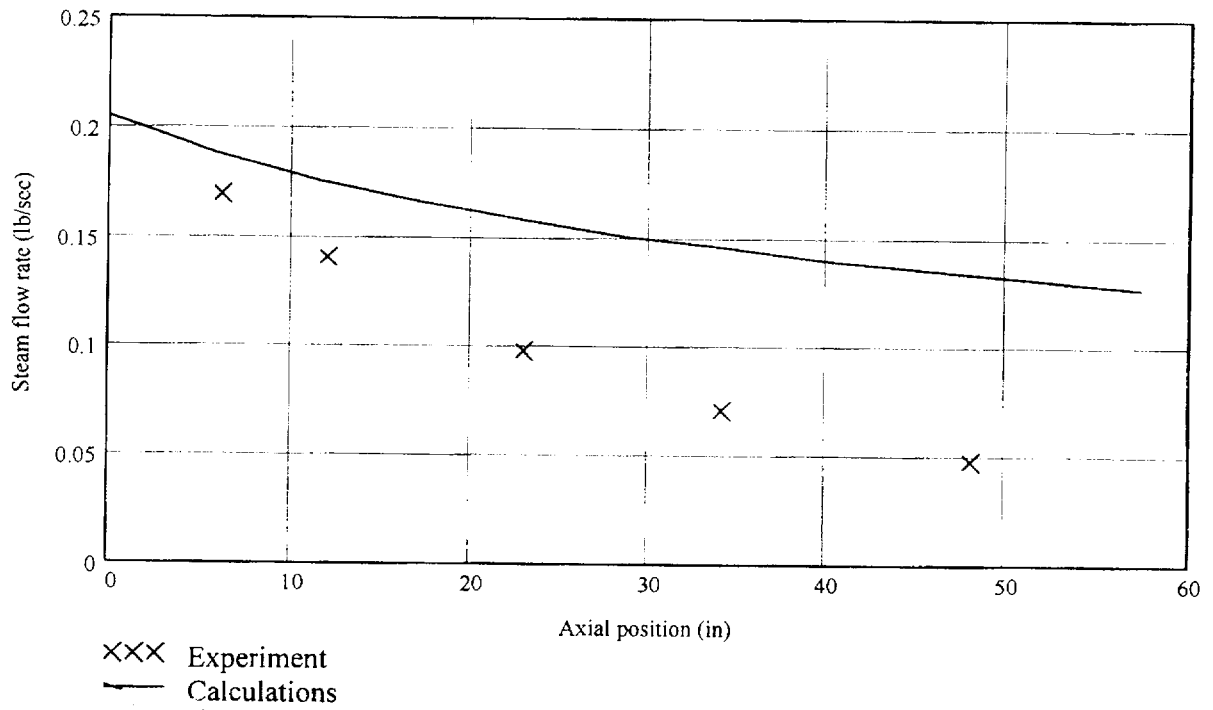


Figure 2-14 Calculated and Measured Steam Flowrate Versus Axial Position (Run 275)

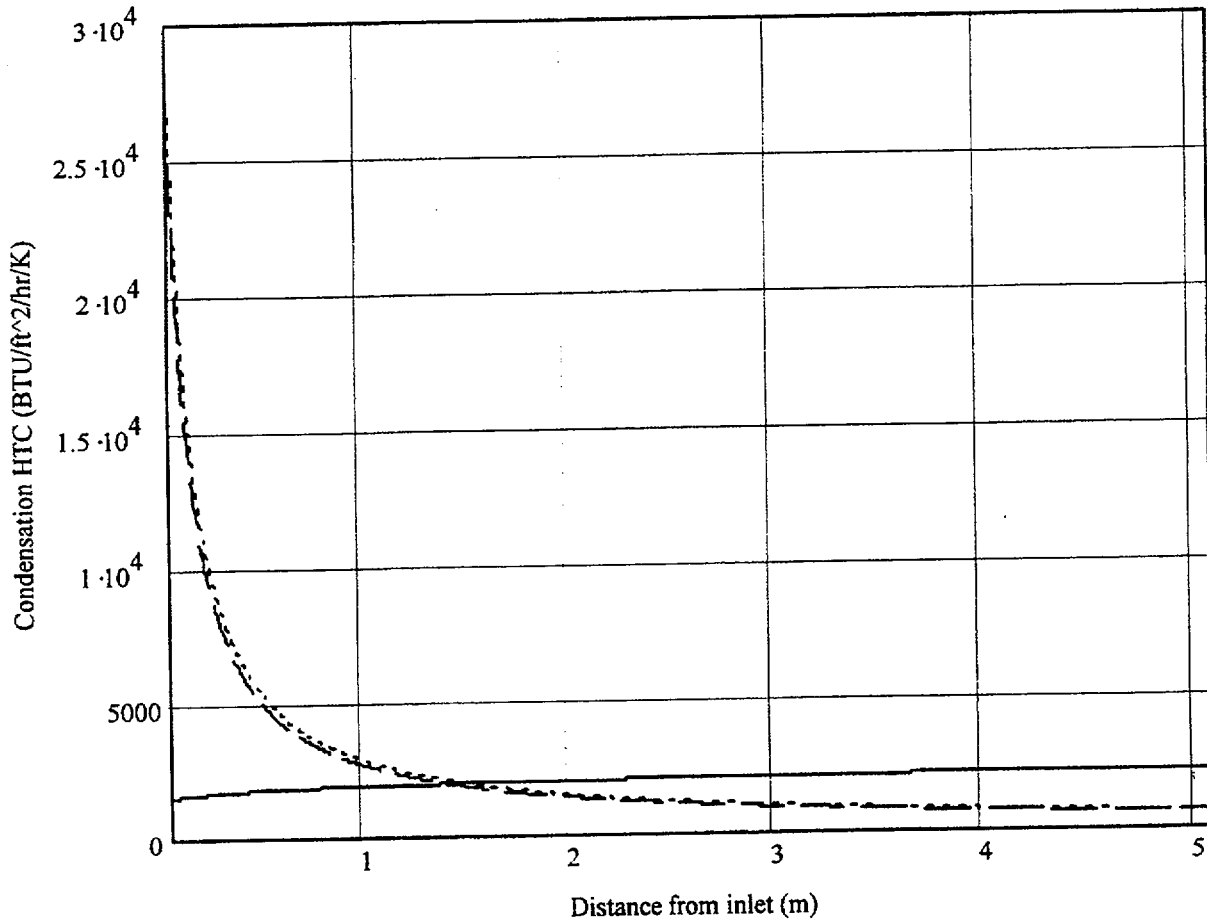


Figure 2-15 Comparison of Condensation Heat Transfer Correlations

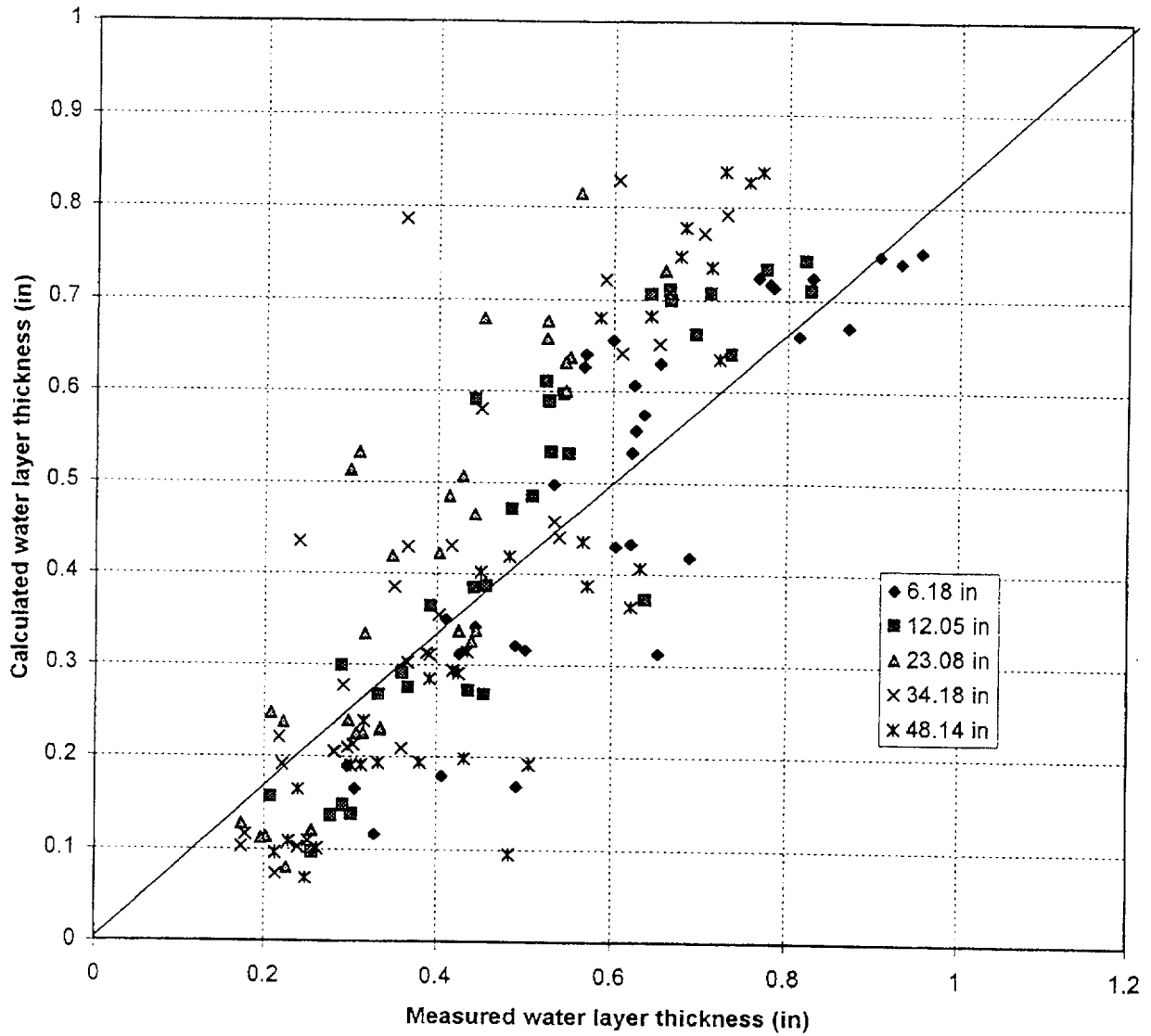


Figure 2-16 Predicted Versus Measured Liquid Level at Various Axial Locations

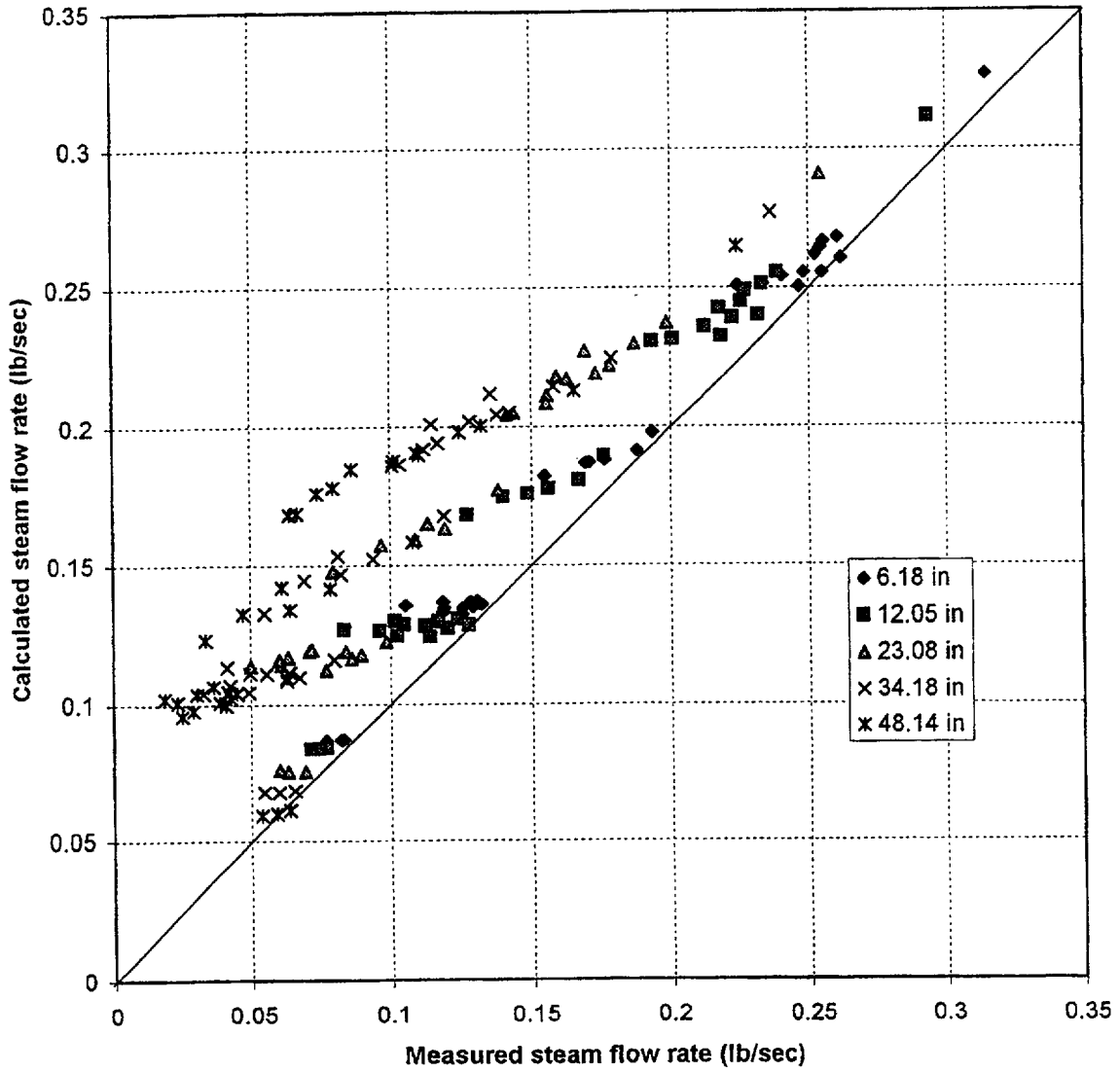


Figure 2-17 Predicted Versus Measured Steam Flowrate at Various Axial Locations

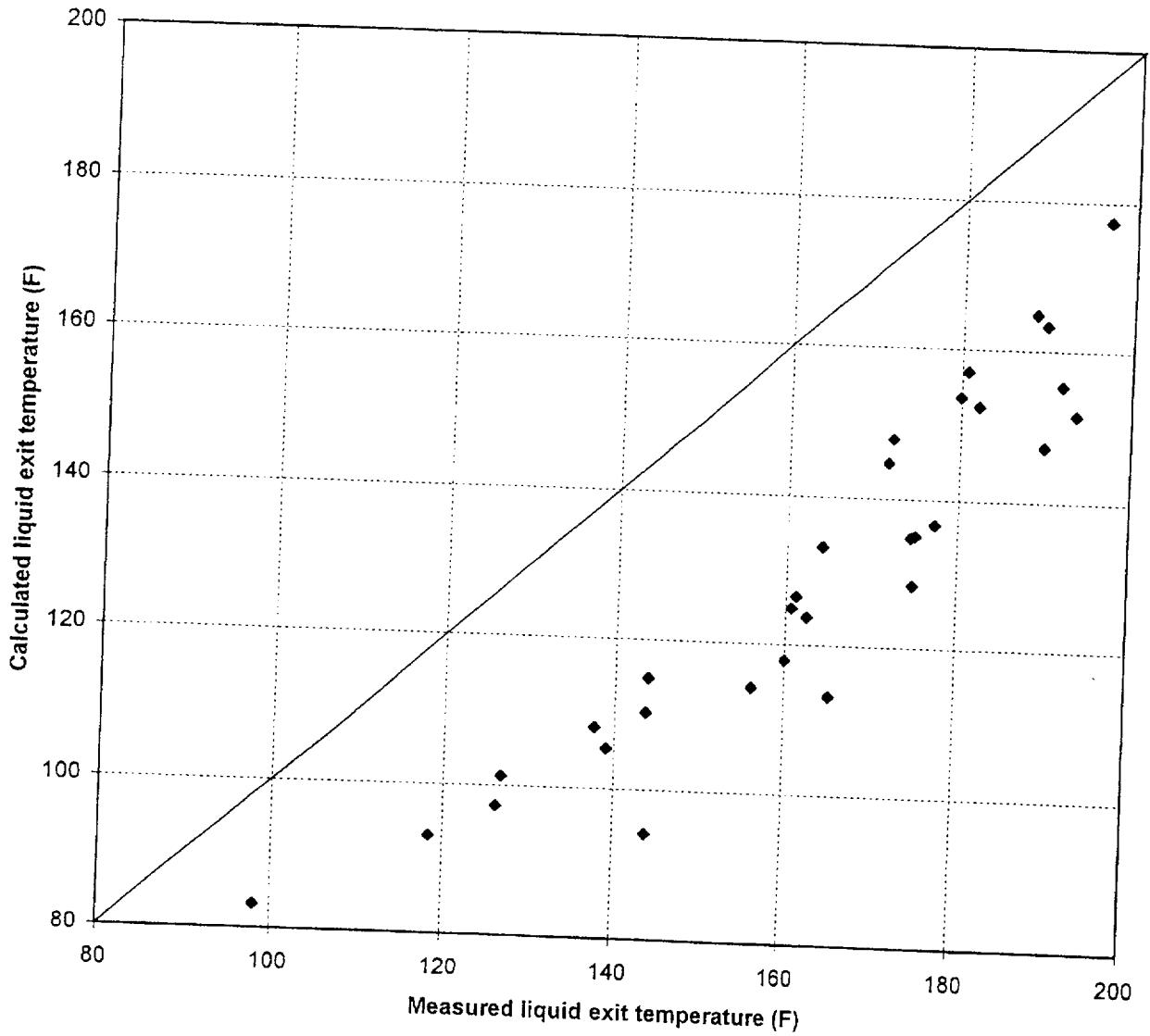
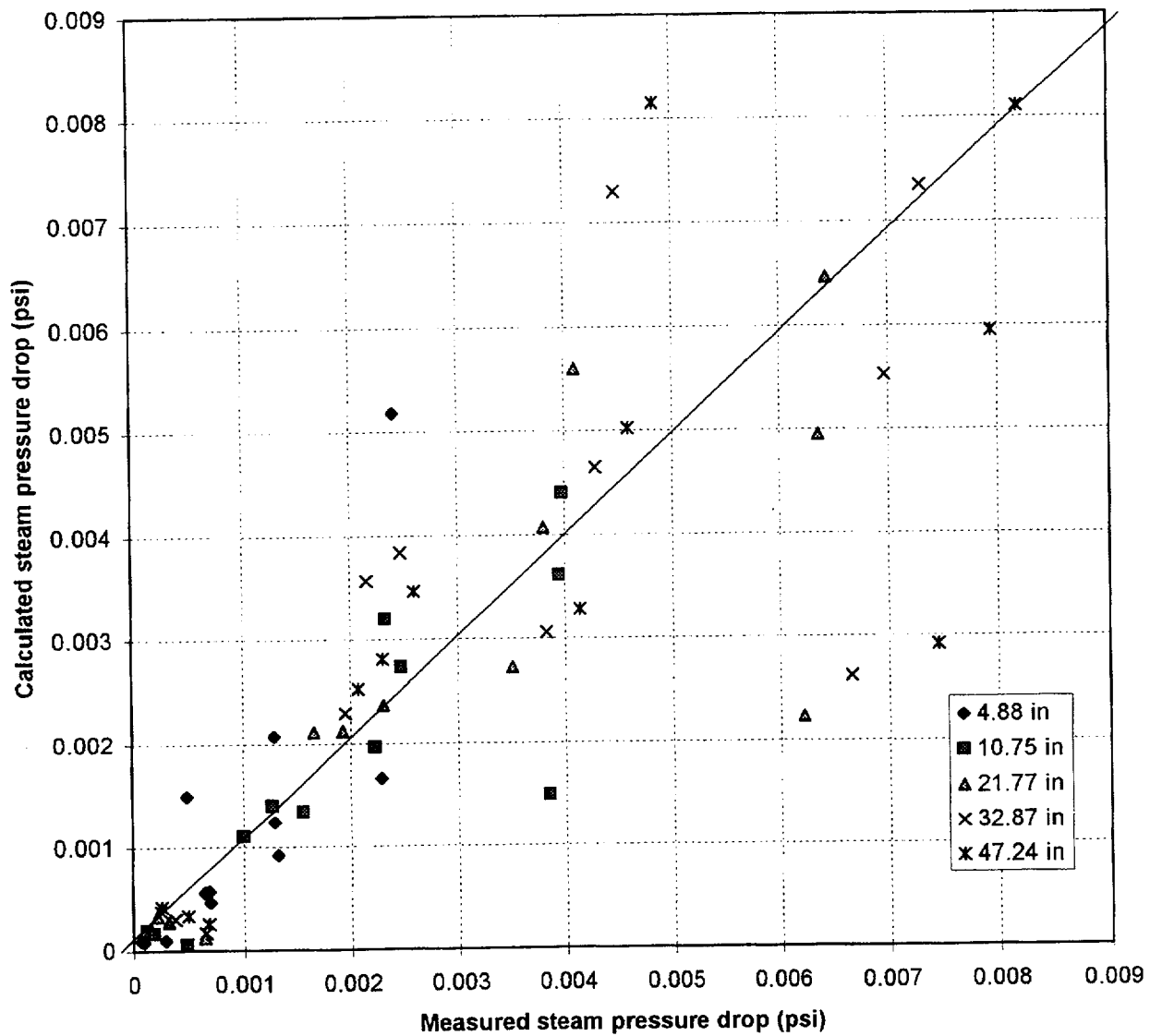


Figure 2-18 Predicted Versus Measured Liquid Temperature at the Channel Exit



(Measurements were taken only during the following runs: 211, 231, 251, 253, 255, 257, 273, 275, 277, 293, 295, and 297)

Figure 2-19 Predicted Versus Measured Steam Pressure Drop at Various Axial Locations

2.3 OSU APEX FACILITY VALIDATION OF WCOBRA/TRAC-AP

In addition to the separate effects test validation reported in the previous section, WCOBRA/TRAC-AP has been validated against Test SB18 of the OSU APEX facility matrix to assess its capability to predict the ADS-4 IRWST initiation phase transient in the upper plenum/hot leg/pressurizer region of interest. The scaling of the OSU APEX facility, which is a 1/4-height, reduced-pressure model of the AP600, has been demonstrated to be adequate for AP1000, such that the data obtained is considered applicable to the larger plant (Reference 1). Test SB18 is simulated [

] ^{a,c}

The WCOBRA/TRAC-AP code version employed in the test SB18 simulation contains the models described in subsection 2.2.1 and the "AP" modeling previously described in Reference 2 superimposed on the Mod 7A Rev. 5 code version, which contains the changes as reported in Reference 3.

The test data report for the OSU tests is given in the OSU Final Data Report (Reference 4), which describes the test facility, the valid instrumentation, and the test facility performance for the different tests. The OSU Test Analysis Report (Reference 5) examines in additional detail the thermal-hydraulic behavior of the test facility and the phenomenon observed in the tests, as identified in the phenomena identification ranking table (PIRT).

The OSU APEX test facility is a 1/4-height, reduced-pressure model of the AP600 and AP1000 and the passive emergency core cooling systems. The test facility located at the Radiation Center at the University in Corvallis, Oregon, includes the RCS, SGs, passive core cooling system (PXS), ADS, and nonsafety-related injection systems, such as the normal residual heat removal system (RNS) and the chemical and volume control system (CVS). The test facility, fabricated from austenitic stainless steel designed for normal operation at 450°F and 400 psig, was scaled using the hierarchical, two-tiered scaling analysis (H2TS) method developed by the U.S. NRC. Simulated piping breaks were tested in the hot leg (HL), cold leg (CL), pressure balance line between the cold leg and the core makeup tank (CMT), and the direct vessel injection (DVI) line. Decay heat that scaled to 3 percent of the full power (about 2 minutes after shutdown) was supplied by electrically heated rods in the reactor vessel. Simulated transients were programmed by the control system to proceed automatically. About 850 data channels were recorded by the data acquisition system (DAS) and downloaded to compact disks for subsequent data reduction and plotting. The OSU test facility was specifically designed to examine the transient (SBLOCA) periods as well as the long-term-cooling (LTC) aspects of the AP600 passive safety systems. The applicability of the OSU APEX facility data to the AP1000 has been demonstrated in Reference 1.

The OSU APEX test facility was constructed specifically to investigate the AP600 passive system characteristics. The facility design models the detail of the AP600 geometry, including the primary system, pipe routings, and layout for the passive safety systems. The primary system consists of one hot leg and two cold legs, with two active pumps and an SG for each of the two loops. There are two CMTs, each connected to a cold leg of one primary loop. The pressurizer is connected to the other primary loop, as in the AP600 plant design. Gas-driven accumulators are connected to the DVI lines. The discharge

lines from a CMT and one of the two IRWST and reactor sump lines are connected to each DVI line. The two independent lines of each stage of ADS 1, 2, and 3 are modeled by one line containing an orifice. Two-phase flow from ADS 1–3 is separated in a swirl-vane separator, and liquid and vapor flows are measured to obtain the total flow rate. The separated flow streams are then recombined and discharged into the IRWST through a sparger. Thus, mass and energy flow from the ADS into the IRWST are preserved. Following actuation, two-phase flow through the ADS-4 flowpaths depressurize the test reactor vessel until IRWST injection is achieved and beyond.

The period for simulation included not only IRWST injection, but also IRWST draining and sump injection to simulate the LTC mode of the AP600. The time scale for the OSU test facility is about one-half; that is, the sequence of events occurred about twice as fast in the test facility as in the AP600. The OSU facility provides data for validating the WCOBRA/TRAC computer code capability to predict the ADS-4 IRWST initiation phase transient.

2.3.1 WCOBRA/TRAC OSU Test Facility Model

The Oregon State University (OSU) test facility is a quarter-scale model of the Westinghouse AP600 and AP1000 systems. It is a low-pressure, integral systems facility designed for test conditions up to 400 psig and 450°F. The facility consists of the following AP600 systems:

- Reactor coolant system (RCS)
- Steam generator (SG) system – primary side
- Passive core cooling system (PXS)
- Partial chemical and volume control system (CVS)
- Partial nonsafety-related normal residual heat removal system (RNS)
- Automatic depressurization system (ADS)

Detailed descriptions of these systems are given in References 4 and 6.

The WCOBRA/TRAC-AP nodalization to analyze the ADS-4 IRWST initiation phase models components of the OSU test facility, as discussed below. Figure 2-20 shows the components simulated in the model. Junctions connecting components are identified with circles. The following subsections describe the main components.

2.3.1.1 Vessel Component

The WCOBRA/TRAC VESSEL component is shown in Figures 2-21 through 2-28. This component simulates the OSU test vessel that contains electrical heater rods as the energy source. As shown,

[] ^{a,c}
 Section 1, shown in Figure 2-22, represents the lower plenum; [] ^{a,c}

Section 2, shown in Figure 2-23, represents [] ^{a,c}

[

] ^{a,c}

Sections 3 through 5, shown in Figures 2-24 to 2-26, represent [

] ^{a,c}

Sections 6 and 7, shown in Figures 2-27 and 2-28, [

] ^{a,c}

2.3.1.2 Primary Loop

The primary loop includes the following major components: [

] ^{a,c}

2.3.1.3 Pressurizer

The pressurizer vent line connects to the ADS Stages 1 to 3 (ADS 1–3) valves. Because [

] ^{a,c}

2.3.1.4 Steam Generators

The code's STGEN component models the SGs [

] ^{a,c}

2.3.1.5 Reactor Coolant Pumps

The RCPs are part of the SG lower plenum. [

] ^{a,c}

2.3.1.6 Loop Lines

The code's PIPE, TEE, and VALVE components [

] ^{a,c}

2.3.1.7 Accumulators

The two accumulators are not modeled because they are empty before the ADS-4 IRWST initiation phase begins.

2.3.1.8 Core Makeup Tanks

The core makeup tanks and the balance lines that connect the top of the CMTs to the cold legs [

] ^{a,c}

2.3.1.9 Passive Residual Heat Removal Heat Exchanger/In-Containment Refueling Water Storage Tank

Test data indicate that the passive residual heat removal heat exchanger (PRHR HX) is [

] ^{a,c}

2.3.1.10 In-Containment Refueling Water Storage Tank (IRWST)

[

] ^{a,c}

2.3.1.11 Automatic Depressurization System Stage 1 to 3 Valves

Component 46 models the ADS 1-3 valves. In the AP600 and AP1000 plants, each set of valves has two flow paths. The OSU test facility [

] ^{a,c}

2.3.1.12 Automatic Depressurization System Stage 4 Valves

Components 64 and 67 represent ADS Stage 4-1 and 4-2 valves, respectively. These valves reduce RCS pressure through HL-1 and HL-2. In the AP600 and AP1000 plants, each fourth stage has two flow paths. In the OSU test facility, [

] ^{a,c}

2.3.1.13 Safety Injection During the ADS-4 IRWST Initiation Phase

As previously noted, [

] ^{a,c}

2.3.1.14 Break Component

The code's BREAK component represents [

] ^{a,c}

2.3.1.15 Boundary Condition Calculations

The phenomena of interest in [

] ^{a,c}

[

] ^{a,c}

2.3.2 Assessment of WCOBRA/TRAC-AP Predictions

The definitions used for quantification are as follows (as excerpted from Section 1.5 of Reference 3):

- **EXCELLENT** – The calculation lies within the data uncertainty band at all times during the transient phase of interest. This is interpreted that the code had no deficiencies that are significant. No action is required for this level of agreement.
- **REASONABLE** – The calculation sometime lies within the data uncertainty bands and shows the same trends as the data. This is interpreted that the code deficiencies are minor. Minor actions and/or discussions are used to explain differences.
- **MINIMAL** – Major data trends and phenomena are not predicted. The code has significant deficiencies, and incorrect conclusions may be drawn based on the calculations without the benefit of data. If the deviation of the code calculations is known, then the minimal agreement may be acceptable for lower-ranked items in the PIRT.
- **INADEQUATE** – Modeling the phenomena is beyond the capability of the code. The question then becomes how important are these phenomena for describing the transient and having confidence in the results and their application to the plant.

This section will focus on the results of the Test SB18 simulation. The time scale of the plots presented is that of the test; the code prediction time values are adjusted so that the ADS-4 actuation time of each is [^{a,c} and in

Figures 2-29 through 2-34. Figure 2-29 compares the pressurizer level predicted by WCOBRA/TRAC with the Test SB18 data as shown in Figure 5.2.2-35 of Reference 5. The WC/T level agrees extremely well with the data through [^{a,c}, at which time it falls below; overall, the agreement is judged as reasonable. The total mass predicted to be released from the ADS-4 flowpaths combined is in reasonable agreement with the data total, as shown in the Figure 2-32 comparison with the test values reported in Reference 5, Figure 5.2.2-62. The code prediction of liquid entrainment through an ADS-4 path is a function of the predicted liquid level in the attached hot leg pipe; subsection 2.2.1 provides discussion of this and other hot leg models developed for this application. The comparison of ADS-4 flow rates is made for only liquid [^{a,c}

The WCOBRA/TRAC predicted collapsed liquid levels in the vessel downcomer, core, and upper plenum are shown in Figures 2-31, 2-32, and 2-33, respectively. These figures show that the code [

] ^{a,c} Figure 2-34 compares the code-predicted downcomer pressure with the Test SB18 value. The agreement is judged to be reasonable. Overall, the WCOBRA/TRAC prediction of the ADS-4 IRWST initiation phase is in reasonable agreement with the Test SB18 data, and the code may be used in AP1000 plant calculations of the ADS-4 IRWST initiation phase to supplement NOTRUMP.

2.3.3 References

1. WCAP-15613, "AP1000 PIRT and Scaling Assessment," Westinghouse Electric Company LLC, February 2001.
2. Garner, D. C., et al., "WCOBRA/TRAC OSU Long-Term Cooling Final Validation Report," March 1998.
3. Letter LTR-NRC-01-6 from H. A. Sepp, Westinghouse, to J. S. Wermiel, USNRC, "10CFR50.46 Annual Notification and Reporting for 2000," March 13, 2001.
4. Dumsday, C. L., Carter, M., Copper, M. H., Lau, L. K., Loftus, M. J., Nayyar, V. K., Tupper, R. B., and Willis, J. W., WCAP-14252, Volumes 1-4, "AP600 Low Pressure Integral Systems Test at Oregon State University, Final Data Report," May 1995.
5. WCAP-14292, Revision 1, "AP600 Low-Pressure Integral Systems Test at Oregon State University Test Analysis Report," September 1995.
6. WCAP-14124, Volume I and Volume II, "AP600 Low Pressure Integral Systems Test at Oregon State University, Facility Description Report," July 1994.
7. Takeuchi, Kenji, Young, M. Y., and Gagnon, A. F., "Flooding in the Pressurizer Surge Line of AP600 Plant and Analyses of APEX Data," Nuclear Engineering & Design 192 (1999), pp. 45-58.

a,c

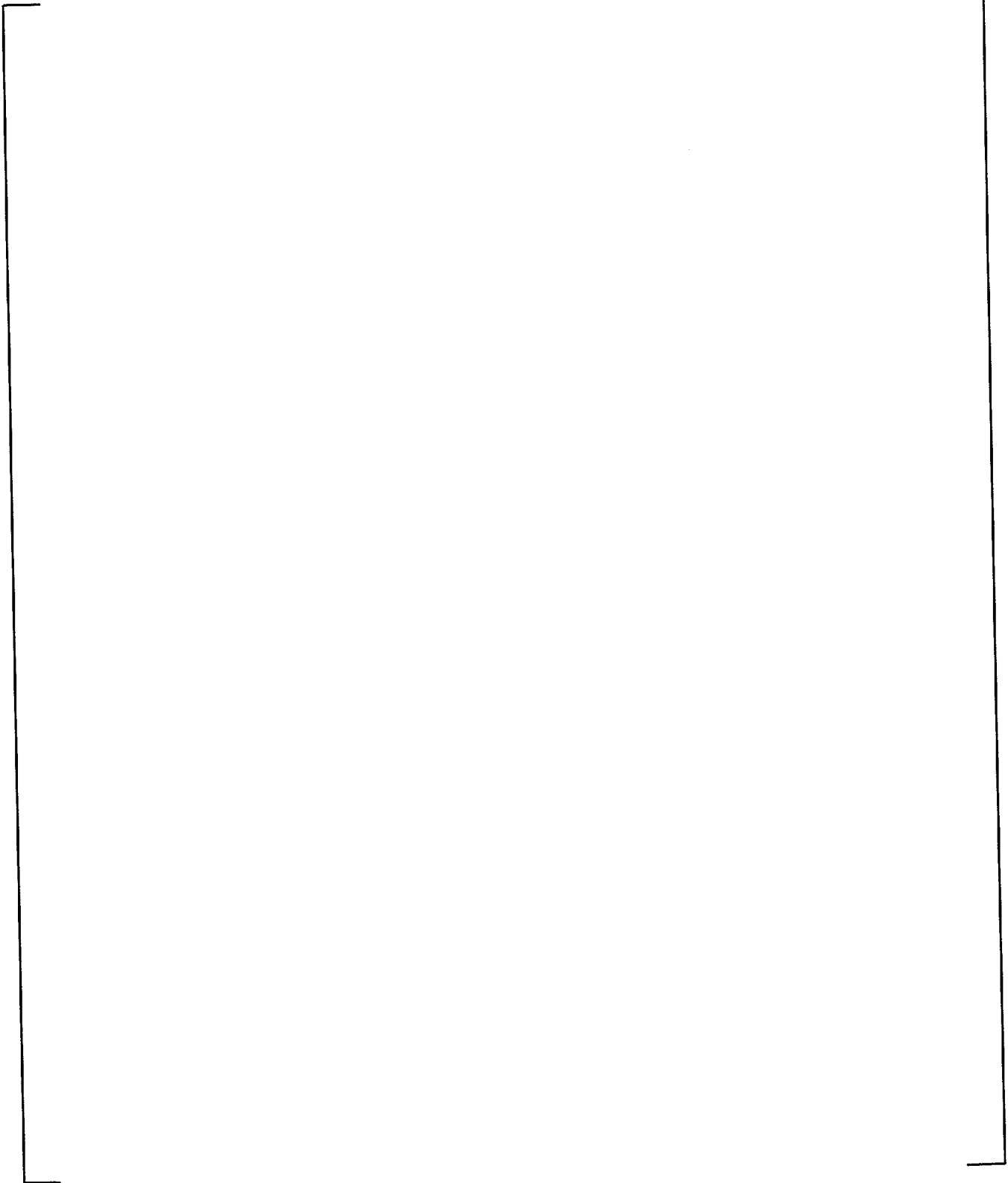


Figure 2-20 OSU WCOBRA/TRAC Schematic Diagram

a,c

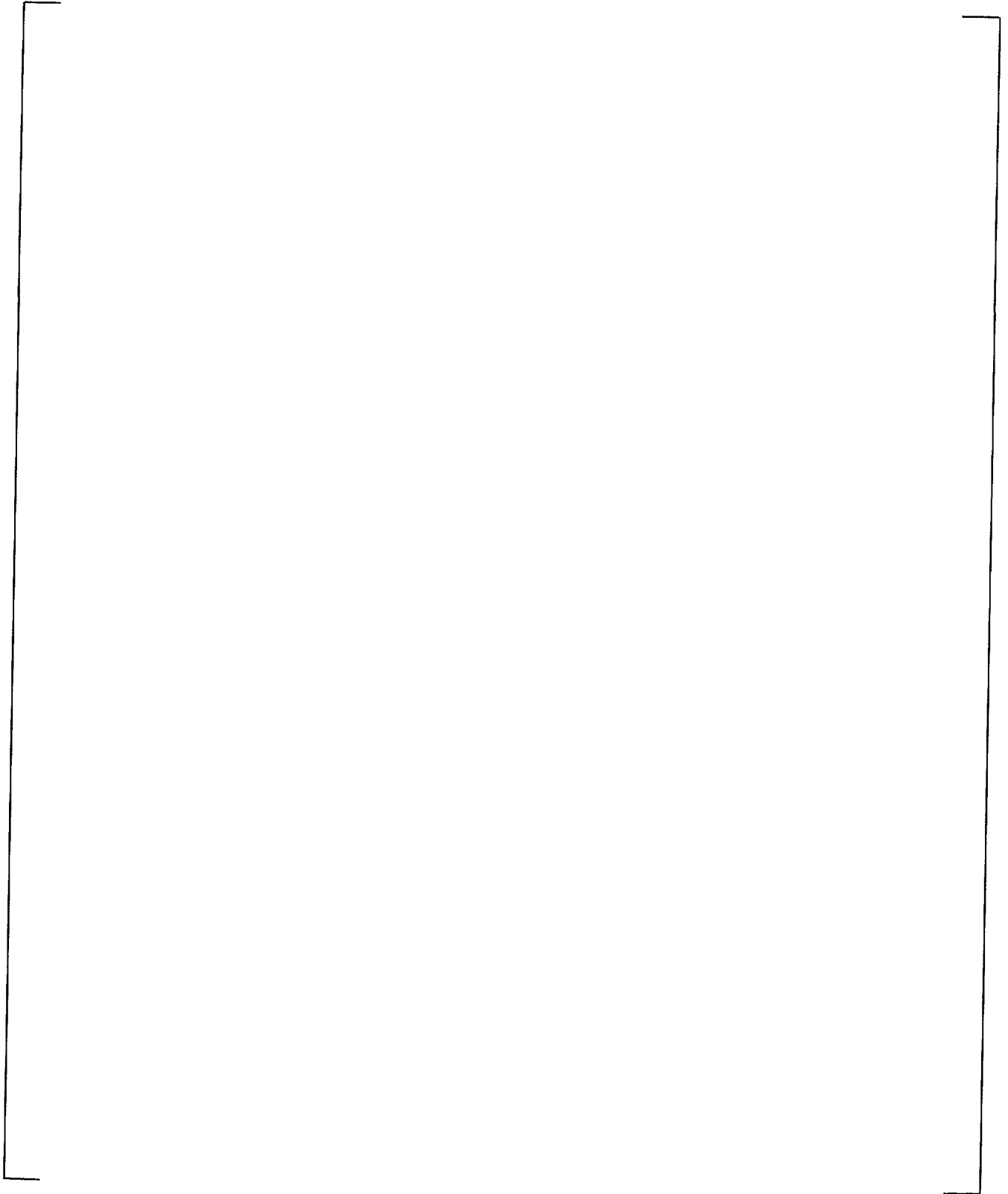


Figure 2-21 OSU WCOBRA/TRAC Vessel Model (Front View)

a,c

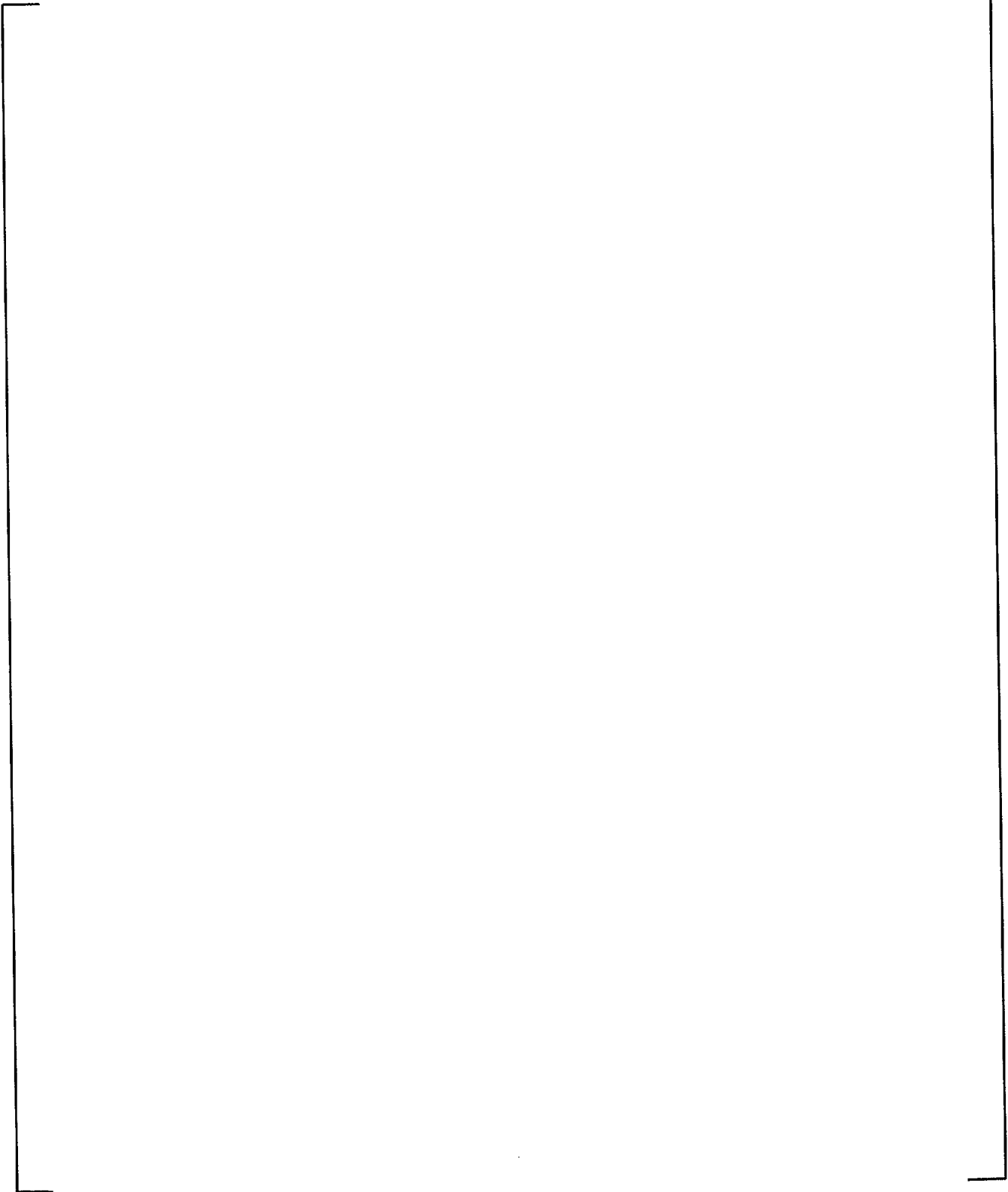


Figure 2-22 OSU Vessel Model – Section 1

a,c

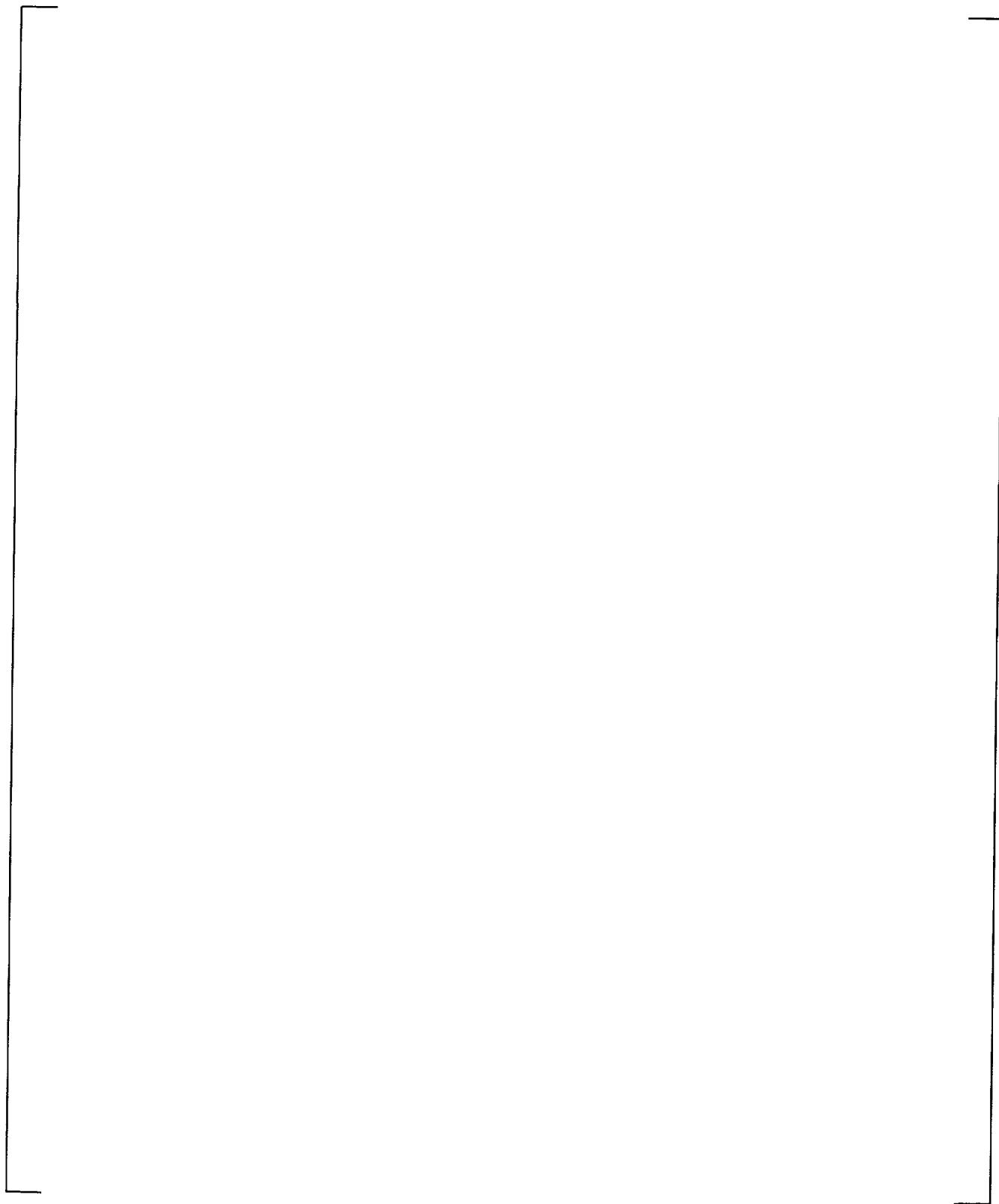


Figure 2-23 OSU Vessel Model – Section 2

a,c

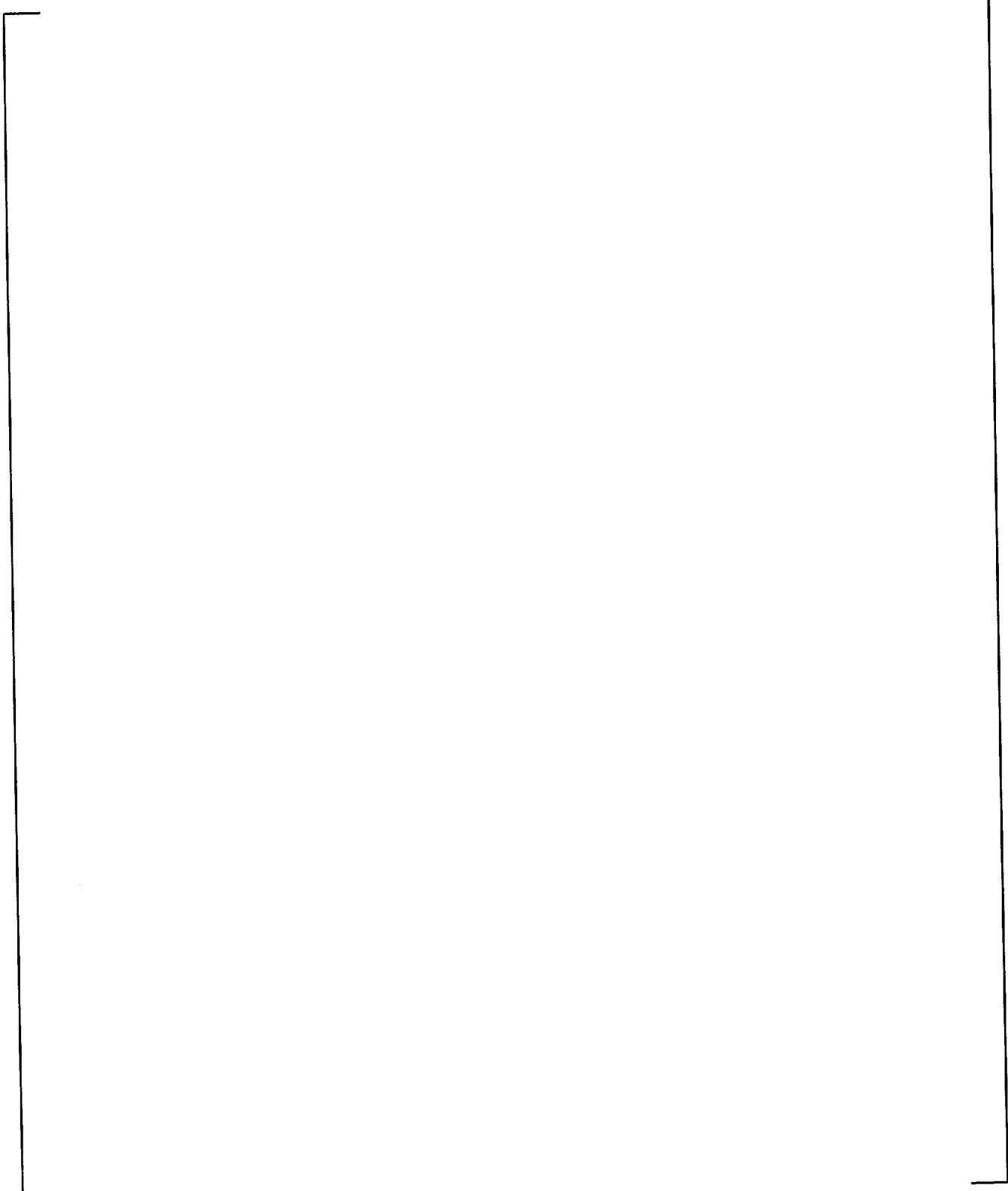


Figure 2-24 OSU Vessel Model – Section 3

a,c

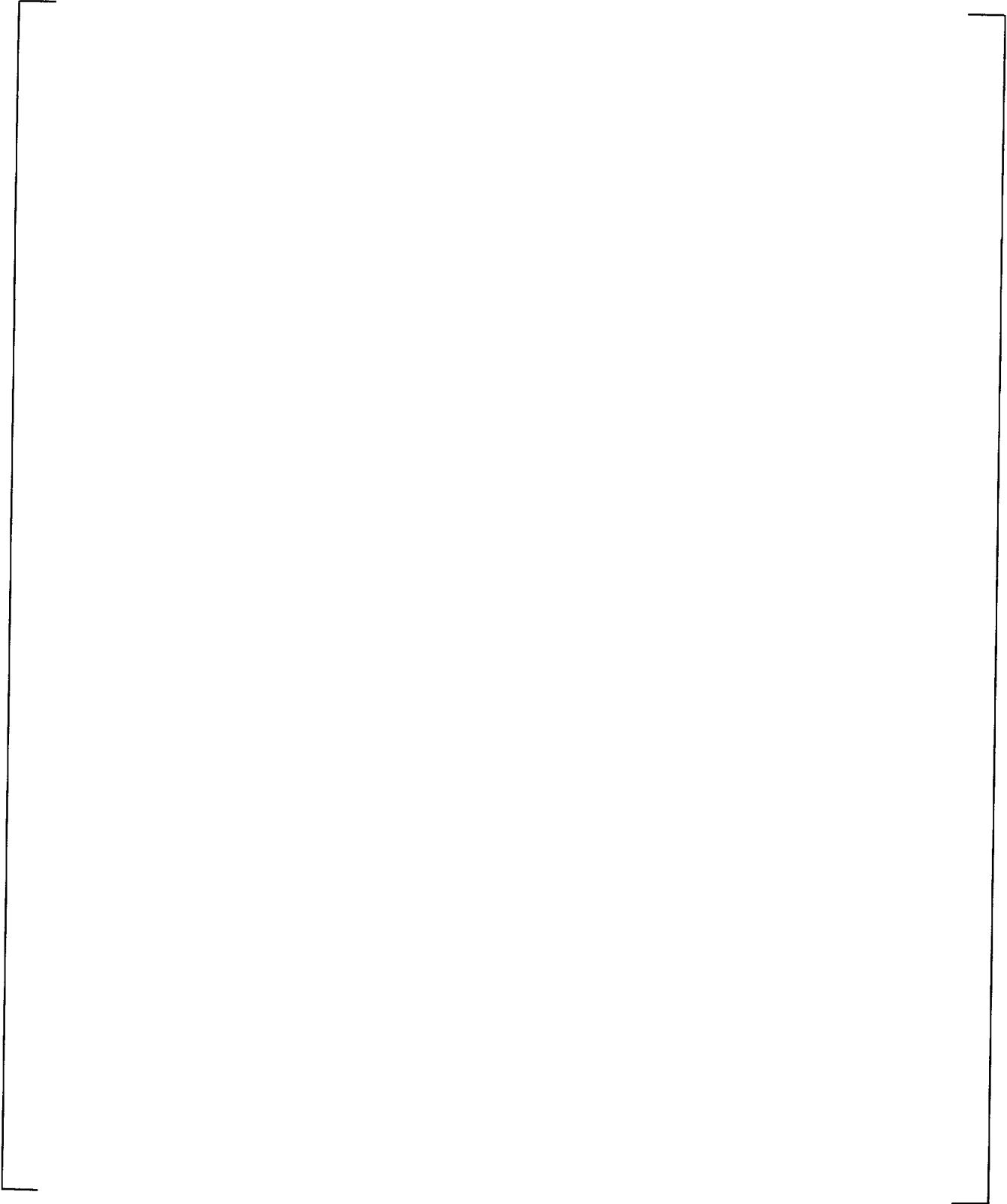


Figure 2-25 OSU Vessel Model – Section 4

a,c

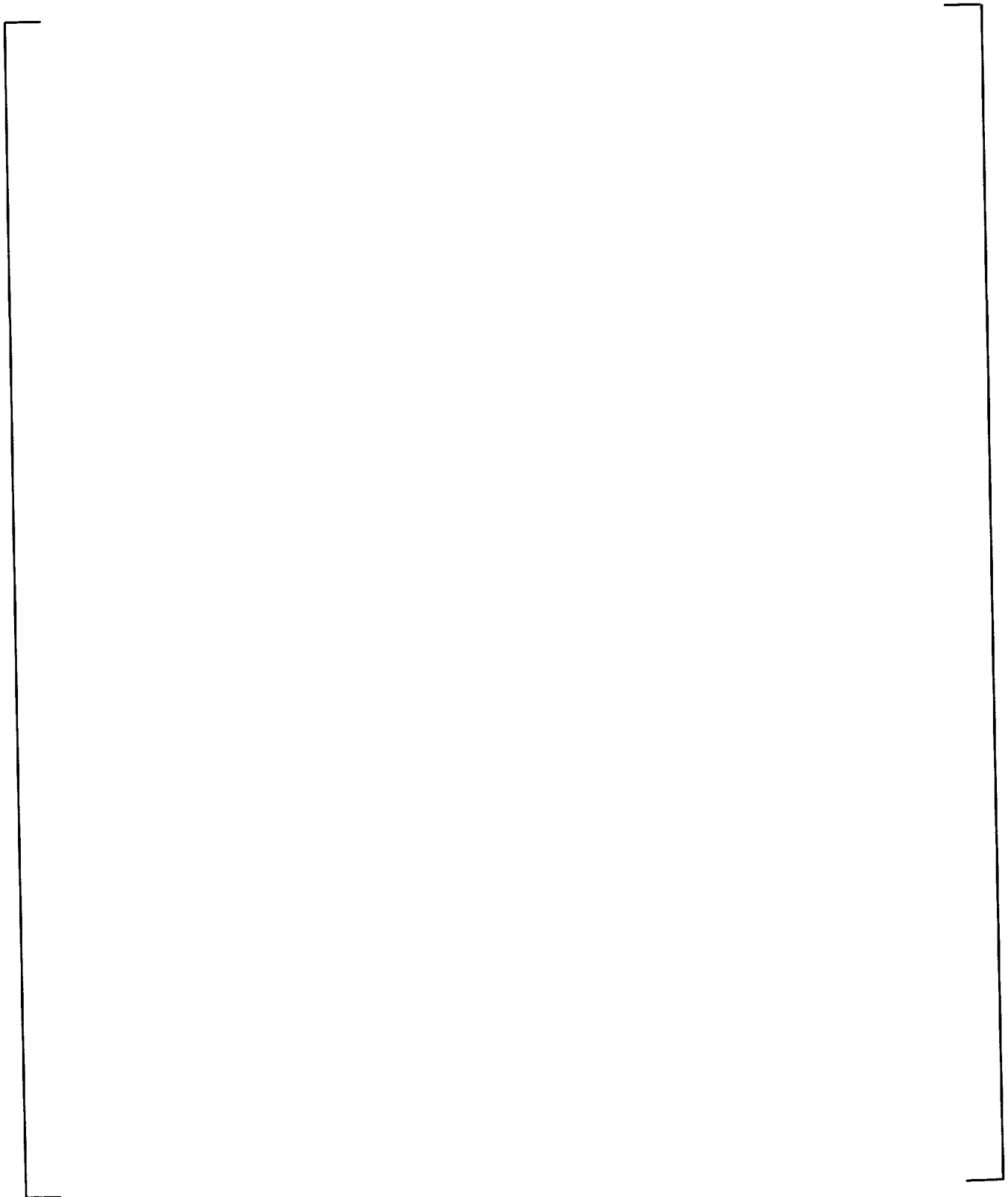


Figure 2-26 OSU Vessel Model – Section 5

a,c

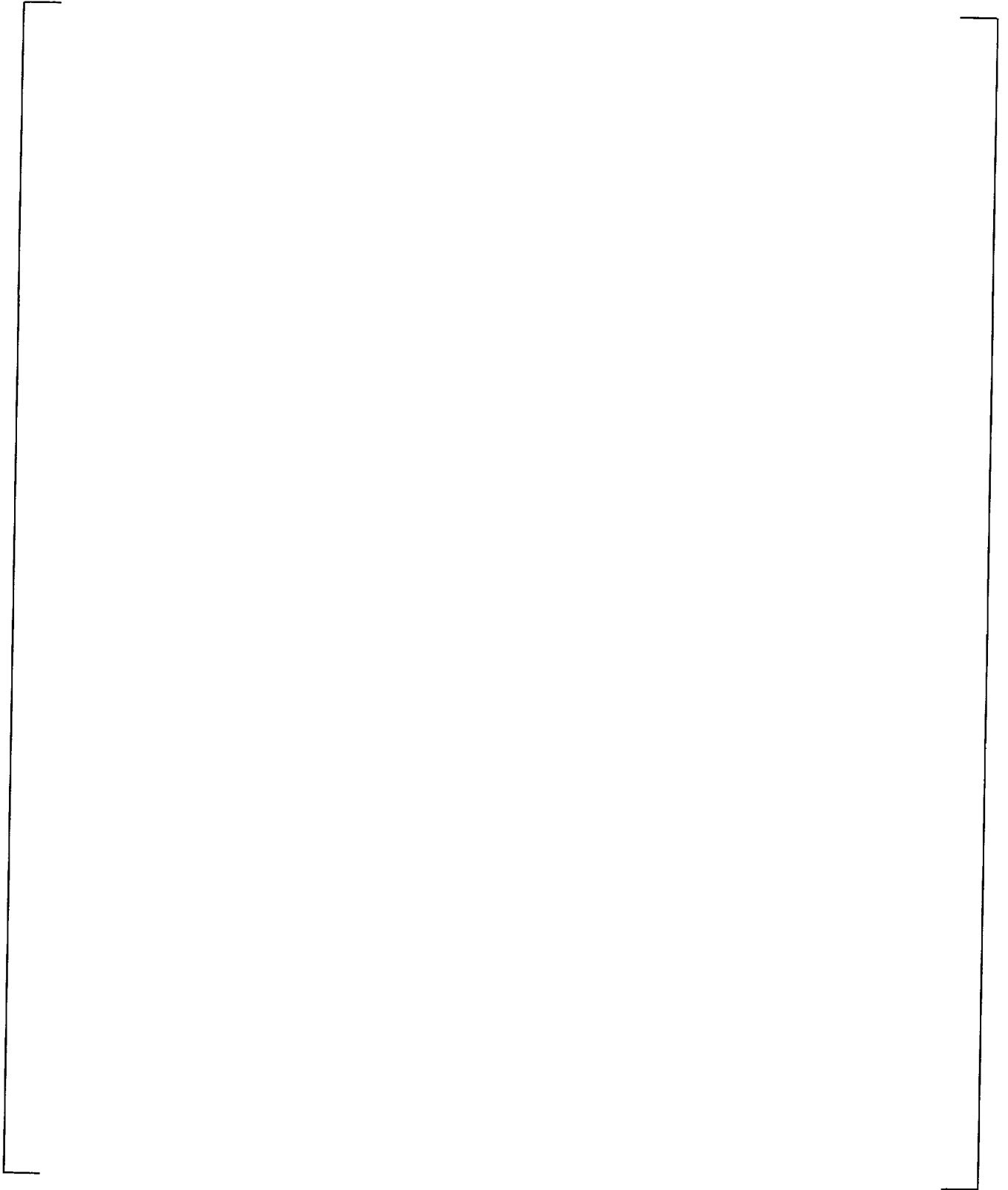


Figure 2-27 OSU Vessel Model – Section 6

a,c

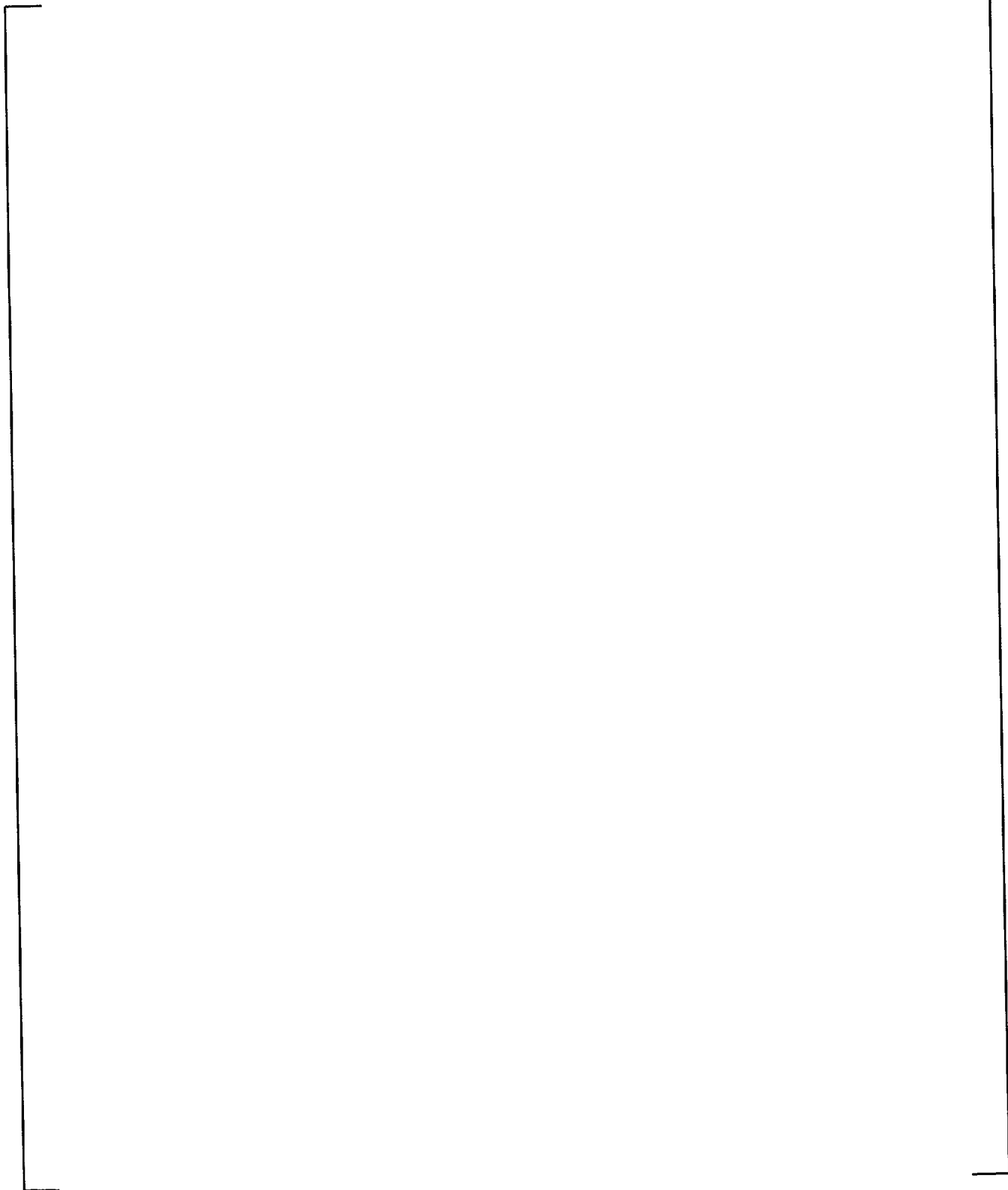


Figure 2-28 OSU Vessel Model – Section 7

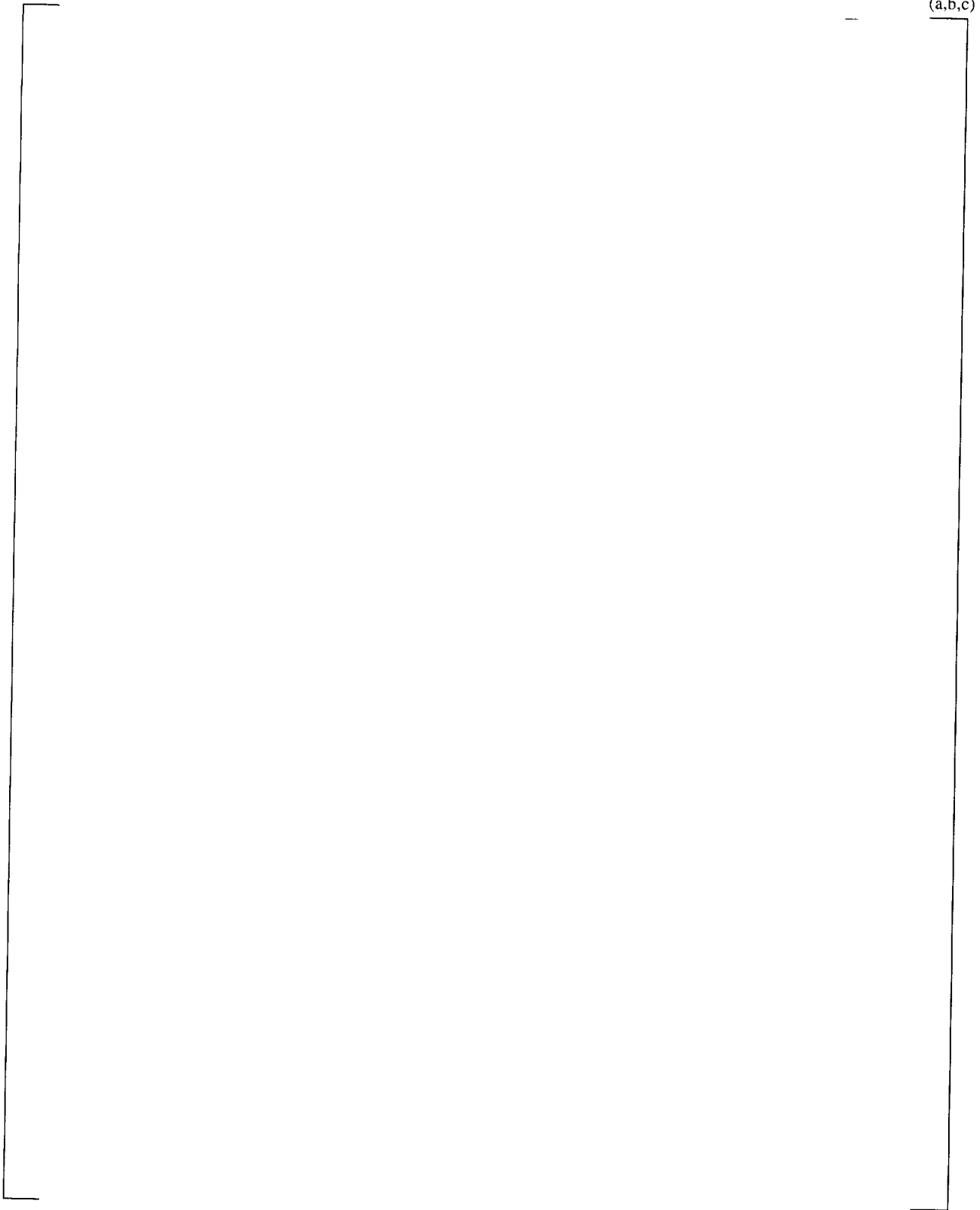


Figure 2-29 WCOBRA/TRAC Prediction vs. Test SB18 Data: Pressurizer Collapsed Liquid Level

(a,b,c)

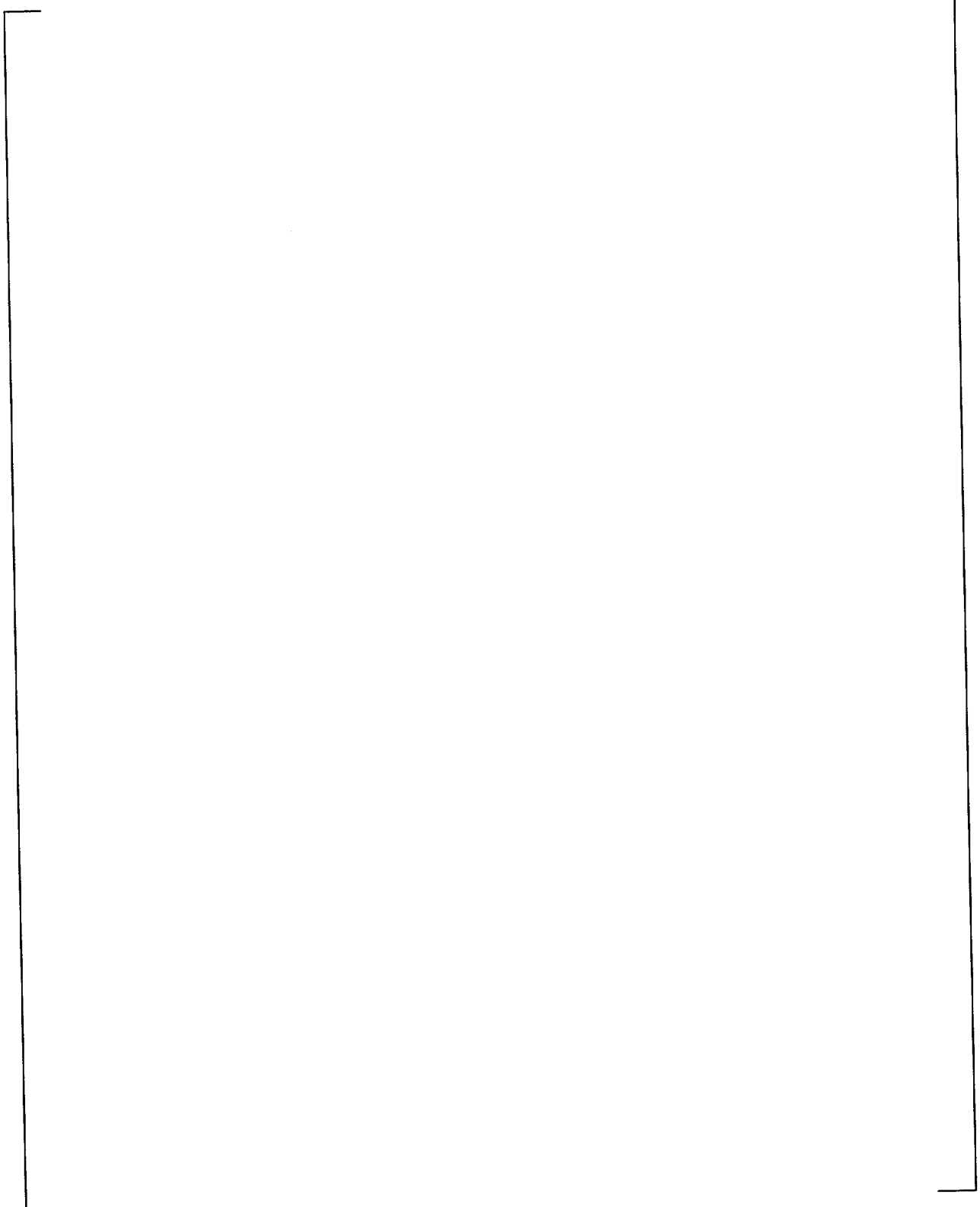


Figure 2-30 WCOBRA/TRAC Prediction vs. Test SB18 Data: Total ADS-4 Integrated Liquid Flow Rate

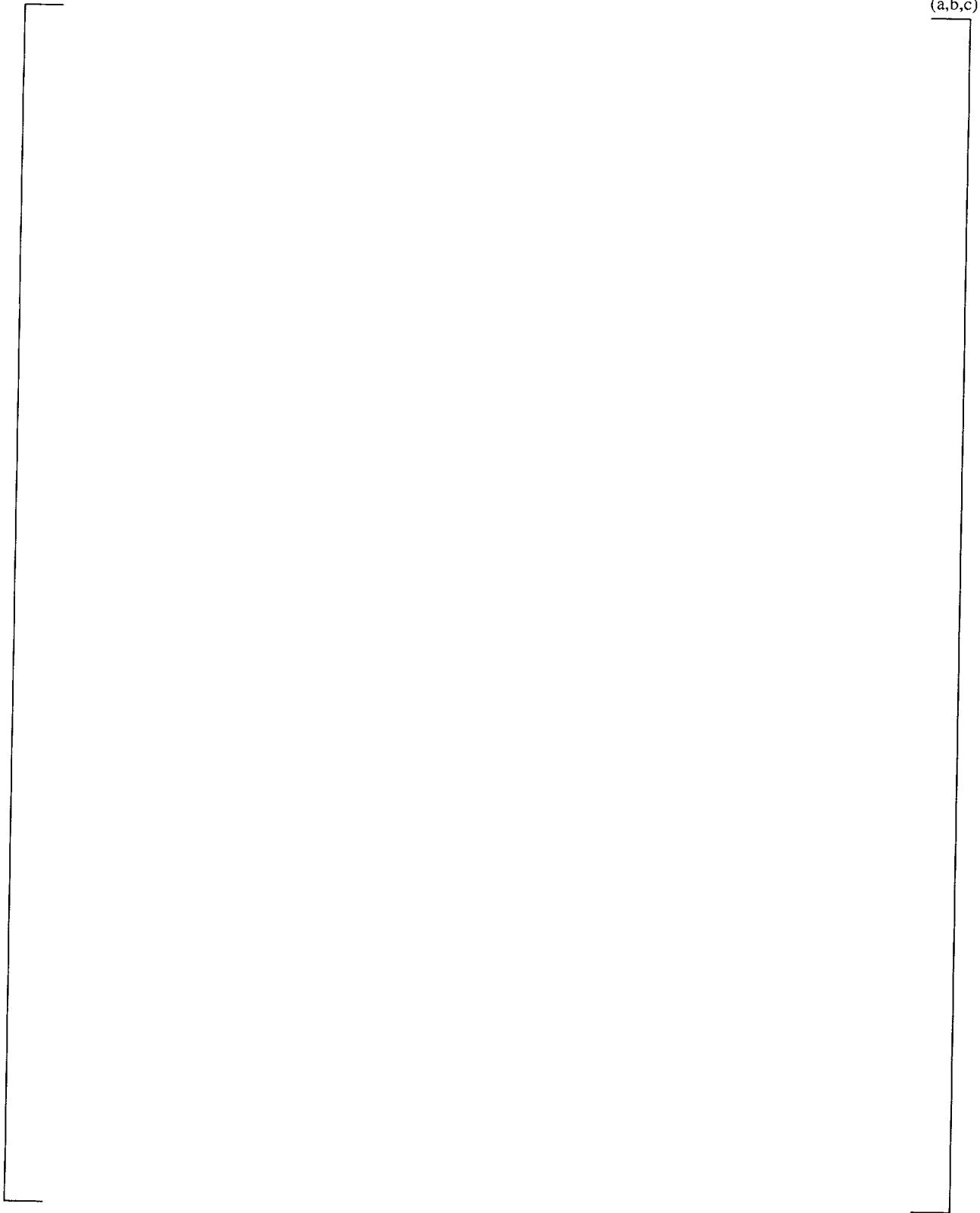


Figure 2-31 WCOBRA/TRAC Prediction of Test SB18 Downcomer Collapsed Liquid Level

(a,b,c)

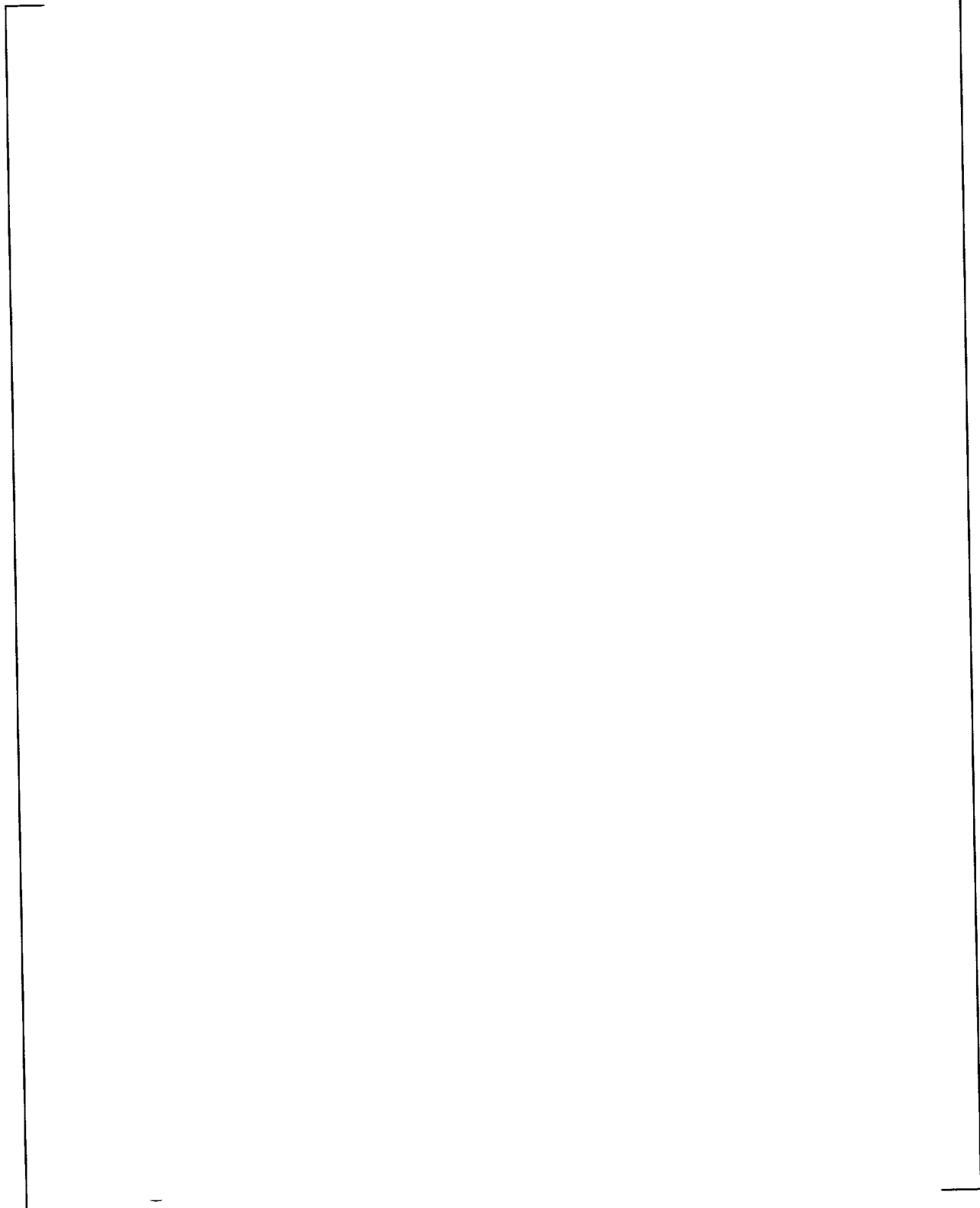


Figure 2-32 WCOBRA/TRAC Prediction of Test SB18 Core Collapsed Liquid Level

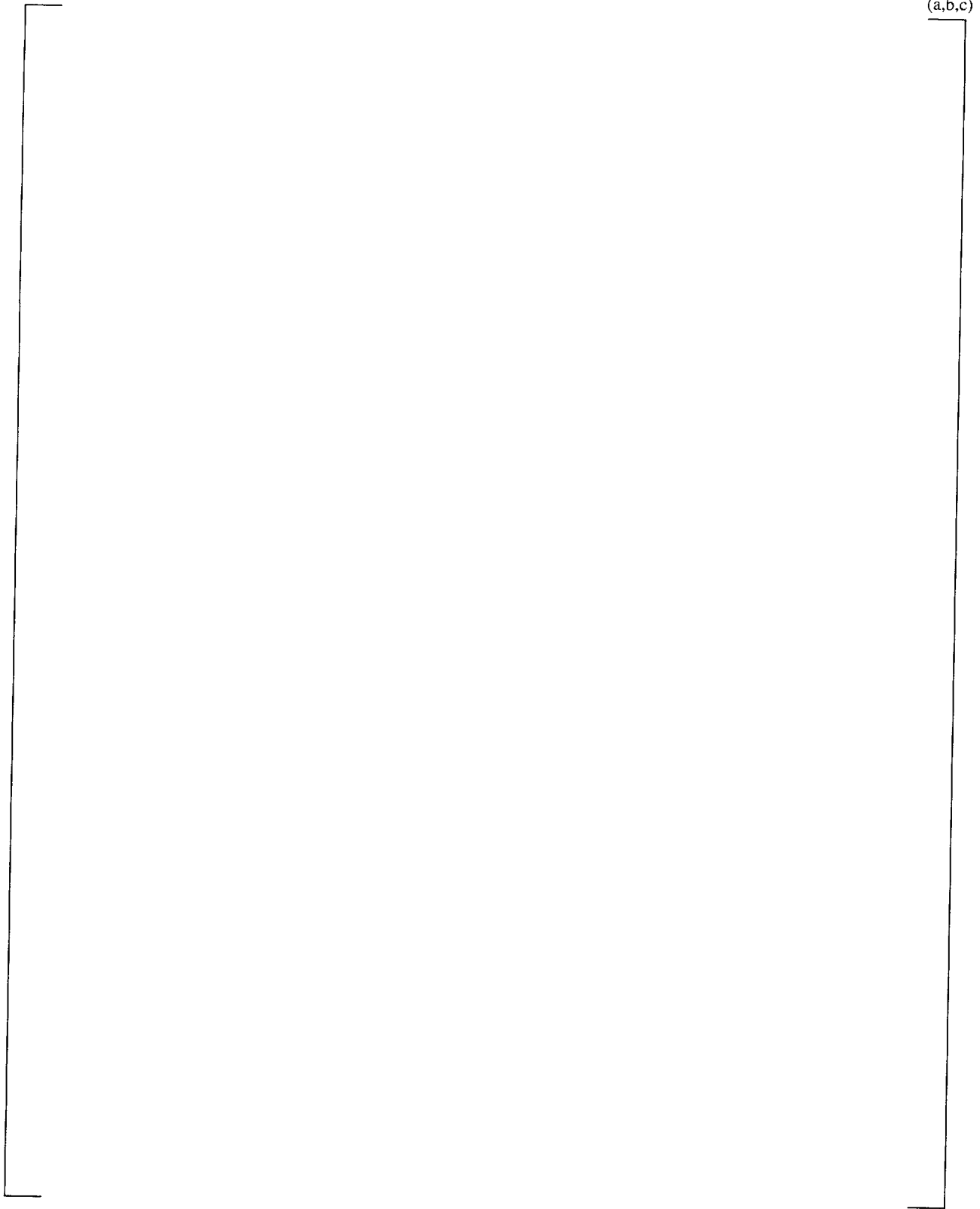


Figure 2-33 WCOBRA/TRAC Prediction of Test SB18 Core/Upper Plenum Collapsed Liquid Level

(a,b,c)

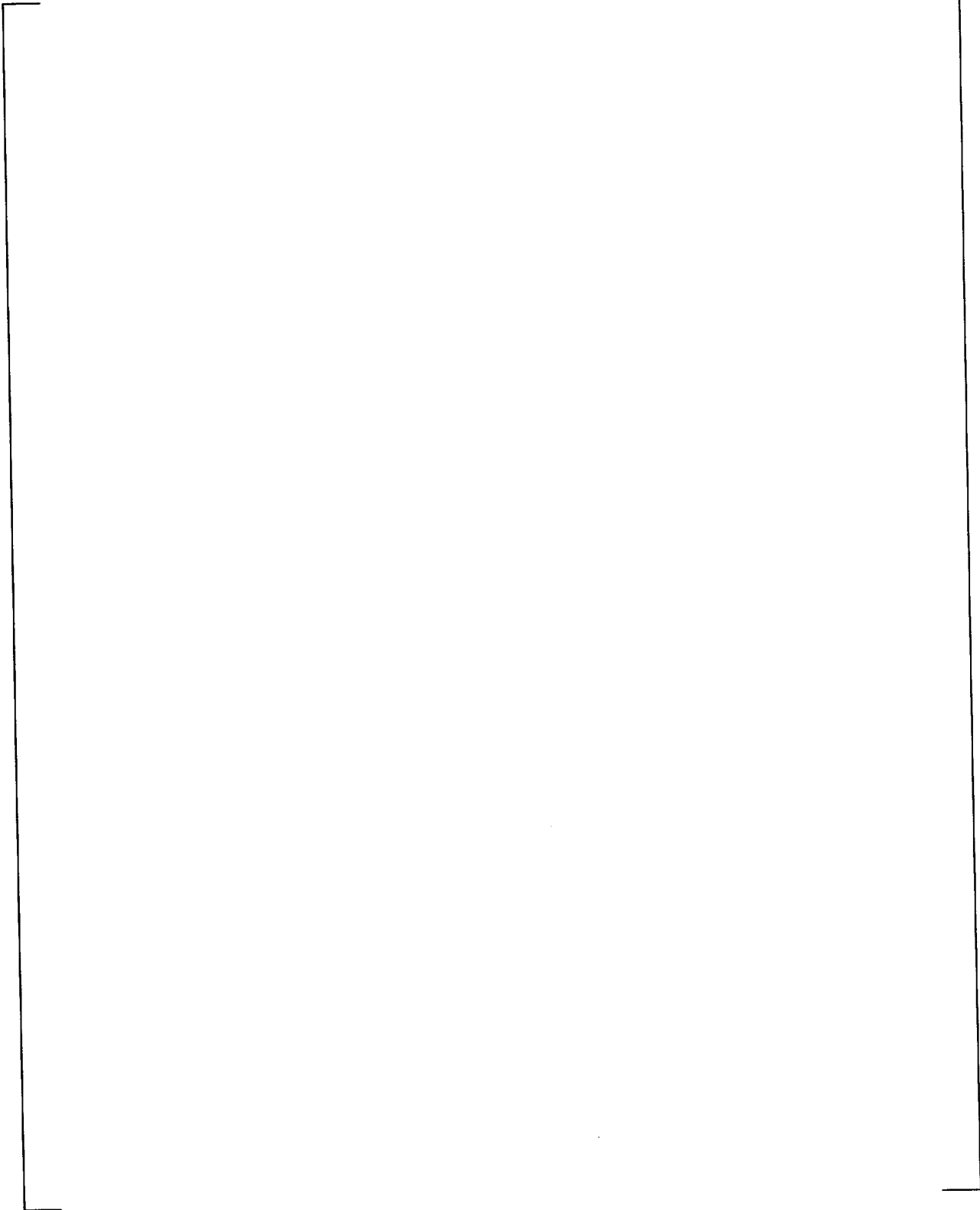


Figure 2-34 WCOBRA/TRAC Prediction vs. Test SB18 Data: Downcomer Pressure

3 AP1000 PLANT SIMULATIONS

The validation presented in Section 2 qualifies WCOBRA/TRAC to predict the ADS-4 IRWST initiation phase behavior of the AP1000. This section presents the AP1000 analyses performed in support of the NOTRUMP small break LOCA analysis in the AP1000 Design Control Document (DCD) (Reference 1).

3.1 PLANT MODELING

The WCOBRA/TRAC-AP nodalization to analyze the ADS-4 IRWST initiation phase transient for AP1000 is consistent with the OSU test facility model discussed in subsection 2.3.1. Figure 3-8 shows the components that are simulated in the AP1000 plant model. Junctions connecting components are identified with circles. The following subsections describe the modeling used to represent the main components.

3.1.1 Vessel Component

The WCOBRA/TRAC VESSEL component is shown in Figure 3-1. As shown, [

] ^{a,c}

Section 1, shown in Figure 3-2, represents the lower plenum; [

] ^{a,c}

Section 2, shown in Figure 3-3, represents [

] ^{a,c}

Sections 3 and 4, shown in Figures 3-4 and 3-5, represent [

] ^{a,c}

Sections 5 and 6, shown in Figures 3-6 and 3-7, both [

] ^{a,c}

Vertical flow channels simulate the axial flow paths, and [

] ^{a,c}

3.1.2 Primary Loop

The primary loop includes the following major components: [

] ^{a,c}

3.1.3 Pressurizer

The pressurizer vent line connects to the ADS Stages 1 to 3 (ADS 1–3) valves. Because [

] ^{a,c}

3.1.4 Steam Generators

The code's STGEN component models the SGs [

] ^{a,c}

3.1.5 Reactor Coolant Pumps

The RCPs are mounted on the SG lower plenums in AP1000. [

] ^{a,c}

3.1.6 Loop Lines

The code's PIPE and TEE components [

] ^{a,c}

3.1.7 Accumulators

The two accumulators are not modeled in the Inadvertent ADS Actuation scenario because they are empty before the ADS-4 IRWST initiation phase begins. For the DEDVI break simulation, [

] ^{a,c}.

3.1.8 Core Makeup Tanks

The core makeup tanks and the balance lines that connect the top of the CMTs to the cold legs [

] ^{a,c}

3.1.9 Passive Residual Heat Removal Heat Exchanger/In-Containment Refueling Water Storage Tank

Test data indicate that the passive residual heat removal heat exchanger (PRHR HX) is [

] ^{a,c}

3.1.10 In-Containment Refueling Water Storage Tank (IRWST)

[

] ^{a,c}

3.1.11 Automatic Depressurization System Stage 1 to 3 Valves

Components 48 and 88 model the ADS 1–3 valves. In the AP1000, each set of valves has two flow paths. These VALVE components are open during the ADS-4 IRWST initiation phase.

[

] ^{a,c}

3.1.12 Automatic Depressurization System Stage 4 Valves

Components 159, 199, 259, and 299 represent ADS Stage 4 valves. Each hot leg has two ADS-4 flow paths. The limiting single failure of an ADS Stage 4 valve to actuate is modeled in WCOBRA/TRAC as the failure of component 159. Component 199 opens when the ADS-4 actuation signal is received, and components 259 and 299 open 60 seconds later.

3.1.13 Safety Injection During the ADS-4 IRWST Initiation Phase

As in the OSU Test SB18 simulation, [

] ^{a,c} Component 777 is the FILL component attached to the second intact DVI line in the Inadvertent ADS scenario.

[

] ^{a,c}

3.1.14 Break Component

The code's BREAK component [

] ^{a,c}

Each open ADS-4 flow path consists of a large diameter pipe leading into a constricted area at the squib valve location. A specific model to simulate this orifice-like break geometry was generated as documented in Reference 3 as the "Small break LOCA break model." This model is applied to calculate the flow rate through the valves at the end of the ADS-4 flow paths. It is also used to model the flow through the venturi of the broken DVI pipe in the DEDVI break simulation.

3.1.15 Initial and Boundary Conditions

The initial conditions used in the AP1000 [

is used in the WCOBRA/TRAC simulation.

] ^{a,c} 10CFR50 Appendix K core decay heat

3.2 LIMITING CASE RESULTS

Two cases from the AP1000 DCD Section 15.6.5.4B small break LOCA analysis are analyzed, the double-ended DVI line break at 25 psia containment pressure and the inadvertent ADS actuation case. These are the minimum passive safety injection flow and the minimum reactor coolant system venting capability cases, respectively, from the AP1000 DCD small break LOCA analyses. In each case, the failure of one ADS-4 valve to open is assumed. For the DEDVI break, Component 778 is the broken DVI pipe instead of an intact injection line. WCOBRA/TRAC simulations of the ADS-4 IRWST initiation phase of these cases are compared with the corresponding NOTRUMP predictions, from Section 15.6.5.4B of the AP1000 DCD, in the following sections.

3.2.1 Double-Ended DVI Line Break

The double-ended DVI line break is the minimum passive safety injection flow capability case from the AP1000 DCD. The failure of one ADS-4 valve to open is assumed in both simulations. The WCOBRA/TRAC simulation of the ADS-4 IRWST initiation phase of the DEDVI line break is compared

with the corresponding NOTRUMP predictions from Section 15.6.5.4B of the AP1000 DCD in this section. The Appendix K-specified ANS 1971 + 20% core decay heat is used in both analyses.

Figure 3-9 presents the WCOBRA/TRAC downcomer pressure prediction of the ADS-4 IRWST initiation phase superimposed on the NOTRUMP result from Section 15.6.5.4B of the AP1000 DCD. The actuation of ADS-4 occurs at 492 seconds. Opening of the ADS-4 flow paths continues the RCS depressurization from approximately 100 psia down to near containment pressure. The RCS pressure tends to stabilize when the energy being discharged from the RCS approaches the energy from the core decay heat and from metal heat. The NOTRUMP prediction levels off in the rate of depressurization at a higher pressure than the WCOBRA/TRAC prediction. This is expected because at a given fluid pressure and quality, the small-break LOCA break flow model in WCOBRA/TRAC delivers more flow through the ADS-4 flow paths than does NOTRUMP using its critical flow model and the ADS-4 flow path resistance increase methodology. Depressurization to the IRWST actuation pressure occurs more rapidly in WCOBRA/TRAC than in NOTRUMP due to the increased rate of energy removal. The IRWST flow rates upon actuation are compared in Figure 3-10. The core makeup tanks still contain a significant amount of water at the time of IRWST injection in the two analyses. The intact CMT and accumulator flow rate is shown in Figure 3-11.

The ADS-4 predicted liquid and vapor flow rates of the two code simulations are compared in Figures 3-12 to 3-15. The more detailed flow regime models and the small-break LOCA break flow model in WCOBRA/TRAC result in higher flow rates through the ADS-4 flow paths.

Comparison of calculated reactor vessel inventory is shown in Figure 3-16. The earlier IRWST injection for the WCOBRA/TRAC case results in the earlier establishment of a stable vessel inventory, which is being replenished by injection from the CMT and IRWST.

The higher WCOBRA/TRAC flow rate through the ADS-4 flow paths also results in a higher mass flow rate through the core than in the NOTRUMP prediction as shown in Figure 3-17. The higher core cooling flow predicted by WCOBRA/TRAC provides a more dynamic heat transfer environment than in NOTRUMP. In both cases, the heat transfer regime on the fuel rods enables the clad temperatures to remain near the coolant saturation temperature.

3.2.2 Inadvertent ADS Actuation Scenario

The Inadvertent ADS scenario is the minimum venting capability case from the AP1000 DCD. The failure of one ADS-4 valve to open is assumed in both simulations. The WCOBRA/TRAC simulation of the ADS-4 IRWST initiation phase of this scenario is compared with the corresponding NOTRUMP predictions from Section 15.6.5.4B of the AP1000 DCD in this section. The Appendix K-specified ANS 1971 + 20% core decay heat is used in both analyses.

Figure 3-18 presents the WCOBRA/TRAC downcomer pressure prediction of the ADS-4 IRWST initiation phase superimposed on the NOTRUMP result from Section 15.6.5.4B of the AP1000 DCD. The actuation of ADS-4 occurs at 1746 seconds. Opening of the ADS-4 flow paths continues the RCS depressurization from approximately 100 psia down to near containment pressure. The RCS pressure tends to stabilize when the energy being discharged from the RCS approaches the energy from the core decay heat and from metal heat. The NOTRUMP prediction levels off in the rate of depressurization at a

higher pressure than the WCOBRA/TRAC prediction. This is expected because at a given fluid condition, the best estimate break flow model in WCOBRA/TRAC delivers more flow through the ADS-4 flow paths than does NOTRUMP using its critical flow model and the ADS-4 flow path resistance increase methodology. Depressurization to the IRWST actuation pressure occurs more rapidly in WCOBRA/TRAC than in NOTRUMP due to the increased rate of energy removal. The IRWST flow rates upon actuation are compared in Figure 3-19. In the WCOBRA/TRAC analysis the IRWST begins to inject before the core makeup tanks have emptied, so there is no gap in safety injection flow. In contrast, NOTRUMP predicts a period almost 10 minutes in length during which no safety injection water is delivered into the reactor vessel. The CMT injection flow rate is shown in Figure 3-20.

The ADS-4 predicted liquid and vapor flow rates of the two code simulations are compared in Figures 3-21 to 3-24. The more detailed flow regime models and the best estimate break flow model in WCOBRA/TRAC result in higher flow rates through the ADS-4 flow paths.

Comparison of calculated reactor vessel inventory is shown in Figure 3-25. The earlier IRWST injection for the WCOBRA/TRAC case results in an earlier recovery of vessel inventory. In both cases the inventory begins to increase once the RCS pressure stabilizes and as decay heat decreases. Inventory is being replenished by injection from the CMT and/or IRWST. The minimum vessel inventory is approximately the same in the WCOBRA/TRAC and NOTRUMP predictions on Figure 3-25. In Figure 3-25 the NOTRUMP plot is adjusted to account for a 3% volume increase introduced according to the Appendix K methodology.

The higher WCOBRA/TRAC flow rate through the ADS-4 flow paths also results in a higher mass flow rate through the core than in the NOTRUMP prediction as shown in Figure 3-26. The higher core cooling flow predicted by WCOBRA/TRAC provides a more dynamic heat transfer environment than in NOTRUMP. In both cases, the heat transfer regime on the fuel rods enables the clad temperatures to remain near the coolant saturation temperature.

3.3 REFERENCES

1. AP1000 Design Control Document, Westinghouse Electric Company LLC, Revision 2, April 2002.
2. Takeuchi, Kenji, Young, M. Y., and Gagnon, A. F., "Flooding in the Pressurizer Surge Line of AP600 Plant and Analyses of APEX Data," Nuclear Engineering & Design 192 (1999), pp. 45-58.
3. WCOBRA/TRAC User's Manual, Revision 9, September 2001, Westinghouse Electric Company, Proprietary.

a,c

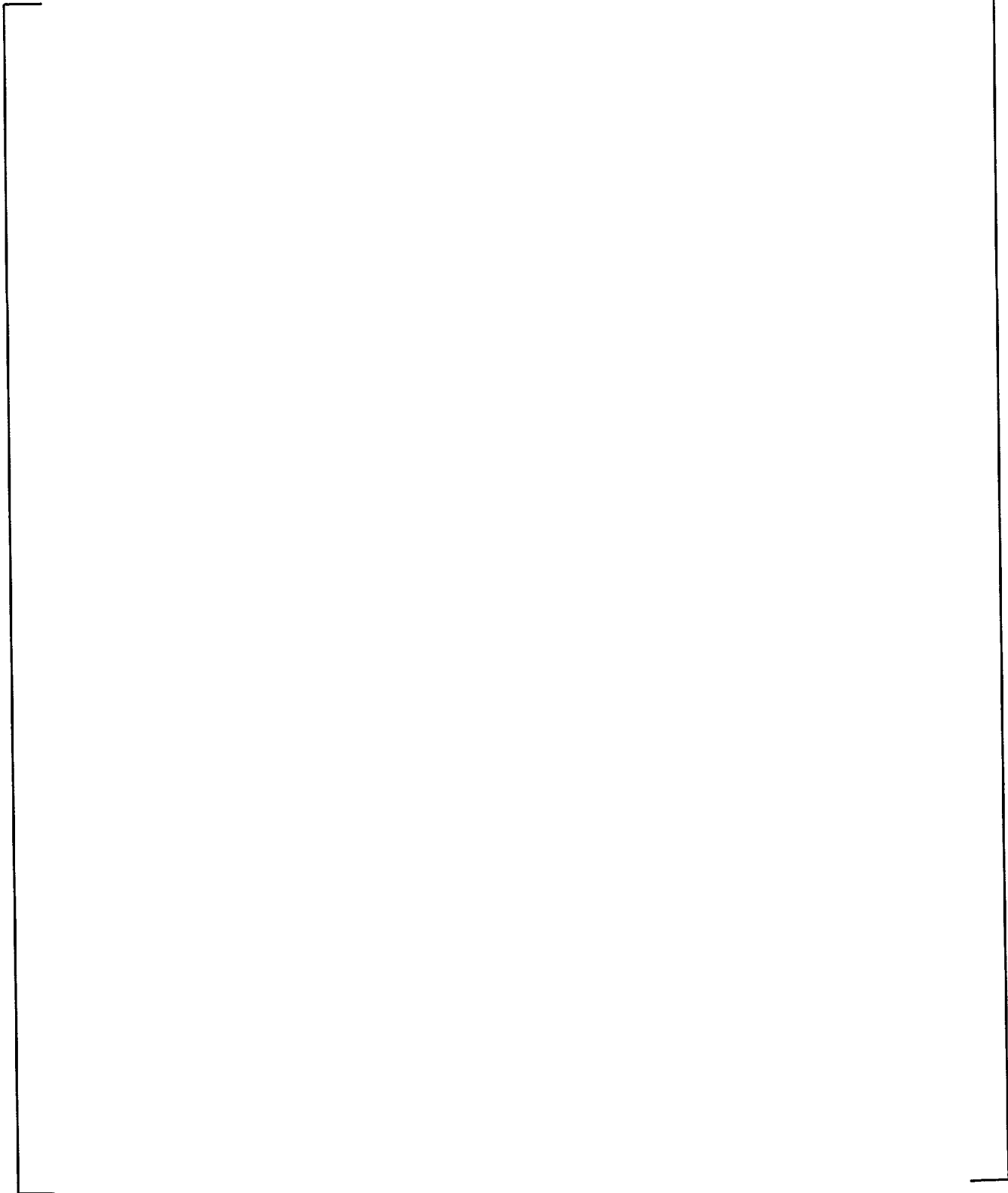


Figure 3-1 AP1000 WCOBRA/TRAC Vessel Model (Front View)

a,c

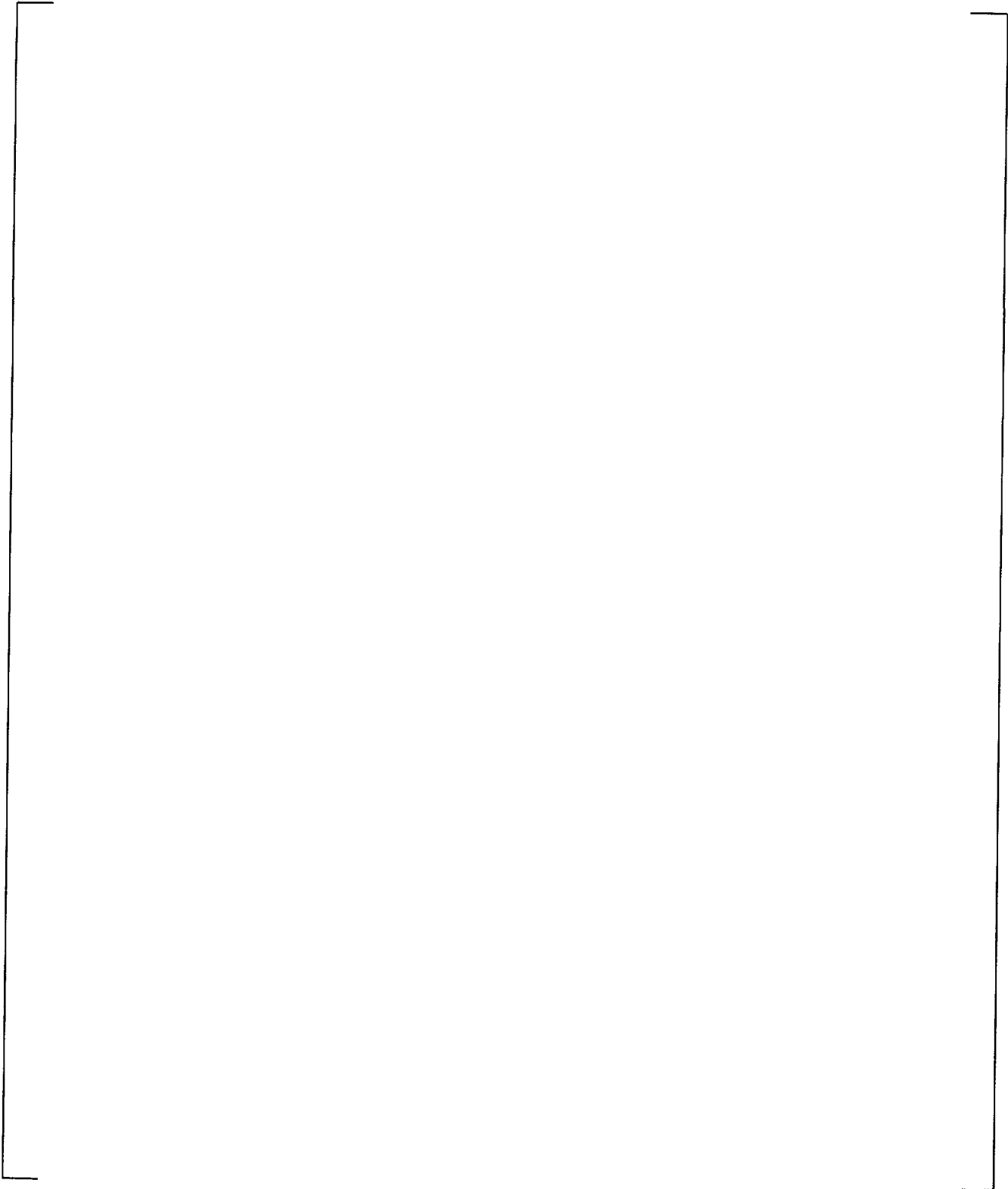


Figure 3-2 AP1000 Vessel Model – Section 1

a,c

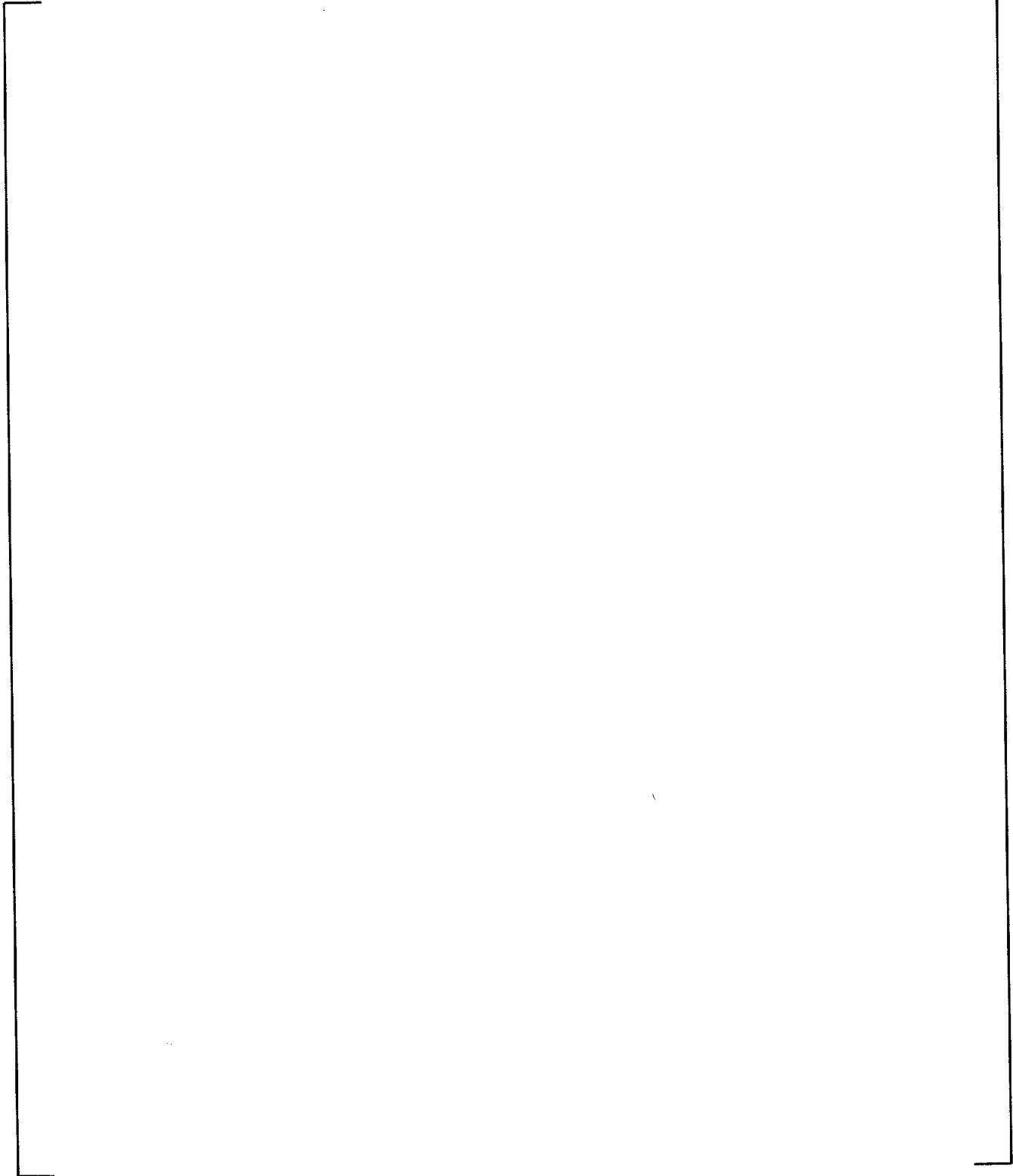


Figure 3-3 AP1000 Vessel Model – Section 2

a,c

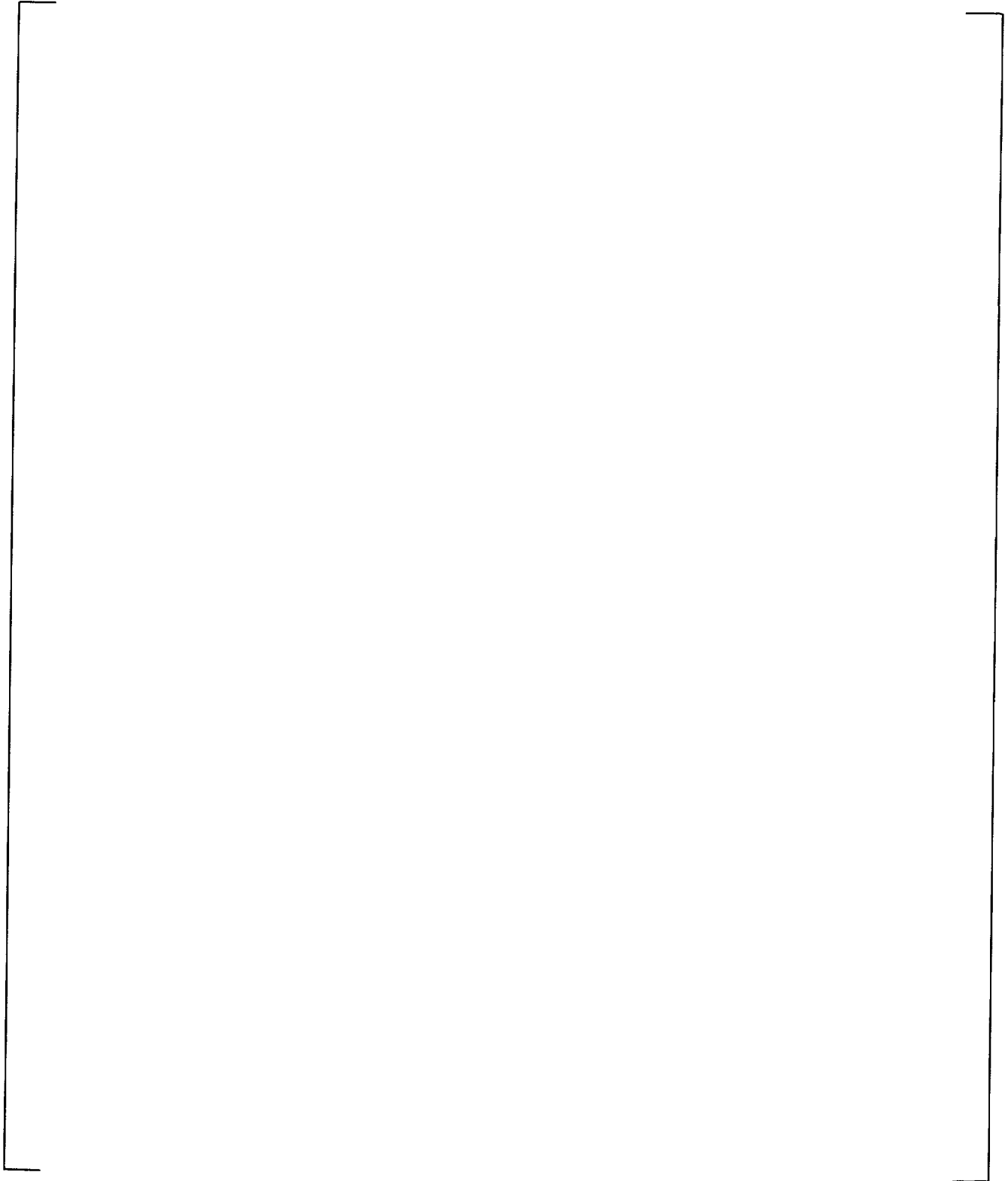


Figure 3-4 AP1000 Vessel Model – Section 3

a,c

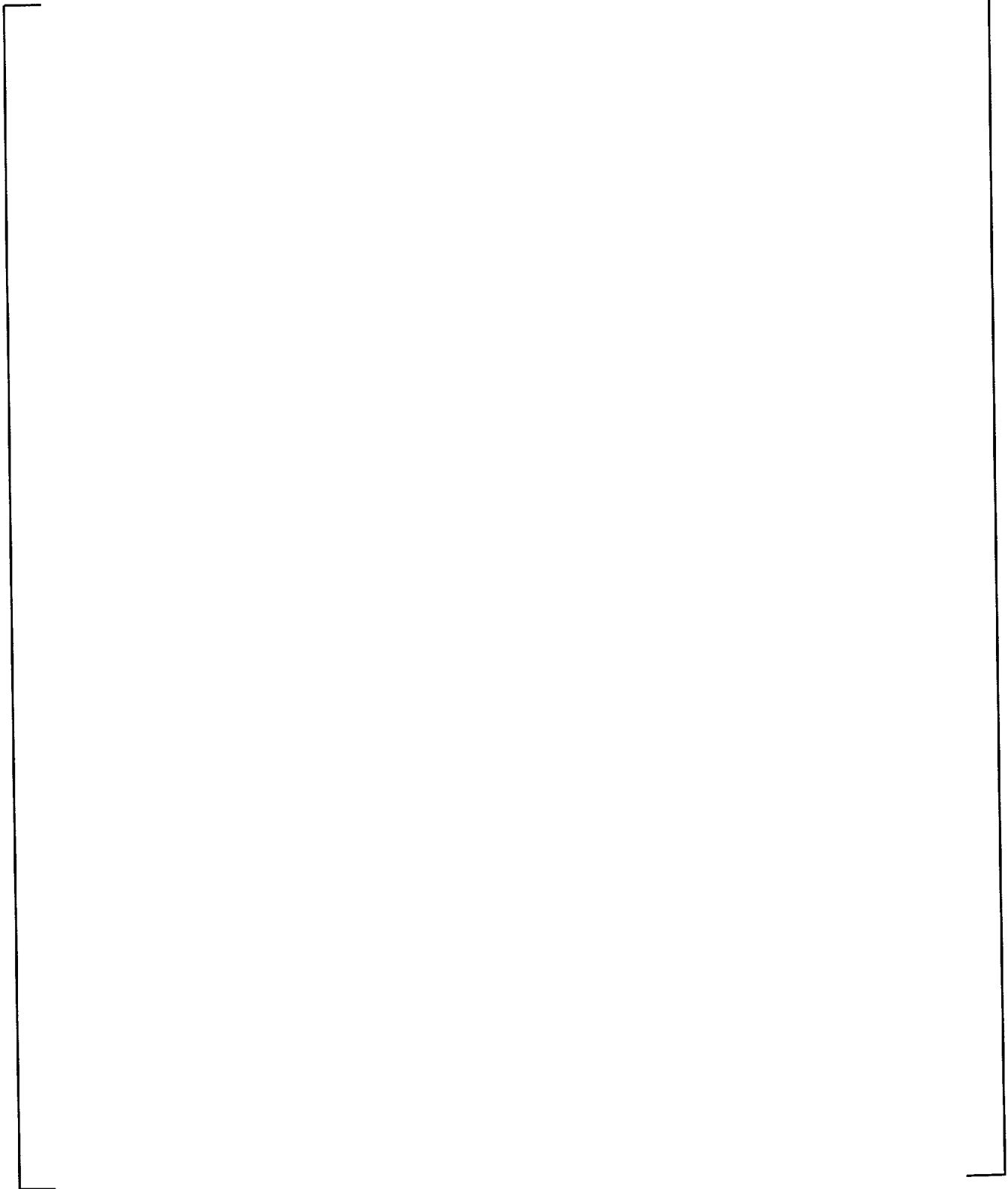


Figure 3-5 AP1000 Vessel Model – Section 4

a,c

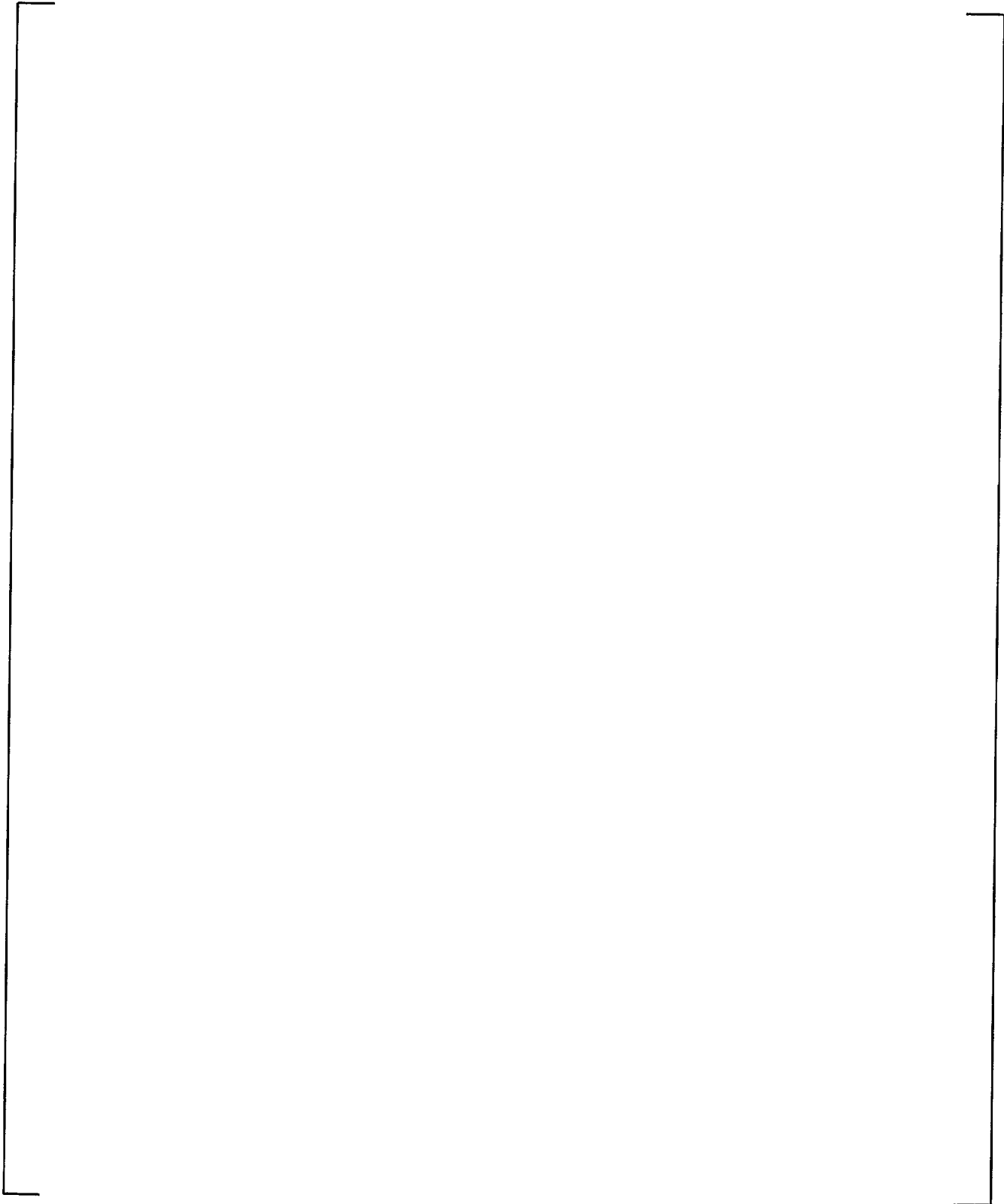


Figure 3-6 AP1000 Vessel Model – Section 5

a,c

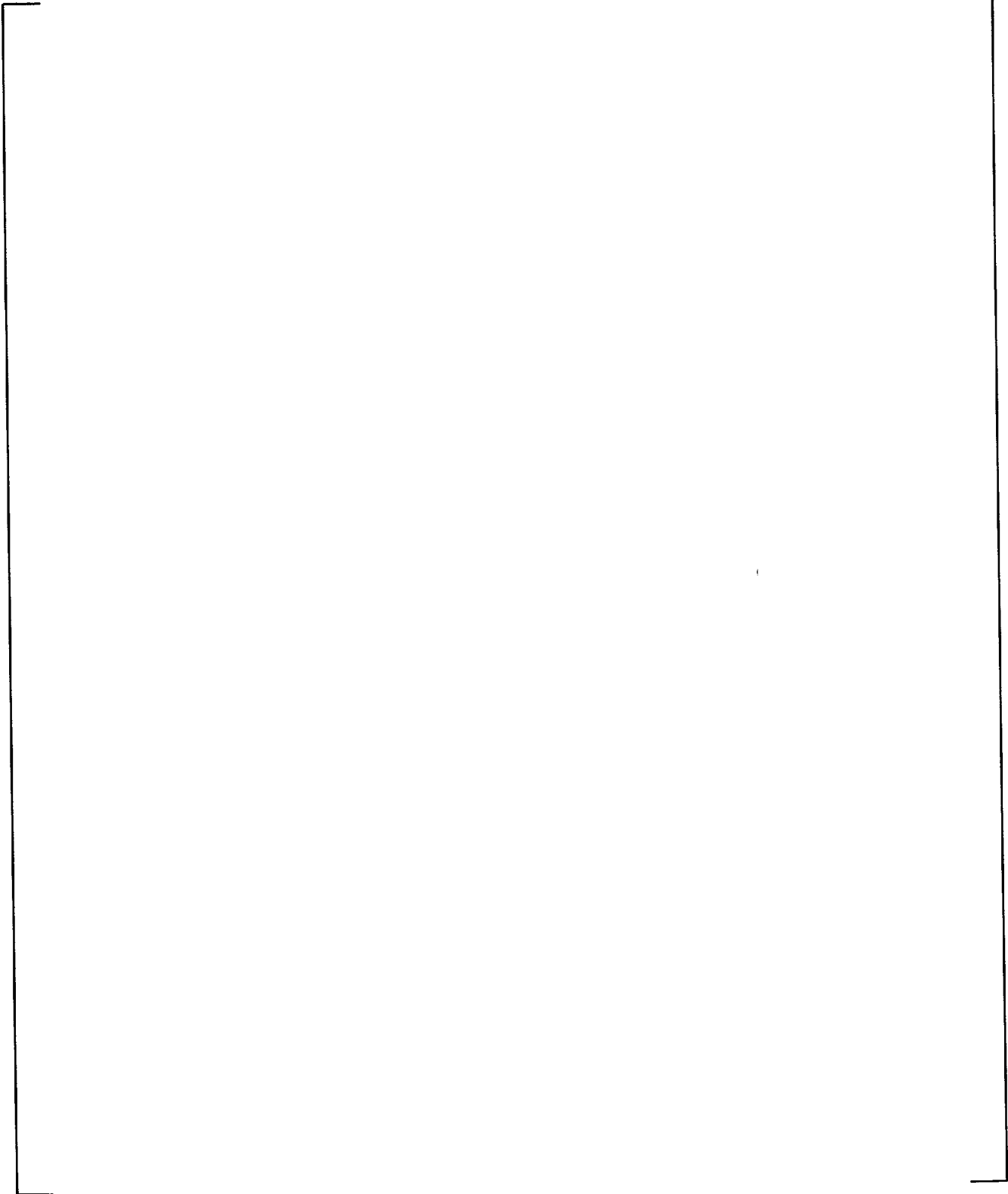


Figure 3-7 AP1000 Vessel Model – Section 6

a,c

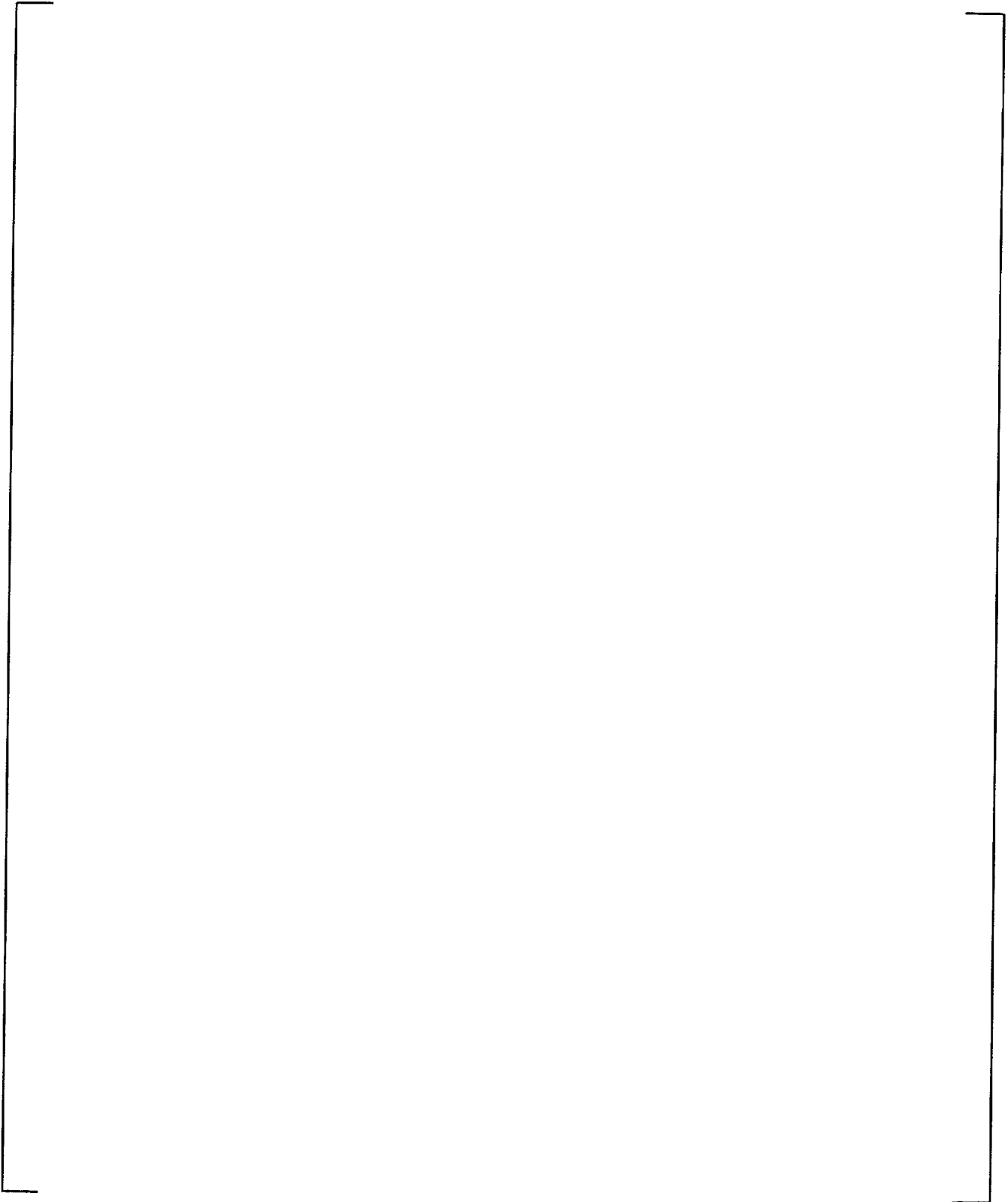


Figure 3-8 AP1000 WCOBRA/TRAC Schematic Diagram

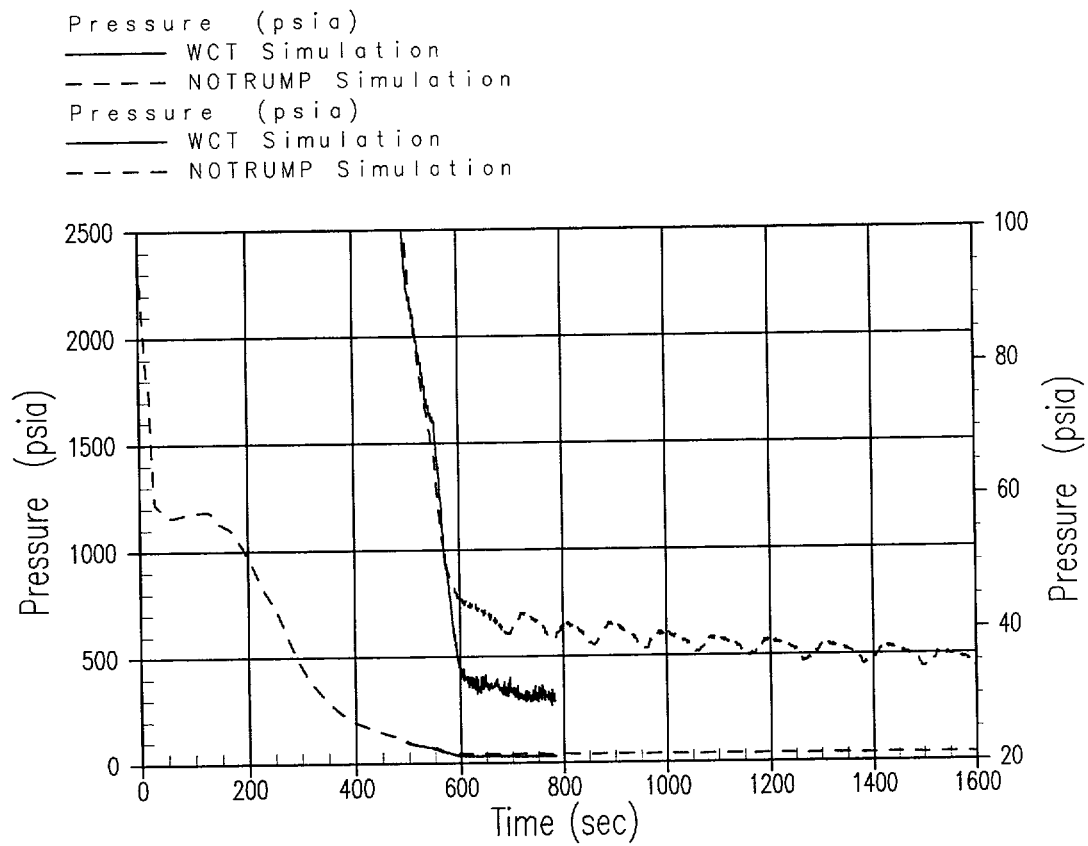


Figure 3-9 AP1000 DEDVI Break Downcomer Pressure

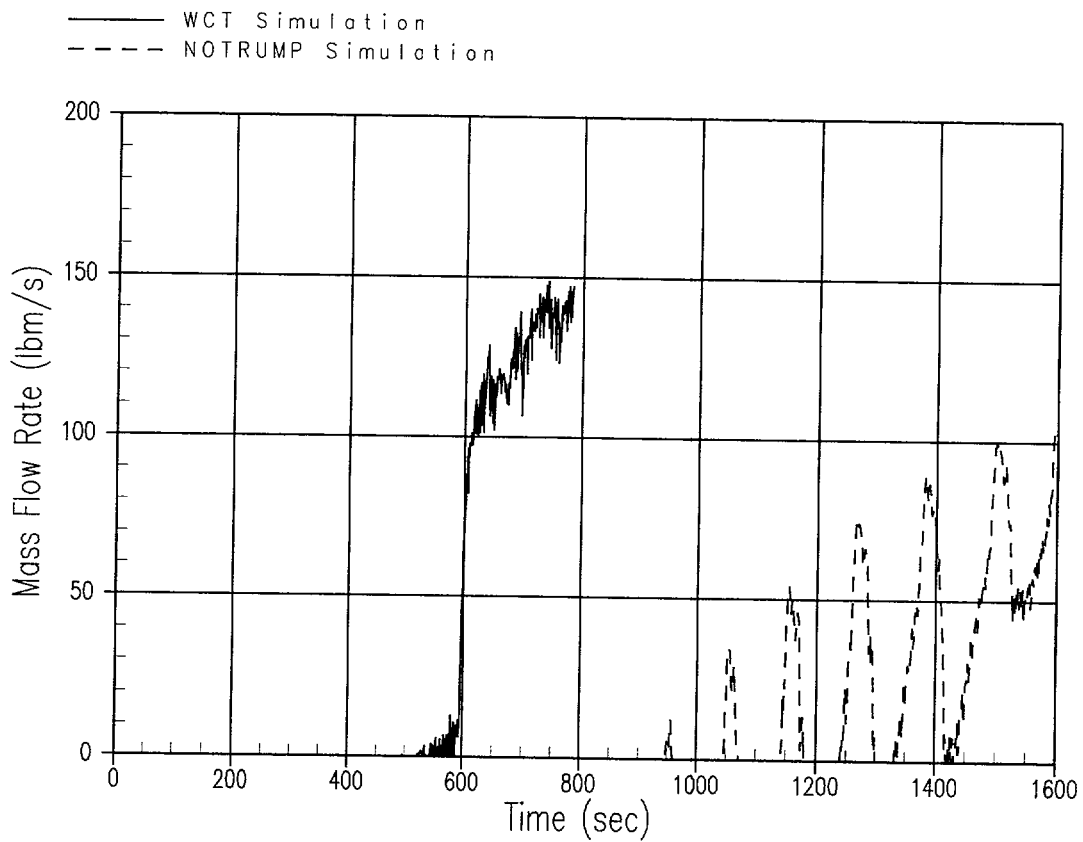


Figure 3-10 AP1000 DEDVI Break IRWST Flow Rate

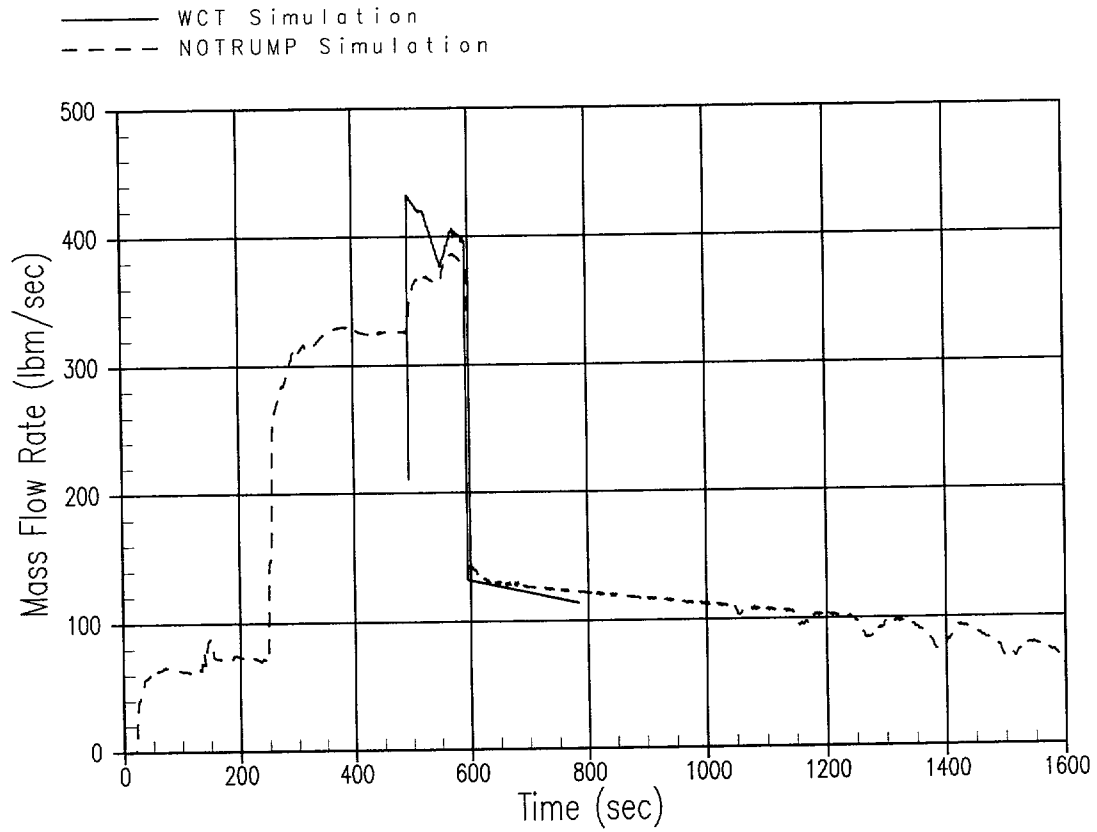


Figure 3-11 AP1000 DEDVI Break CMT and Accumulator Flow Rate

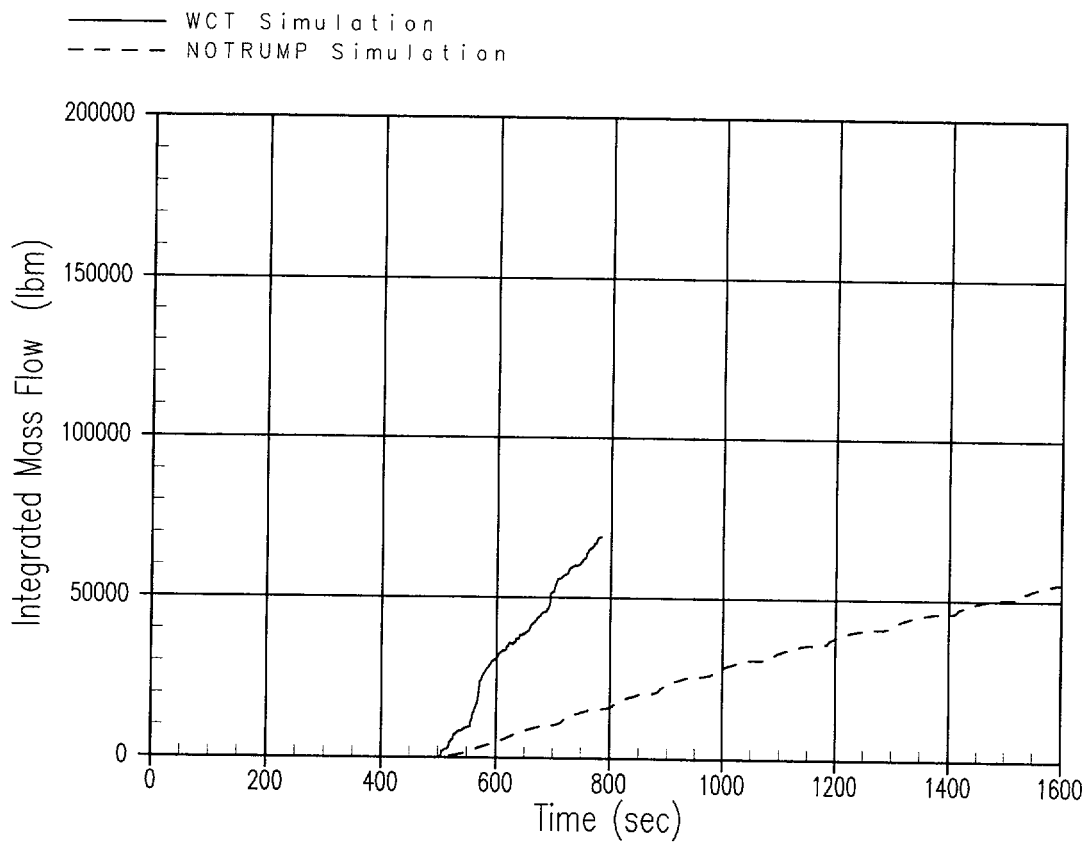


Figure 3-12 AP1000 DEDVI Break Intact Loop ADS-4 – Integrated Liquid Flow

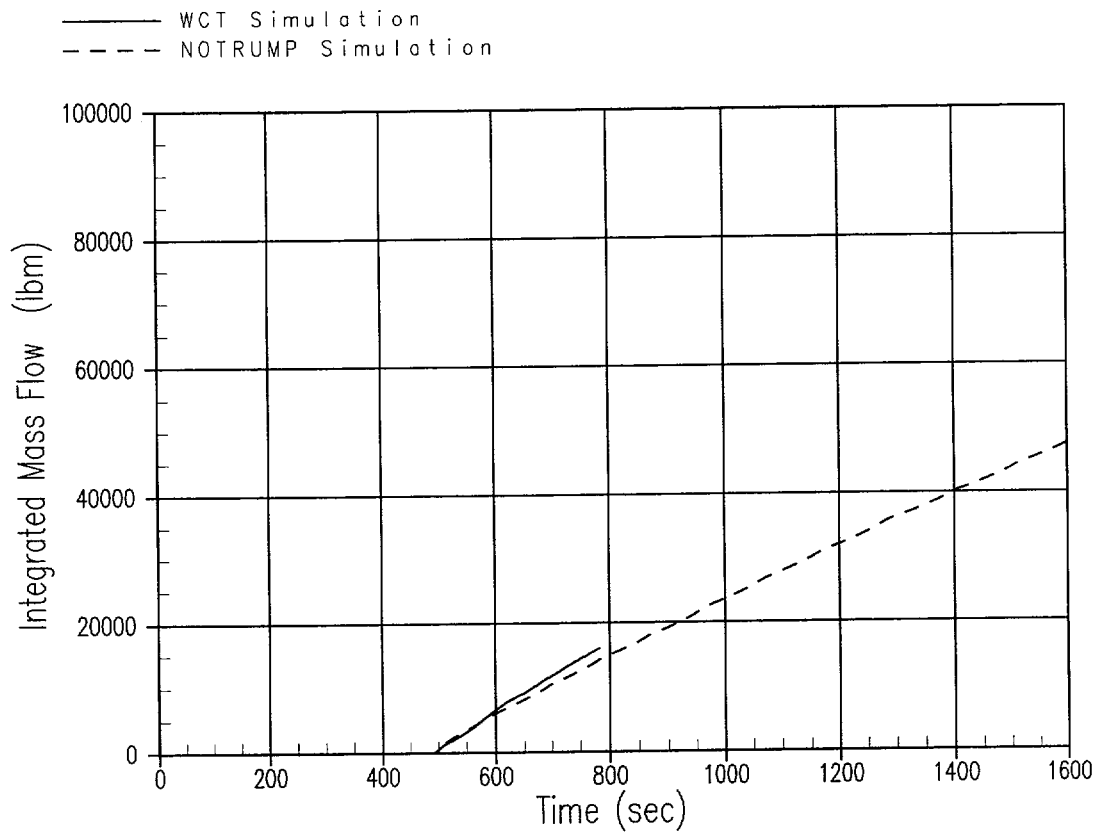


Figure 3-13 AP1000 DEDVI Break Intact Loop ADS-4 – Integrated Vapor Flow

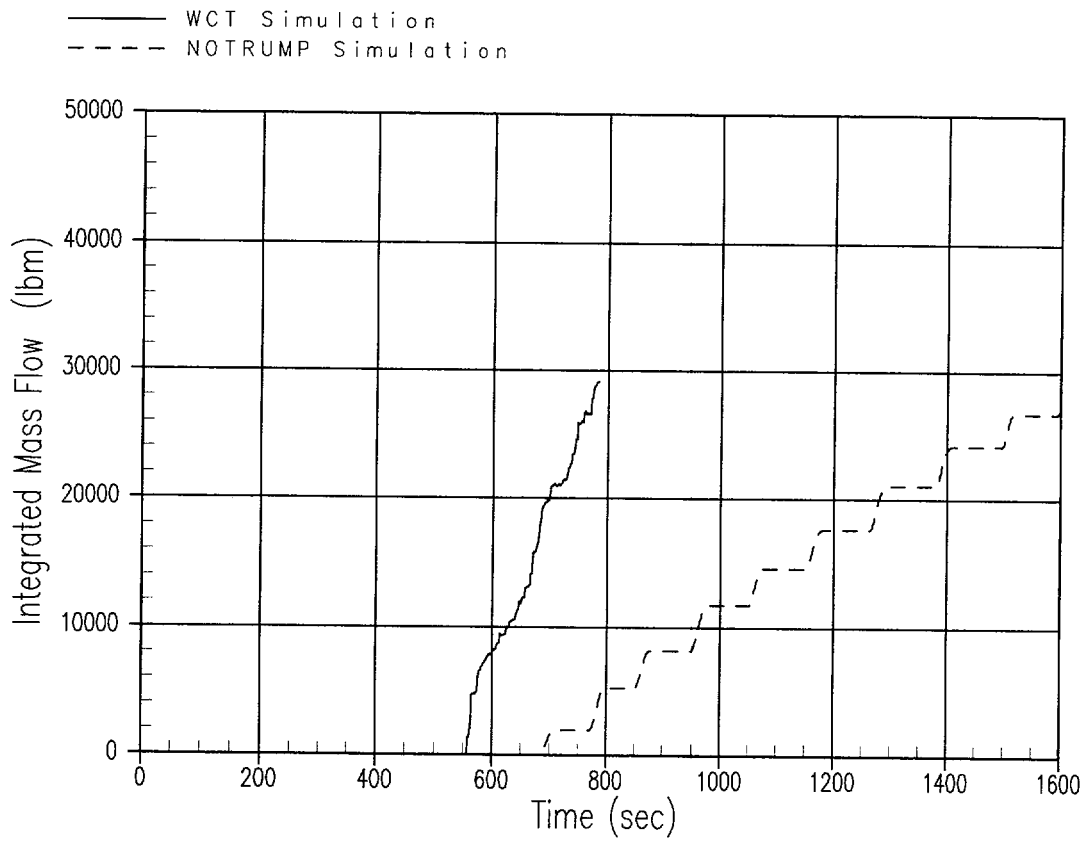


Figure 3-14 AP1000 DEDVI Break Single Failure Loop ADS-4 – Integrated Liquid Flow

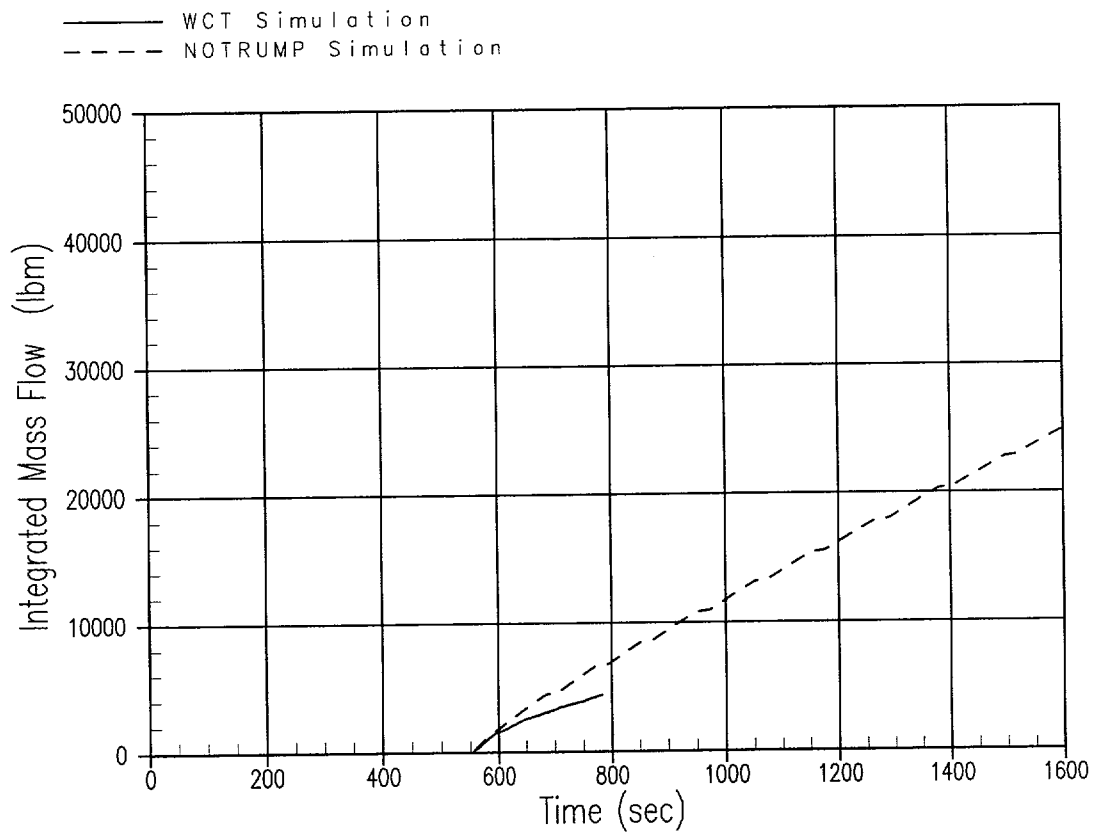


Figure 3-15 AP1000 DEDVI Break Single Failure Loop ADS-4 – Integrated Vapor Flow

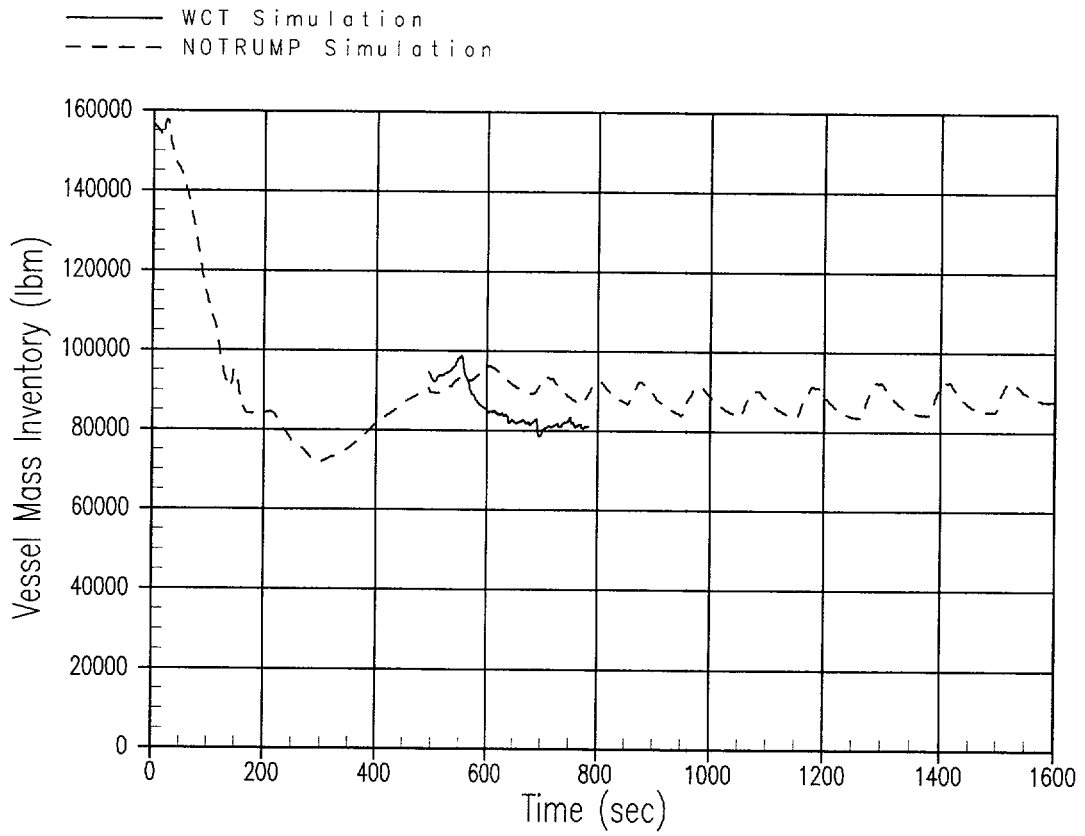


Figure 3-16 AP1000 DEDVI Break Vessel Mass Inventory

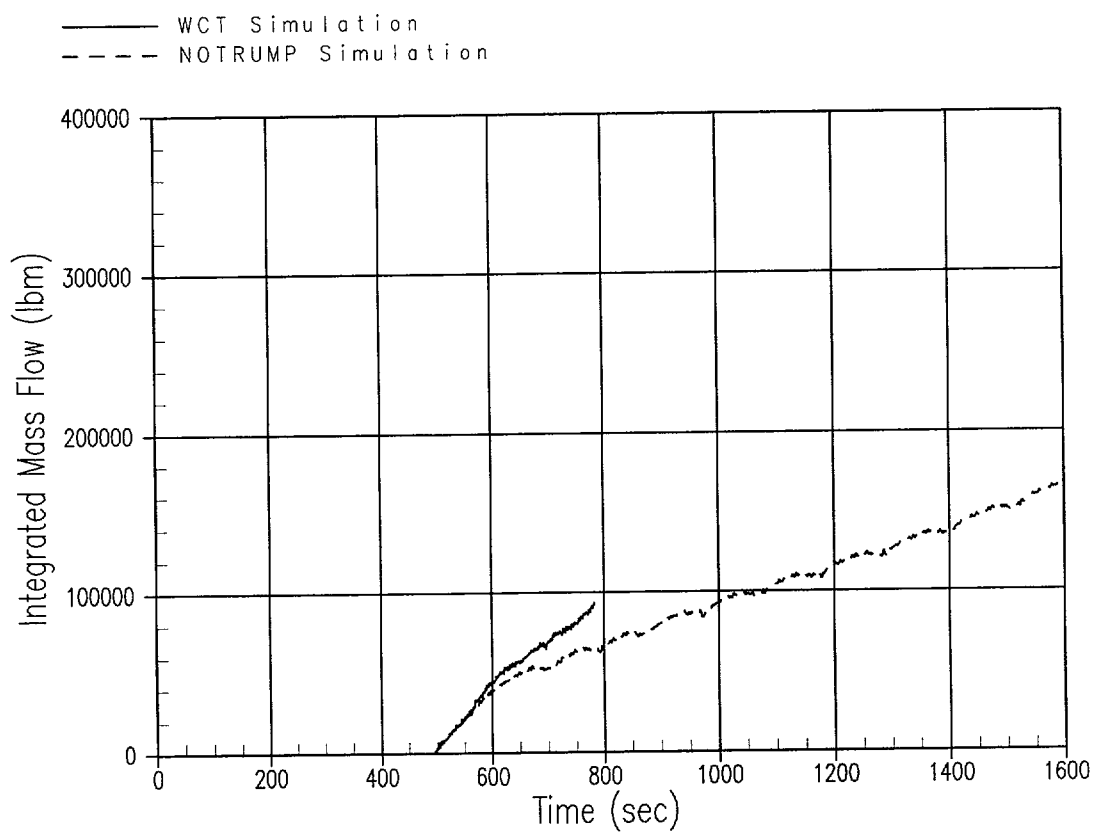


Figure 3-17 AP1000 DEDVI Break Integrated Core Inlet Flow

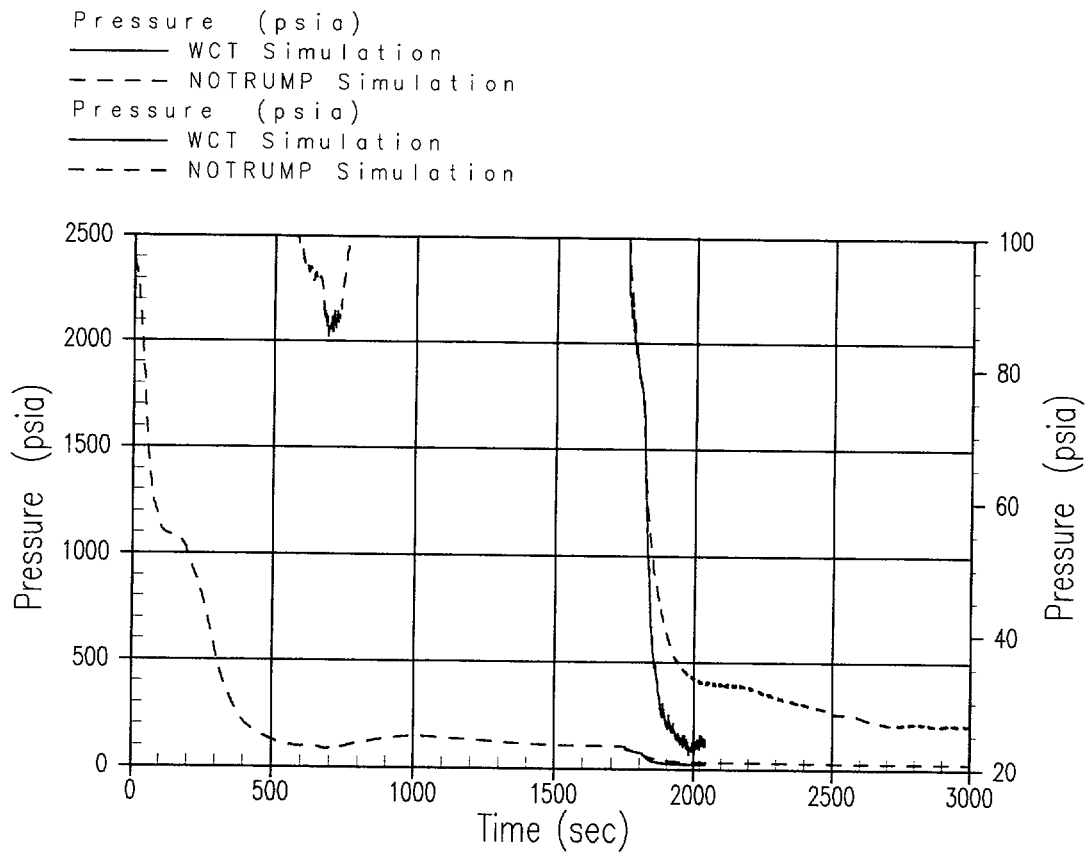


Figure 3-18 AP1000 Inadvertent ADS Actuation Scenario – Downcomer Pressure

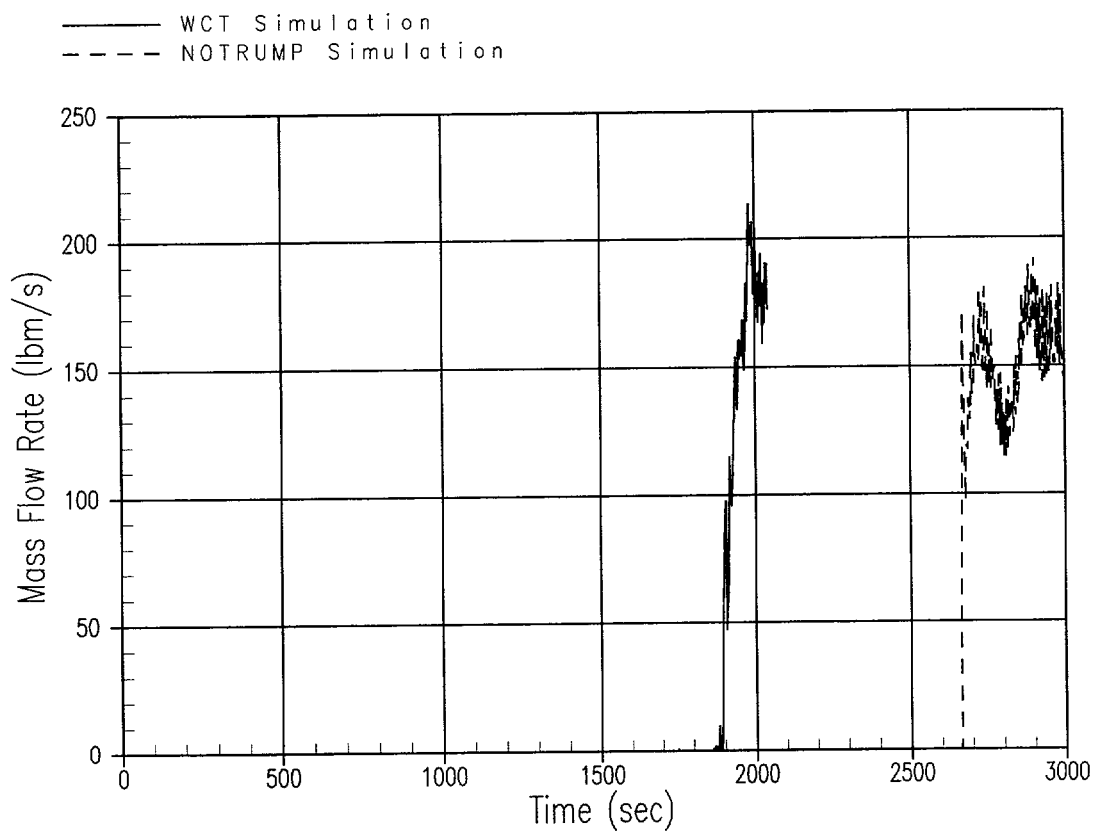


Figure 3-19 AP1000 Inadvertent ADS Actuation Scenario – Total IRWST Injection Flow Rate

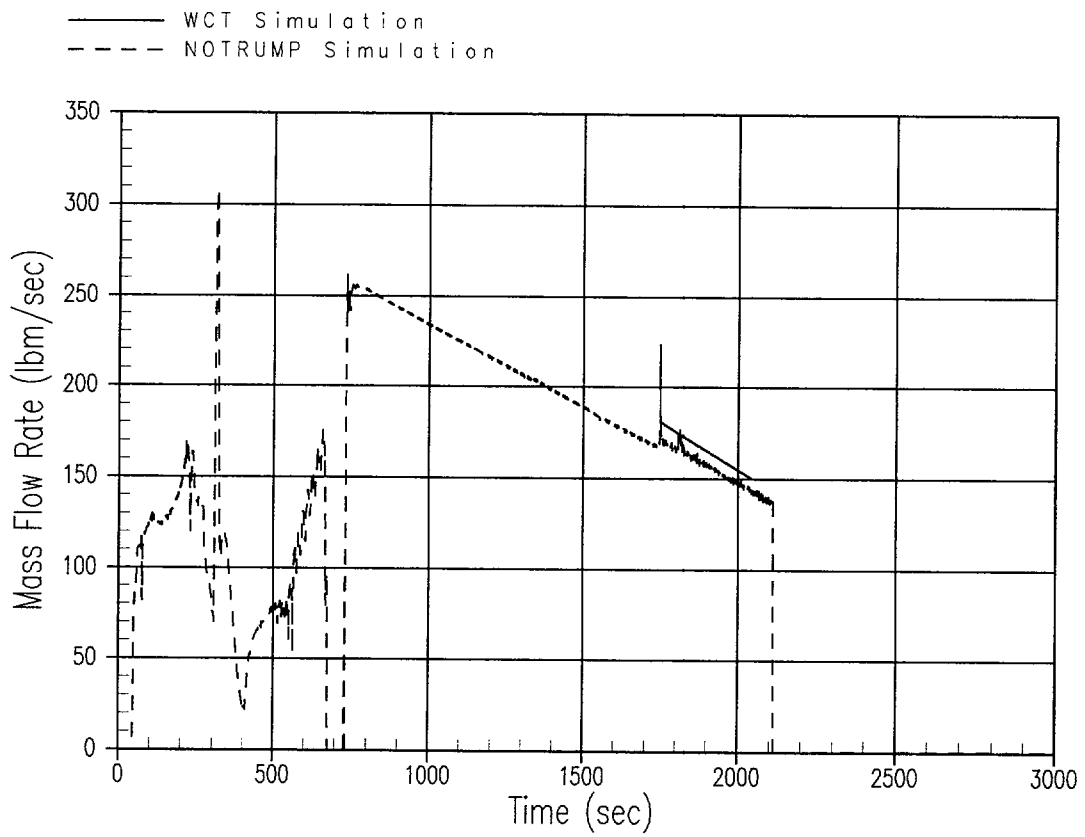


Figure 3-20 AP1000 Inadvertent ADS Actuation Scenario – Total CMT Injection Flow Rate

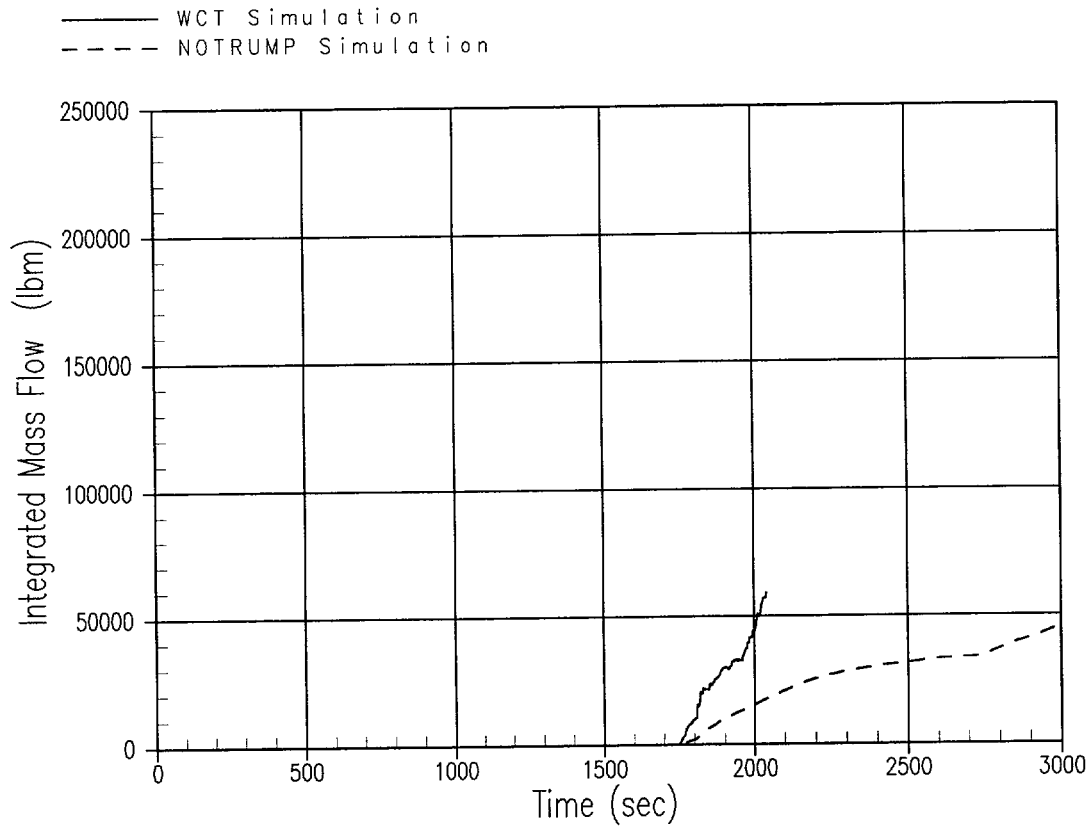


Figure 3-21 AP1000 Inadvertent ADS Actuation Scenario Intact Loop ADS-4 – Integrated Liquid Flow

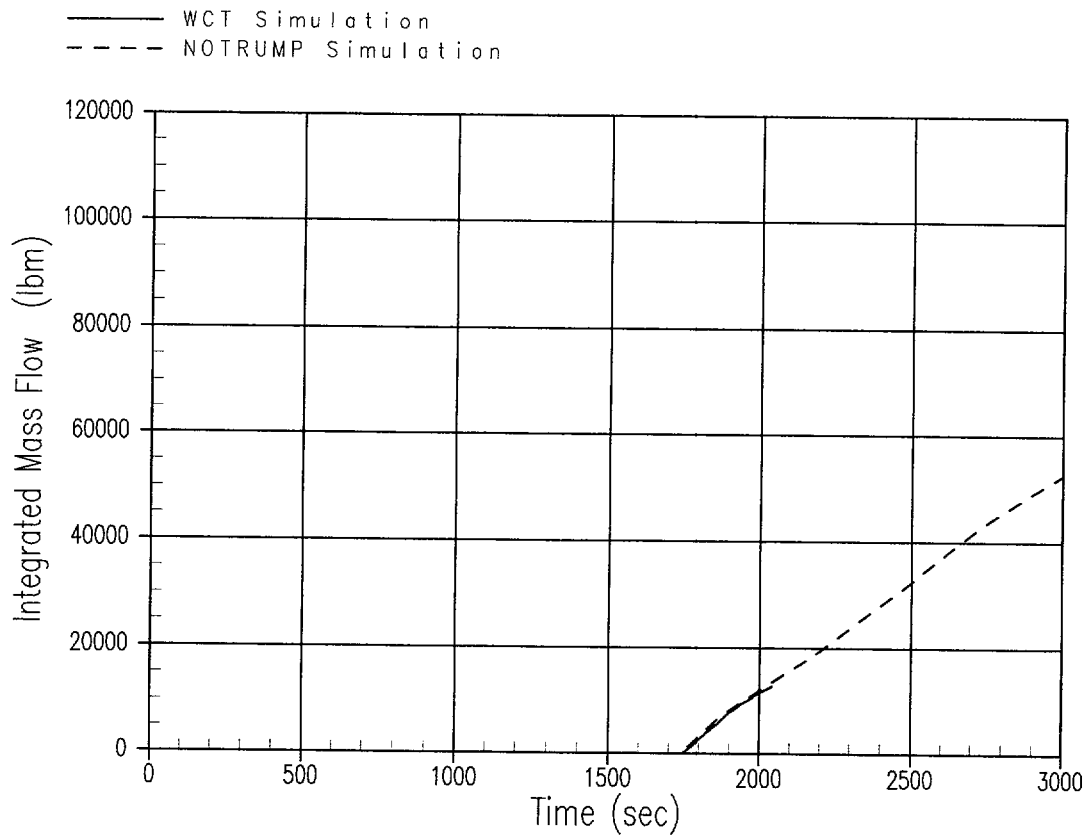


Figure 3-22 AP1000 Inadvertent ADS Actuation Scenario Intact Loop ADS-4 – Integrated Vapor Flow

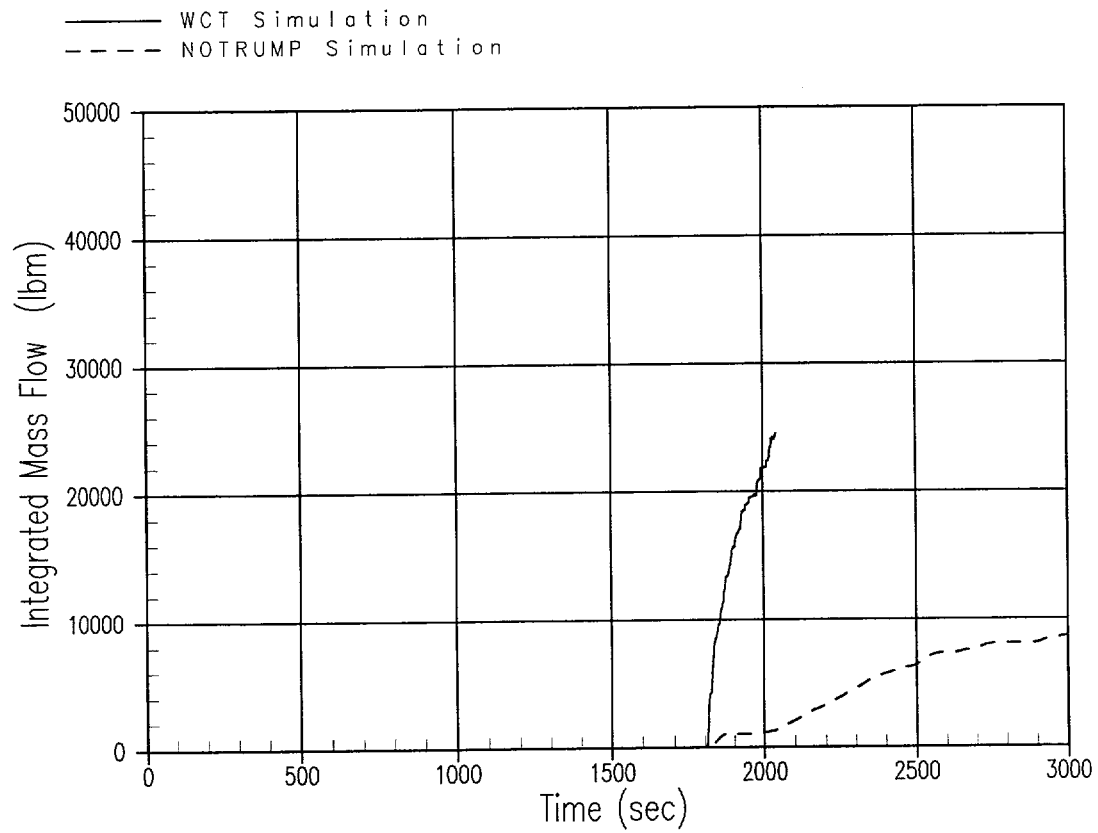


Figure 3-23 AP1000 Inadvertent ADS Actuation Scenario Single Failure Loop ADS-4 – Integrated Liquid Flow

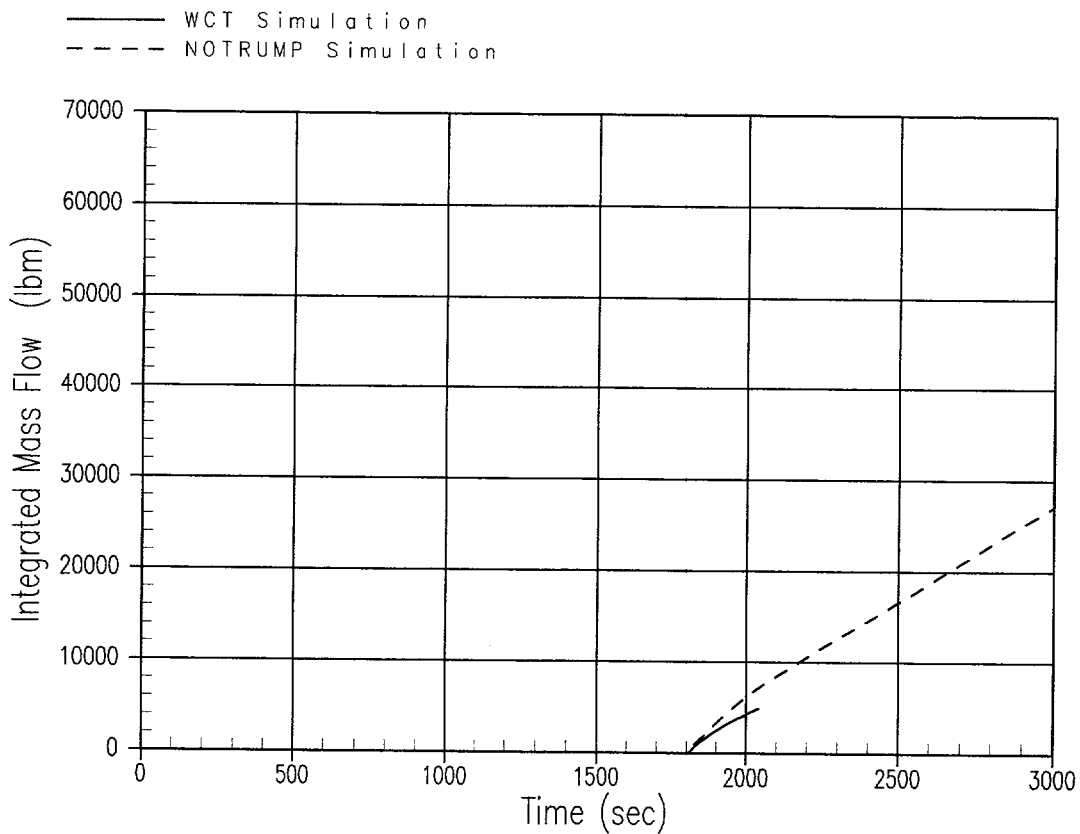


Figure 3-24 AP1000 Inadvertent ADS Actuation Scenario Single Failure Loop ADS-4 – Integrated Vapor Flow

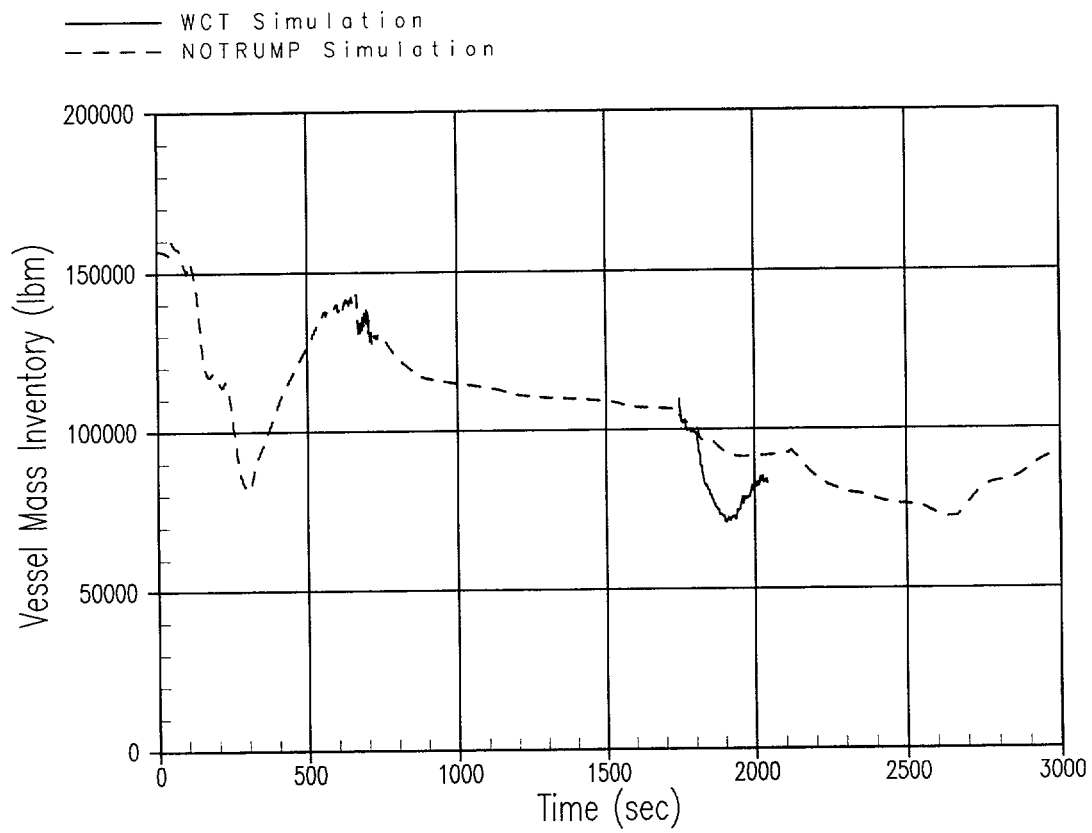


Figure 3-25 AP1000 Inadvertent ADS Actuation Scenario Break Vessel Mass Inventory

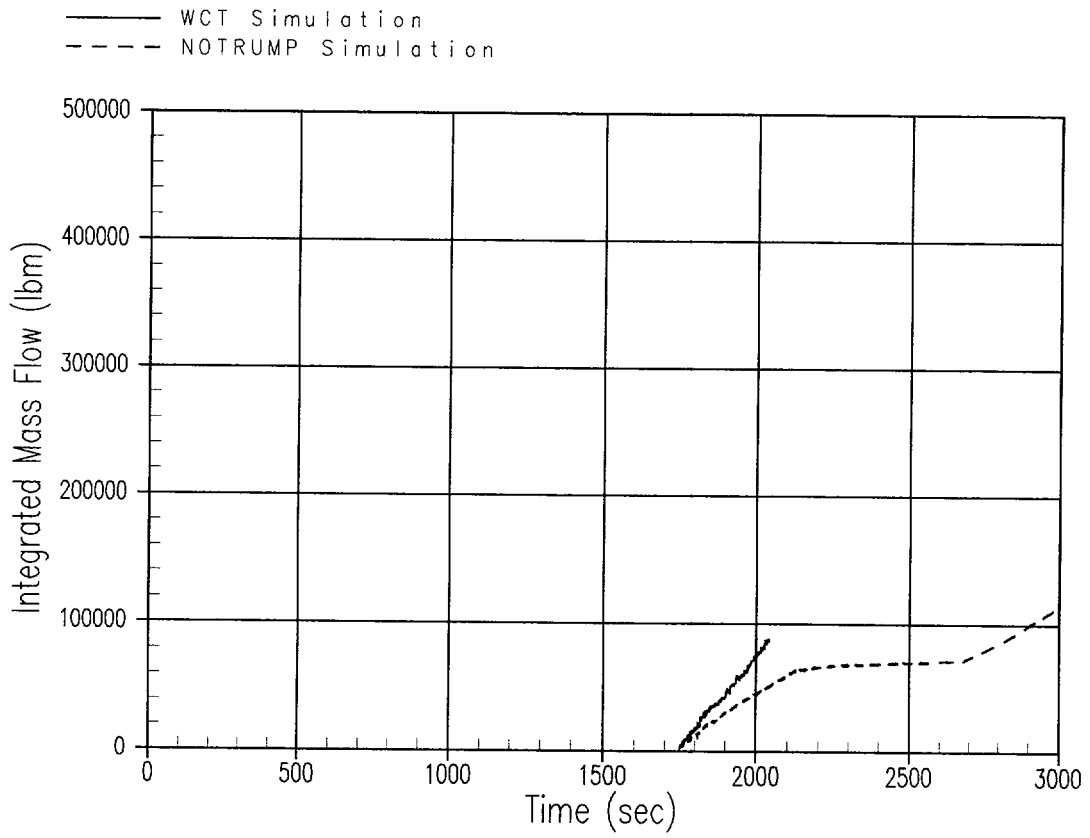


Figure 3-26 AP1000 Inadvertent ADS Actuation Scenario Break Integrated Core Inlet Flow

4 CONCLUSIONS

A version of the WCOBRA/TRAC computer code which contains physically based models for hot leg flow and entrainment phenomena has been created to analyze the AP1000 ADS-4 IRWST initiation phase. The code version has been validated against separate effects test data and against OSU APEX Facility Test SB18. The WCOBRA/TRAC-AP code version is then used to analyze the ADS-4 IRWST initiation phase transients for the DEDVI break and inadvertent ADS actuation AP1000 plant scenarios, using the same methodology as in the test simulations.

Core cooling heat transfer is a function of mass flow rate through the core. During the ADS to IRWST transition the flow through the core is controlled by the ability to remove mass and energy via flow out the ADS vents. WCOBRA/TRAC predicts more flow through the core as expected due to its small-break LOCA break flow modeling. NOTRUMP stabilizes at somewhat higher pressure as the energy being discharged comes into near equilibrium with the decay heat and metal heat.

This comparison of NOTRUMP and WCOBRA/TRAC for the ADS to IRWST transition phase shows that:

- NOTRUMP modeling of ADS venting results in a slower depressurization of the primary system following a SBLOCA in comparison to the prediction with WCOBRA/TRAC.
- The higher pressure in NOTRUMP delays the onset of IRWST injection relative to WCOBRA/TRAC.
- Minimum vessel inventory during the ADS to IRWST transition phase is predicted to occur later for NOTRUMP relative to WCOBRA/TRAC, mainly due to the delayed depressurization in NOTRUMP.
- NOTRUMP and WCOBRA/TRAC both predict core heat transfer rates that maintain clad temperatures near the fluid saturation temperature.

The comparison of NOTRUMP with WCOBRA/TRAC for the limiting SBLOCA events confirms that NOTRUMP can adequately simulate the overall core cooling behavior during the ADS to IRWST transition phase of an AP1000 SBLOCA event. The methodology developed for NOTRUMP for AP600 provides a conservative simulation of ADS-4 venting and the onset of IRWST injection for AP1000.

The NOTRUMP DCD analysis is performed under Appendix K restrictions, including the use of ANS 1971 + 20% core decay heat. Additional conservatism account for plant design uncertainties: the passive safety systems resistances are set at design upper bound values, and the minimum effective critical flow area and maximum flow resistance are used in the ADS flow paths. Overall, the NOTRUMP thermal-hydraulic model predictions of critical flow and ADS-4 flow path pressure drop with the flow resistance penalty included adequately compensate for the lack of detailed momentum flux and liquid entrainment models in the code. The NOTRUMP DCD analysis provides a conservative prediction of the ECCS performance of the AP1000 for postulated small break LOCA events.